KERNFORSCHUNGSZENTRUM KARLSRUHE

Institut für Neutronenphysik und Reaktortechnik

The Influence of Nuclear Data Uncertainties of Reactor Materials on the main Safety and Stability Parameters of a Large Steam-Cooled Fast Reactor (D-1 Design) *)

C.H.M. BROEDERS

September 1968

*) Work performed as final part of the study for electrotechnical engineer at the T.H. Eindhoven.

TABLE OF CONTENTS

Introduction

Investigations of the D-1 design for a 1,000 MWe steam-cooled fast breeder reactor showed that the D-1 core is near the boundary of inherent stability. Within the expected uncertainties of the feedback coefficients the core may become unstable. In earlier studies, mainly on sodium-cooled fast breeder reactors, it was found that the feedback coefficients are rather sensitive to the nuclear data uncertainties.

Therefore, in this study the influences of the nuclear data uncertainties on the main parameters for the safety and stability of the D-1 design are primarily investigated. These parameters are the Doppler coefficient and the steam-density coefficient. Moreover, the influence of the data uncertainties on the loss of coolant reactivity, the conversion ratio of the core and the amount of fissile material required is considered.

Mainly the influence of the uncertainties of the capture and fission cross-sections is examined. Only for the materials U^{238} and Pu^{239} the influence of the inelastic cross-section uncertainties is considered too.

Most investigations were performed with the help of multi-group diffusion calculations in a fundamental mode approximation. For these calculations the KFK-SNEAK set was used as basic group constant set.

After each cross-section variation the reactor parameters considered were calculated for a critical reactor.

In order to obtain some general information about the influence of the nuclear data uncertainties on the Doppler coefficient and the steam-density coefficient, the effect on these parameters following a 10% increase in the macroscopic cross-sections for capture and fission are first investigated.

After that the influences of the data uncertainties of the reactor materials are calculated. Moreover, for the Doppler effect the results of different calculation methods are compared.

In the last chapter the influence of the reactor parameter uncertainties (found in this study) on safety, stability and dynamic behaviour of the D-1 design is investigated.

1. THE REACTOR CONSIDERED AND THE MODEL APPLIED FOR THE CALCULATIONS

1.1. Features of the reactor considered

The study is carried out for the D-1 design for a large steam-cooled fast breeder reactor which is the first detailed design for a 1,000 MWe reactor of this type undertaken by the Kernforschungszentrum Karlsruhe. It has been pointed out that the D-1 design does not claim to be the optimum of possible steam-cooled breeder reactors; the intention rather was that further analyses of the design would lead to a more optimal design.

The design is described in detail elsewhere [1,2]. Figure 1 shows a simplified diagram of the reactor. Only a short summary of the most important features will be given here.

Power

1,000 MWe or about 2,500 MWth.

Cooling

The cooling is by superheated H_2O steam. The steam enters the pressure vessel at the bottom, goes upward through the radial blanket, passes the core in downward direction and leaves the vessel at the bottom. The normal mean pressure of the steam in the core is 170 ata $\triangleq$ 2,600 p.s.i. (steam-density ρ = 0.0706 g/cm^3).

Fuel

The fuel is in the form of oxide. The D-1 design contains primarily U^{238} as fertile material and Pu^{239} as fissile material. Due to the neutron capture in Pu^{239} a second fertile isotope Pu^{240} is built up which may be converted into Pu^{241} and Pu^{242}.

The long-time behaviour of fast power reactors with Pu recycling is described in more detail in (3,4).

The D-1 concept provides fuel exchanging of 1/3 of the fuel, after that maximum permissible burn-up is reached in this part. For this purpose, the fuel subassemblies are divided into a number of groups. Each of these groups contains 3 subassemblies. The only difference between these is the burn-up. At maximum burn-up in one subassembly the other ones reach 1/3 and 2/3 of the maximum burn-up respectively.

It is intended to treat the blanket and fission core material together during the recycling. After a number of recyclings a nearly constant isotopic composition of the plutonium will be reached. For the D-1 design this composition was calculated to be [5]:

Pu^{239} 74%; Pu^{240} 22.7%; Pu^{241} 2.3%; Pu^{242} 1%.

Core

The core has a cylindrical form with H/D = 0.575. A division into 7 zones is provided (figure 2).

- 3 radial zones
  - 2 fission zones with a different ratio of fertile to fissile material
  - 1 blanket (breeding) zone with natural uranium-oxide and a small amount of Pu^{239}-oxide.
- 4 axial zones
  - 1 zone for collecting fission-product gasses
  - 1 fission zone
  - 2 blanket zones

The 2 radial fission zones have a different ratio of fertile to fissile material so that the maximum power densities are nearly equal in these zones.

Cladding

For cladding the following materials will be used:

- For the blankets:

  Incoloy 800 with the composition
  Cr 20%; Fe 48%; Ni 32%.

- For the fission-core zones
  Inconel 625 with
  Cr 22%; Fe 3%; Mo 9%; Nb 4%; Ni 62%

An analysis of the power coefficient of the D-1 core [34,35] yielded a small negative value. However, within the expected uncertainty of the calculated reactivity effects the power coefficient may be positive, which implies an inherent unstable core.

In order to obtain more information about the uncertainty of the power coefficient, the dependence of the Doppler effect and the steam-density coefficient on the nuclear cross section uncertainties is examined in this study.

1.2. The approximation model for the calculations

The effect of the data uncertainties on the safety parameters was studied with the help of a homogenized model. The core geometry was taken into account by a geometrical buckling. With this model zero-dimensional or fundamental mode calculations may be made. The required computing time for these calculations is relatively small while the effect on the parameters is in rather good agreement with more detailed calculations.

The parameters are calculated at maximum burn-up. It is assumed that in this case no absorbing control materials are in the reactor any more but the control rod followers of Al_2O_3.

The design parameters for the homogenized core in the reference point are given in table 1.1.

Description	Material	Volume fraction
Fuel	PuO_2-UO_2	0.454
Cladding + Structure	Inconel 625	0.206
Coolant	H_2O steam	0.32
Control rod follower	Al_2O_3	0.02

Table 1.1.

The fuel-density is assumed to be 0.87 of the theoretical values. These are

UO_2 10.96 g/cm^3
PuO_2 11.46 g/cm^3

The normal mean steam-density is

$\rho = 0.0706$ g/cm^3 ($\hat{=}$ 170 ata $\hat{=}$ 2,600 p.s.i.)

The isotopic composition of the plutonium is

Pu^{239} 74%; Pu^{240} 22.7%; Pu^{241} 2.3%; Pu^{242} 1%

Geometrical buckling

The geometrical buckling is determined with the help of

$$B_g^2 = \left(\frac{\pi}{H'}\right)^2 + \left(\frac{2.405}{R'}\right)^2$$

with

$H' = H_c + 2S$
$R' = R_c + S$

H_c height of the fission zone of the core: 150 cm
R_c radius " " " " " " " : 130 cm
S saving " " blanket

The saving is determined by comparison of fundamental mode calculations with one- and two-dimensional calculations for the reflected system. For the dimensions of the D-1 core the saving is determined to be about 16 cm.

Therefore:

$$B_g^2 = \left(\frac{\pi}{150+2.16}\right)^2 + \left(\frac{2.405}{130+16}\right)^2 = 5.69\ 10^{-4}\ \text{cm}^{-2}$$

Burn-up

The maximum permissible burn-up is 55,000 MWd/T. This is defined to be the maximum permissible axial averaged burn-up in the fuel rods situated in the core where the radial flux distribution has its maximum.

For the calculations the equivalent atom burn-up is required. The latter is calculated in appendix A.

The burn-up is 3.45 atom per cent.

With these parameters and the group cross-section constants of the KFK-SNEAK set [7] the homogenized core is just critical at 900°K with the following atom-densities (table 1.2)

Material	Atom-density 10^{24} |cm^{-3}|		Material	Atom-density 10^{24} |cm^{-3}|	
Al	7.34	10^{-4}	O	2.12903	10^{-2}
Cr	4.42974	10^{-3}	Pu^{239}	1.12238	10^{-3}
Fe	5.62485	10^{-4}	Pu^{240}	3.44298	10^{-4}
H	1.49785	10^{-3}	Pu^{241}	3.48849	10^{-5}
Mo	9.82257	10^{-4}	Pu^{242}	1.51673	10^{-5}
Nb	4.50843	10^{-4}	U^{238}	7.86809	10^{-3}
Ni	1.10588	10^{-2}	pairs of fission products	3.35346	10^{-4}

Table 1.2

In figure 3 the neutron flux distribution for the steam-densities $\rho = 0$ and $\rho = 0.0706$ is plotted. Fig. 4 shows the adjoint flux. Figures 5,6 and 7 show the energy dependence of the capture and fission rates of the most important reactor materials.

Some reactor parameters are *)

Loss of coolant reactivity	ΔK_L	$= 3.64\ 10^{-2}$	at 900°K
Reduced steam-density coefficient	R.S.D.C.	$= -2.14\ 10^{-2}$	at 900°K
Conversion ratio	C.R.	$= 0.9857$	at 900°K
Doppler constant	A_D	$= -1.386\ 10^{-2}$	at 900°K

*) For the description of these parameters see chapters 2 and 3.

2. THE REACTOR PARAMETERS CONSIDERED

The most important coefficients for the safety and stability of a fast steam-cooled reactor are the Doppler coefficient and the steam-density coefficient since they form the largest feedback reactivity effects.

In a large fast reactor the Doppler coefficient is a prompt negative reactivity effect [9]. Because of the small neutron life-times in fast reactors this prompt negative reactivity is important for the control and safety of the reactor.

In [34] is shown that large steam-cooled fast reactors are inherent stable only if the steam-density coefficient is negative and if its absolute value is not too large.

For the safety of the reactor also the loss of coolant reactivity is important because it is significant for the reactivity ramp after large disturbances in the cooling system.

With the calculation methods applied also the ratio of the fertile to the fissile material and the conversion ratio of the core could be easily determined.

Therefore, the following parameters are considered:

1) Doppler coefficient
2) Steam-density coefficient
3) Loss of coolant reactivity
4) Ratio of the fertile to the fissile material
5) Conversion ratio of the core

3. CALCULATION METHODS

In this chapter some general features of the calculation methods suitable for the intended study are described.

3.1. The multi-group diffusion equations

The behaviour of a neutron chain reactor is defined by the production and losses of the neutrons in this reactor. The behaviour of the neutrons in the reactor may be described exactly by the transport theory (10).

The number of neutrons with energy E and direction $\vec{\Omega}$ at time t at point $\vec{x}$ in the reactor is given by $f(\vec{x},E,\vec{\Omega},t)$. Then, the space and time dependent flux is equal to

$$\phi(\vec{x},t) = \int_E dE \int_{\vec{\Omega}} d\vec{\Omega}\, f(\vec{x},E,\vec{\Omega},t) \tag{3.1}$$

The neutron balance for the reactor leads to the Boltzmann equation

$$\begin{aligned}\frac{1}{v}\frac{\partial f(\vec{x},E,\vec{\Omega},t)}{\partial t} = &- \vec{\Omega}\ \text{grad}\ f(\vec{x},E,\vec{\Omega},t)\\ &- f(\vec{x},E,\vec{\Omega},t)\ [\Sigma_s(\vec{x},E,\vec{\Omega},t)+\Sigma_a(\vec{x},E,\vec{\Omega},t)]\\ &+ S(\vec{x},E,\vec{\Omega},t)\\ &+ \int_{E'} dE' \int_{\vec{\Omega}'} d\vec{\Omega}'\,[f(\vec{x},E,\vec{\Omega},t)\Sigma_s(\vec{x},t,E'\to E,\vec{\Omega}'\to\vec{\Omega})]\end{aligned} \tag{3.2}$$

with

- v neutron velocity
- Σ_s scattering cross-section
- Σ_a absorption cross-section
- $\Sigma_s(E'\to E,\vec{\Omega}'\to\vec{\Omega})$ cross section for the scattering of neutrons with energy E' and direction $\vec{\Omega}'$ to E and $\vec{\Omega}$
- S source term

For solving the Boltzmann equation many approximation methods exist. In this study the multi-group diffusion approximation will be used for the calculations.

The energy dependent diffusion equation reads

$$\mathrm{div}D(\vec{x},E)\,\mathrm{grad}\phi(\vec{x},E) + \left[\Sigma_s(\vec{x},E)+\Sigma_a(\vec{x},E)\right]\phi(\vec{x},E) = \int_{E'} dE'\ \Sigma_s(\vec{x},E'\to E)\phi(\vec{x},E') + \frac{\chi(\vec{x},E)}{K_{eff}}\int_{E'} dE'\ \nu(\vec{x},E')\Sigma_f(\vec{x},E')\phi(\vec{x},E') \qquad (3.3)$$

with

χ	number of fission neutrons
ν	mean number of fission neutrons per fission
Σ_f	fission cross-section
K_{eff}	multiplication factor of the system

The multi-group equations are for each group i

$$\nabla D_i(\vec{x})\nabla\phi_i(\vec{x})+\Sigma^i_{rem}(\vec{x})\phi_i(\vec{x}) = \sum_{j\neq i}\Sigma_{j\to i}(\vec{x})\phi_j(\vec{x})+\frac{\chi_i(\vec{x})}{K_{eff}}\sum_j \nu_j\Sigma^j_f\phi_j \qquad (3.4)$$

with

i,j	group indices
D_i	diffusion constant $D_i = \frac{1}{3\Sigma_{tr_i}}$
Σ_{tr_i}	transport cross-section constant in group i
ϕ_i	neutron flux " " "
Σ^i_{rem}	removal cross-section constant " " "
Σ_f^j	fission cross-section constant " " j
$\Sigma_{j\to i}$	scattering cross-section constant for scattering from group j to i
χ_i	fraction of fission neutrons in group i
ν_j	mean number of fission neutrons per fission in group j

The adjoint flux or importance function $\phi^+(\vec{x},E)$ may be defined as the number of daughter neutrons due to the neutron energy distribution caused by a neutron put in the reactor with energy E at point $\vec{x}$.

The multi-group equation for the adjoint flux reads

$$\nabla D_i(\vec{x})\nabla\phi_i^+(\vec{x})+\Sigma^i_{rem}(\vec{x})\phi_i^+(\vec{x}) = \sum_{j\neq i}\Sigma_{i\to j}\phi_j^+(\vec{x})+\frac{\nu_i(\vec{x})\Sigma^i_f(\vec{x})}{K_{eff}}\sum_j \chi_j(\vec{x})\phi_j^+(\vec{x}) \qquad (3.5)$$

Usually, further approximations are applied for the space dependence. This is done by separating coordinates. The coordinates separated are taken into account by bucklings.

For fundamental mode or zero-dimensional calculations the system is homogenized and the geometry is taken into account by the geometrical buckling Bg^2.

The equation

$$\Delta\phi_i + Bg_i^2\,\phi_i = 0 \qquad (3.6)$$

has to be satisfied by the flux.

Substitution of equations (3.6) in (3.4) and (3.5) gives the relative simple set of equations:

$$(\Sigma^i_{rem}+Bg_i^2)\phi_i = \sum_{j\neq i}\Sigma_{j\to i}\phi_j+\frac{\chi_i}{K_{eff}}\sum_j \nu_j\Sigma^j_f\phi_j \qquad (3.7a)$$

$$(\Sigma^i_{rem}+Bg_i^2)\phi_i^+ = \sum_{j\neq i}\Sigma_{i\to j}\phi_j^+ + \frac{\nu_i\Sigma^i_f}{K_{eff}}\sum_j \chi_j\phi_j^+ \qquad (3.7b)$$

Calculations with the multi-group diffusion equations have uncertainties by several origins:

1) The approximation of the transport equation.
2) Uncertainties of the group constants.

   The latter are introduced by:

   2.1) Uncertainties in the basic nuclear data.

   2.2) The way the energy dependent nuclear data are condensed in the group constants.

In this study mainly uncertainties caused by the basic nuclear data on the group constants will be examined.

3.2. The group constants for the multi-group diffusion equations

For the multi-group diffusion calculations the energy dependent nuclear data have to be worked up into group constants.

The group constants required are:

$$D_i = \frac{1}{3\Sigma^i_{tr}} \; ; \; \Sigma^i_{rem} \; ; \; \Sigma_{i\to j} \; ; \; \nu_i\Sigma^i_f \; ; \; \chi_i$$

The transport and removal cross-sections are defined by

$$\Sigma_{tr} = \Sigma_t - \mu\Sigma_s \tag{3.8}$$

$$\Sigma_{rem} = \Sigma_\gamma + \Sigma_f + \Sigma_{bin} + \Sigma_{be} \tag{3.9}$$

with (only symbols occurring for the first time are explained)

Σ_t	total cross-section
μ	mean cosine of the scattering angle in the laboratory system
Σ_γ	capture cross-section
Σ_{bin}	cross-section for inelastic removal
Σ_{be}	cross-section for elastic removal

The condensation of the energy dependent cross-sections into group constants has to be done carefully in a way that the energy dependent diffusion equation (3.3) is approximated as accurate as possible by the set multi-group equations(3.4). The preparation of a group constant set for fast reactor calculations is described detailed in [6,7,8].

In this study the resonance self-shielding effect is taken into account with the help of the σ_o concept (described in this chapter).

A short description of the determination of the group constants is given below.

1) The group constants for the absorption cross-sections are determined by the requirement:

$$\int_{\Delta E_i} \Sigma_x(E)\phi(E)dE = \Sigma_x^i \phi_i \qquad x = \gamma, f \tag{3.10}$$

The group flux is defined by:

$$\phi_i = \int_{\Delta E_i} \phi(E)dE \tag{3.11}$$

With the help of (3.10) and (3.11) we obtain:

$$\Sigma_x^i = \frac{\int_{\Delta E_i} \Sigma_x(E)\phi(E)dE}{\int_{\Delta E_i} \phi(E)dE} \qquad x = \gamma, f \tag{3.12}$$

2) For the fission neutron source term we have

$$\int_{\Delta E_i} dE \frac{\chi(E)}{K_{eff}} \int_{E'} dE' \left[\nu(E')\Sigma_f(E')\phi(E')\right] = \frac{\chi_i}{K_{eff}} \sum_j (\nu\Sigma_f)^j \phi_j \tag{3.13}$$

It follows:

$$\chi_i = \int_{\Delta E_i} \chi(E)dE \tag{3.14}$$

Usually, the following normalization is applied:

$$\int_E \chi(E)dE = 1$$

This means

$$\sum_i \chi_i = 1 \tag{3.15}$$

Further, we obtain from (3.13)

$$\int_{E'} \nu(E')\Sigma_f(E')\phi(E')dE' = \sum_j (\nu\Sigma_f)^j\phi_j \qquad (3.16)$$

With (3.11) and (3.16) follows

$$(\nu\Sigma_f)^j = \frac{\int_{\Delta E_j} \nu(E)\Sigma_f(E)\phi(E)dE}{\int_{\Delta E_j} \phi(E)dE} \qquad (3.17)$$

3) The group constants for inelastic and elastic removal and the scattering matrix elements $\Sigma_{i\to j}$ are more complicated to calculate and are not described in detail here. See for these constants [7].

4) For the calculation of the transport cross section from equation (3.8) the total cross-section is required.

The condensing procedure for this total cross-section group constant is based on the following considerations. The diffusion constant is equal to $D = \frac{1}{3\Sigma_{tr}}$ with $\Sigma_{tr} = \Sigma_t - \mu\Sigma_s$. In many cases $\mu\Sigma_s << \Sigma_t$ and $D \approx \frac{1}{3\Sigma_t}$. For this reason it is required that

$$\int_{\Delta E_i} dE\left[D(E)\nabla^2\phi(E)\right] = D_i\nabla^2\phi_i \qquad (3.18)$$

or

$$\int_{\Delta E_i} dE\left[\frac{\phi(E)}{3\Sigma_t(E)}\right] = \frac{1}{3\Sigma_t^i}\int_{\Delta E_i}\phi(E)dE \quad , \quad \Sigma_t^i = \frac{\int_{\Delta E_i}\phi(E)dE}{\int_{\Delta E_i} dE\,\frac{\phi(E)}{\Sigma_t(E)}} \qquad (3.19)$$

From these considerations follows that for the preparation of group constants the actual neutron flux spectrum $\phi(E)$ is required as weighting spectrum.

However, the ABN, SNEAK and most other group constant sets are intended to be used in more general reactor calculations. For this reason the neutron flux spectrum is approximated.

Usually, the narrow resonance (N.R.) approximation is applied. This means that the collision density is considered to be a slowly varying function of the energy

$$\Sigma_t(E)\phi(E) = F(E) \tag{3.20}$$

In the ABN set is

$F(E)$: constant for $E \leq 2.5$ MeV (Fermi spectrum)
: the fission neutron spectrum for $E > 2.5$ MeV

In the KFK-SNEAK set $F(E)$ is determined with the help of the smoothed neutron spectrum of the SNEAK 3A-2 core (similar to the spectrum of a large steam-cooled fast reactor with $\rho = 0.07$ g/cm^3). The spectrum was calculated with the help of the ABN set and the KFK-26-10 set [7].

With the narrow resonance approximation the material dependent group constants are

$$K_{\Sigma_x}^{i} = \frac{\int_{\Delta E_i} K_{\Sigma_x}(E)\,\frac{F(E)}{\Sigma_t(E)}\,dE}{\int_{\Delta E_i} \frac{F(E)}{\Sigma_t(E)}\,dE} \qquad \begin{array}{l} x = \gamma, f \\ K = \text{reactor material} \end{array} \tag{3.21}$$

In equation (3.21) the self-shielding effect may be observed. The group constant $K_{\Sigma_x}^{i}$ depends on the ratio $\frac{K_{\Sigma_x}(E)}{\Sigma_t(E)}$, that means the concentration of material K in the reactor (K_{Σ_x} macroscopic cross-section for process x of material K, Σ_t total macroscopic cross-section of the material mixture considered).

The σ_o concept includes that $\Sigma_t(E)$ is approximated by

$$\Sigma_t(E) = K_{\Sigma_t}(E) + K_{\sigma_o}\,K_N \tag{3.22}$$

K_N atom density of material K
K_{σ_o} background total cross-section per atom of material K

It is assumed that $^{K}\sigma_o$ is independent of energy in the group i just considered.

Then

$$^{K}\Sigma_x^i\,(^{K}\sigma_o) = \frac{\int_{\Delta E_i} \frac{^{K}\Sigma_x(E)\,F(E)}{^{K}\Sigma_t(E)+{}^{K}\sigma_o\,{}^{K}N}\,dE}{\int_{\Delta E_i} \frac{F(E)}{^{K}\Sigma_t(E)+{}^{K}\sigma_o\,{}^{K}N}\,dE} \qquad x = \gamma, f \qquad (3.23)$$

For an infinite dilute concentration of the material K: $^{K}\sigma_o\ {}^{K}N\to\infty$

$$^{K}\Sigma_x^i(\infty) = \lim_{{}^{K}\sigma_o\,{}^{K}N\to\infty} (^{K}\Sigma_x^i(^{K}\sigma_o\,{}^{K}N)) = \frac{\int_{\Delta E_i} {}^{K}\Sigma_x(E)F(E)dE}{\int_{\Delta E_i} F(E)dE} \qquad x = \gamma, f \qquad (3.24)$$

For materials with temperature dependent cross-sections the definitions are

$$^{K}\Sigma_x^i\,(^{K}\sigma_o,T) = \frac{\int_{\Delta E_i} \frac{^{K}\Sigma_x(E,T)\,F(E)}{\Sigma_t(E,T)+{}^{K}\sigma_o\,{}^{K}N}\,dE}{\int_{\Delta E_i} \frac{F(E)}{\Sigma_t(E,T)+{}^{K}\sigma_o\,{}^{K}N}\,dE} \qquad x = \gamma, f \qquad (3.25)$$

and

$$^{K}\Sigma_x^i\,(\infty,o) = \lim_{\substack{{}^{K}\sigma_o\,{}^{K}N\to\infty \\ T=o}} (^{K}\Sigma_x(^{K}\sigma_o,T)) = \frac{\int_{\Delta E_i} {}^{K}\Sigma_x(E,o)F(E)dE}{\int_{\Delta E_i} F(E)dE} \qquad x = \gamma, f \qquad (3.26)$$

The self-shielding factor $^{K}f_x^i(\sigma_o,T)$ is defined by

$$^{K}\Sigma_x^i\,(\sigma_o,T) = {}^{K}f_x^i\,(\sigma_o,T)\ {}^{K}\Sigma_x^i\,(\infty,o)$$

or

$$^{K}f_x^i\,(\sigma_o,T) = \frac{^{K}\Sigma_x^i\,(\sigma_o,T)}{^{K}\Sigma_x^i\,(\infty,o)} \qquad (3.27)$$

The self-shielding factor (equation 3.27) is calculated and tabulated for 3 temperatures (T = 300°K, 900°K and 2100°K) and 7 values of σ_o ($0, 10^i$; i=1 to 6). For σ_o values not tabulated interpolations have to be made.

The group constants and self-shielding factors for the capture, fission and total cross-sections are calculated straight forward with the help of the formulae given before. Also the group constants for the removal and transport cross-sections are calculated and tabulated. This is done with the help of the following formulae (material and group indices are omitted)

$$f_{rem}\,\Sigma_{rem} = f_\gamma\Sigma_\gamma + f_f\Sigma_f + f_e\Sigma_{be} + \Sigma_{bin} \tag{3.28}$$

$$f_{tr}\,\Sigma_{tr} = \{f_t\Sigma_t - (f_\gamma\Sigma_\gamma + f_f\Sigma_f + \Sigma_{in})\}\,(1-\mu) + (f_\gamma\Sigma_\gamma + f_f\Sigma_f + \Sigma_{in}) \tag{3.29}$$

The group constant $K_{(\nu\Sigma_f)^i}$ is not calculated with the help of formula (3.17) but with

$$K_{(\nu\Sigma_f)^i} = K_{\nu_i}\,K_{\Sigma_f^i} \tag{3.30}$$

and

$$K_{\nu_i} = \frac{\int_{\Delta E_i} K_\nu(E)\,dE}{\int_{\Delta E_i} dE} \tag{3.31}$$

This approximation introduces small errors since the energy dependence of $\nu(E)$ is very weak. For most fissile materials $\nu(E)$ may be approximated by

$$\nu(E) = \nu_o + aE$$

ν_o constant (about 1.8 to 3.0)
a " (" 0.1 " 0.16)
E energy in MeV

A crude calculation for group 1 (6.5 MeV to 10.5 MeV) of Pu^{239} shows a difference of about 3% between $\nu'\Sigma_f'$ and $(\nu\Sigma_f)'$. For the higher groups (E<6.5 MeV) the differences will be much smaller because of the smaller energy intervals and the less steep decreasing of the flux. Below 100 keV $\nu(E)$ varies less than 1% over the group width.

3.3. Perturbation calculations

The perturbation theory allows calculating directly the effects due to macroscopic cross section variations in a reactor from its flux and adjoint flux spectra. These calculations often provide sufficient accuracy with relative small computing time.

In appendix B a perturbation calculation is described. The latter is applied for the examination of the energy dependence of some reactivity effects.

3.4. The calculation of the reactor parameters considered.

3.4.1. The Doppler coefficient

The Doppler effect in a nuclear reactor is the prompt temperature effect on the reactivity due to the temperature dependence of the cross sections in the resonance energy region. The Doppler coefficient (D.C.) is defined by $D.C. = \frac{dk}{dT}$. (3.32)

If the cross sections for a reactor calculation change, the D.C. is changing for the following reasons:

a) Due to the variation of the flux and adjoint flux spectrum.

b) In order to maintain criticality the ratio of fertile to fissile material has to be changed. The main fertile material U^{238} has a negative Doppler effect while the main fissile material Pu^{239} has no Doppler effect or only a small positive one. Therefore, the ratio of these materials influences the total Doppler effect of the system.

c) If the cross sections in the resonance region change the resonance parameters are changing too generally. This variation also influences the Doppler effect.

For the calculation of the D.C. several methods may be used, e.g.

a) Method developed by Nicholson and Froelich [11,12]. With the help of the temperature derivatives of the cross sections $\frac{d\Sigma_x}{dT}$ in a perturbation calculation the D.C. is determined.

b) Successive k-calculation method. The multiplication factor k of the system is calculated for different temperatures. For the determination of the D.C. a temperature law has to be assumed. Generally $\frac{dk}{dT} = \frac{a}{T^x}$. (3.33)

c) Calculation of $\Delta k(\Delta T)$ with a perturbation code. With the cross section differences $\Delta\Sigma_x$ due to a temperature difference ΔT in a perturbation calculation the reactivity effect $\Delta k(\Delta T)$ is determined. Again a temperature law is required for the determination of the D.C.

d) Monte Carlo methods. With the Monte Carlo methods both $\frac{dk}{dT}$ and $\Delta k\ (\Delta T)$ may be calculated [13].

For some of these methods a short description follows below.

3.4.1.1. The method of Nicholson-Froelich.

This method is usually applied at the Kernforschungszentrum Karlsruhe. Froelich has developed a computer program [14] based on the theory of KFK 367 [12] in order to calculate the temperature derivatives of the capture and fission cross-sections of the fuel materials. Since his theory is based on the statistical distributions of the resonance parameters the results are sufficiently accurate only if the number of resonances in an energy group is sufficiently large. That is why the D.C. is calculated only for energies above 100 eV.
In a succeeding perturbation calculation the D.C. is calculated.

For the intended study, this method has some disadvantages:

a) The D.C. is calculated only in the energy region 100 eV<E<100 keV. The lower limit certainly is allowed for sodium-cooled fast reactors. However, in a steam-cooled fast reactor with a considerably weaker neutron spectrumthe contribution of the energy region below 100 eV may be significant.

b) The temperature derivatives of the cross sections are calculated with fixed resonance parameters from a special tape. Variation of the cross-section in the resonance energy region would require variations on this special tape to take into account the resonance parameter variations [9].

3.4.1.2. Successive k-calculations.

In this method the multiplication factor k of the system is calculated for different temperatures. For the temperature dependence of the D.C., generally the relation $\frac{dk}{dT} = \frac{a}{T^x}$ is assumed. From theoretical considerations it may be expected that x lies between $x = \frac{1}{2}$ (for thermal reactors [15]) and $x = \frac{3}{2}$ (for reactors with a very hard neutron spectrum [11]). The constants a and x may be calculated from 3 k-calculations in the following way:

If $T_1 < T_2 < T_3$ and $x \neq 1$, it may be shown easily

$$\Delta k(T_1 \to T_2) = \frac{-a}{1-x}\left[T_1^{(1-x)} - T_2^{(1-x)}\right] \tag{3.34}$$

and

$$\frac{\Delta k(T_1 \to T_2)}{\Delta k(T_2 \to T_3)} = \frac{(T_1/T_2)^{(1-x)}-1}{(T_3/T_2)^{(1-x)}-1} \tag{3.35}$$

With the formulae (3.34) and (3.35) a and x may be calculated if k is known for the temperatures T_1, T_2, T_3.

In the special case that x=1 (the often assumed inverse proportionality of the D.C. with the absolute temperature) we obtain:

$$\Delta k(T_1 \to T_2) = a \ln T_2/T_1 \tag{3.36}$$

and

$$D.C. = \frac{\Delta k(T_1 \to T_2)}{T \ln T_2/T_1} \tag{3.37}$$

The usefulness of this method for the intended study is defined by the way in which the temperature dependent cross-sections are obtained.

As pointed out in chapter 3.2. the temperature dependence of the group cross-section constants in the KFK-SNEAK set is taken into account by means of the self-shielding factors. The latter are calculated with the help of resonance parameters recently recommended [7].

In order to take into account the uncertain-ties of the resonance parameters in a correct way both the group constants for infinite dilution and the self-shielding factors should be modified for variations in the resonance energy region. However, it is expected that the f-factors do not depend very strongly on the resonance parameters.

3.4.1.3. $\Delta\Sigma_x(\Delta T)$ in a perturbation calculation.

This method does not differ much from the preceding one. The usefulness of the method is mainly defined by the way in which $\Delta\Sigma_x(\Delta T)$ are obtained. As described by Kiefhaber [16] a modified perturbation code may be advantageous with respect to the accuracy and to the computing time.

3.4.2. The steam-density coefficient

The steam-density coefficient (S.D.C.) is a measure for the reactivity effect due to variations of the density of the steam coolant. The S.D.C. is defined by:

$$S.D.C. = \frac{dk}{d\rho} \quad \text{for } \rho = \rho_N \text{ ; } \rho_N \text{ normal steam-density} \tag{3.38}$$

In this study the reduced steam-density coefficient (R.S.D.C.) will be considered:

$$R.S.D.C. = \frac{dk}{k} \Big/ \frac{d\rho}{d\rho} \quad \text{for } \rho = \rho_N$$

or

$$R.S.D.C. = \frac{\rho_N}{k}\frac{dk}{d\rho} \quad \text{for } \rho = \rho_N \tag{3.39}$$

Earlier studies, e.g. by Kiefhaber [17] and Jirlow [18], give the qualitative dependence of k on the steam-density for large burn-up as plotted in figure 8. The S.D.C. and R.S.D.C. have to be calculated with the help of the tangent on this curve at normal steam-density.

The simpliest way to determine this tangent sufficiently accurate is to assume that $k = k(\rho)$ is linear in the interval $\rho_N - \delta\rho < \rho < \rho_N + \delta\rho$ and to calculate the reactivity effects $\Delta k(-\delta\rho)$ and $\Delta k(+\delta\rho)$ with the help of successive k calculations or with a perturbation code. $\delta\rho$ has to be chosen in a way that minimum errors are introduced by

a) the linear approximation of $k(\rho)$ in the interval $\rho_N - \delta\rho < \rho < \rho_N + \delta\rho$

b) in the case of successive k-calculations

the uncertainty in

$$\Delta k = k(\rho_N+\delta\rho) - k(\rho_N-\delta\rho)$$

caused by the truncation error in the calculation of the multiplication factor $k(\rho)$.

The linearity may be expressed in the value

$$p = \frac{k(\rho_N+\delta\rho)-k(\rho_N)}{k(\rho_N)-k(\rho_N-\delta\rho)} \qquad (3.40)$$

For exact linearity in the interval considered $p=1$. (Equation (3.40) only is valid if $\frac{dk}{d\rho}$ has no maximum or minimum in the interval considered.)

3.4.3. Loss of coolant reactivity

The loss of coolant reactivity is defined by

$$\Delta k_L = k(\rho=o)-k(\rho=\rho_N) \qquad (3.41)$$

In this study only one group constant set is used: the KFK-SNEAK set with the weighting spectrum of a large steam-cooled reactor with approximately $\rho=\rho_N$.

However, the calculation of the parameter Δk_L is complicated by the hardening of the neutron energy spectrum due to the loss of the (moderating) coolant. For an exact multi-group calculation using the same basic nuclear data, different group constant sets would be required for the cases $\rho=o$ and $\rho=\rho_N$ in order to take into account for the neutron spectrum hardening

Application of only one group constant set may introduce considerable errors in the absolute value of Δk_L. However, it may be expected that the influence of the cross-section uncertainties on this parameter Δk_L may be studied rather well with one-group constant set.

3.4.4. Ratio of the fertile to fissile material

The ratio $y = \frac{\text{volume fraction of fertile material}}{\text{volume fraction of fissile material}}$

is varied in order to keep the reactor critical after the cross-section variations.

The value of $\frac{1}{1+y}$ is a significant measure for the amount of fissionable material required.

3.4.5. Conversion ratio of the core

As measures for the breeding quality of a reactor or of parts of it the following quantities may be defined

a) breeding ratio of volume V of a reactor with volume R

$$B.R.(V) = \frac{\int_V dV \int_E dE \; {}^{FERT}\Sigma_\gamma(\bar{x},E)\;\phi(\bar{x},E)}{\int_R dV \int_E dE \; \{{}^{FISS}\Sigma_\gamma(\bar{x},E)+{}^{FISS}\Sigma_f(\bar{x},E)\}\phi(\bar{x},E)} \qquad (3.42)$$

b) conversion ratio of volume V of a reactor with volume R

$$C.R.(V) = \frac{\int_V dV \int_E dE \; {}^{FERT}\Sigma_\gamma(\bar{x},E)\,\phi(\bar{x},E)}{\int_V dV \int_E dE \; \{{}^{FISS}\Sigma_\gamma(\bar{x},E)+{}^{FISS}\Sigma_f(\bar{x},E)\}\phi(\bar{x},E)} \qquad (3.43)$$

FERT all fertile materials

FISS all fissile materials

With fundamental mode calculations a good approximation of the conversion ratio of the core may be obtained by calculating the ratio of the captures per volume unit in the fertile material to the absorption per volume unit in the fissile material.

$$C.R. = \frac{\sum_i FERT_{\Sigma_\gamma^i}\,\phi_i}{\sum_i (FISS_{\Sigma_\gamma^i} + FISS_{\Sigma_f})\phi_i} \qquad (3.44)$$

The influence of the cross-section uncertainties on the conversion ratio of the core may be examined rather well with the help of the C.R. from equation (3.44) and fundamental mode calculations for the fluxes.

4. THE UNCERTAINTIES OF THE CROSS-SECTIONS OF THE MATERIALS IN THE REACTOR CONSIDERED

4.1. Materials and cross sections considered

4.1.1. Materials

The D-1 design includes the following materials

Fuel: PuO_2 and UO_2 with the following isotopes

Pu^{239}, Pu^{240}, Pu^{241}, Pu^{242}, U^{238} and in a very small amount U^{235}.

Structural materials: Cr, Fe, Mo, Nb, Ni and in a small amount Al.

Coolant: Light water steam: H_2O

Also, the fission products of Pu^{239} are considered.

Al and U^{235} will not be considered here because of the very small amounts.

4.1.2. Cross sections

From similar studies on sodium-cooled reactors [19,20] it may be expected that the most important influence will be due to capture and fission cross-section uncertainties. Moreover, in this chapter the uncertainties of the total inelastic scattering cross sections and of ν for Pu^{239} will be considered.

Not considered are the uncertainties of the resonance parameters of the fuel materials. The latter may be important for the Doppler coefficient calculations with the help of the method of Froelich (chapter 3.4.1.1)

4.2. Basic group constant set

As basic group constant set the KFK-SNEAK set was used. The energy spectrum is divided into 26 groups. The group boundaries are the same as in the Russian ABN set [8]. For some less important materials the group constants of the KFK-SNEAK set are taken from the ABN set.

The KFK-SNEAK set was chosen for the following reasons:

a) Recent nuclear data are incorporated for the most important reactor materials.

b) For the calculation of the group constants the expected neutron energy spectrum of a steam-cooled fast reactor is used, namely the calculated spectrum of the SNEAK 3A-2 core with an equivalent steam-density as in the large reactor (ρ=0.07 g/cm^3) [7].

4.3. Sources of information for the evaluation of the data uncertainties

The basic source of information was KFK 120 part I by J.J. Schmidt [21].

For the higher Pu isotopes and the structural material Nb, in this reference no data are available. Here, BNL 325 second edition [22] and evaluations by Yiftah et al [23] and Pitterle et al. [24] were used.

In addition for some materials recent publications were considered.

a) For Pu^{239} the effect of recent α-measurements by Schomberg et al. [25] The latter result in remarkable uncertainties of α and σ_γ in the energy region 0.5 keV to 30 keV.

b) For Pu^{239} the effect of recent σ_f data for U^{235} by Beckurts et al. [26] on the normalization of σ_f measurements for Pu^{239} by White et al. [27] in the energy region 40 keV to 500 keV.

c) For U^{238} the effect of σ_γ measurements by Pönitz et al. [28]

4.4. Some aspects in the resonance energy region

In this energy region 3 subjects are important

a) Resonance parameters

b) Group constants

c) Self-shielding factors

4.4.1. Resonance parameters

The resonance region may be divided into

- region with resolved resonances
- " " unresolved resonances

The unresolved resonances may be

- not or only weakly overlapping
- considerably overlapping
- strongly overlapping

The resolved resonances may be described well by the single level Breit-Wigner formula. For a resonance at energy E_r:

$$\sigma_x(E) = 4\pi\lambda^2 g \frac{\Gamma_n^r \Gamma_x^r}{\Gamma_T^{r\,2}} \frac{1}{\left(\frac{E-E_r}{\Gamma_T^r/2}\right)^2+1} \qquad (4.1)$$

with

λ	reduced neutron wave length
g	statistical factor
Γ_f	halfwidth for fission
Γ_γ	" " capture
Γ_n	" " scattering
Γ_T	total halfwidth ($\Gamma_T=\Gamma_f+\Gamma_\gamma+\Gamma_n$)

It was shown (see [12]) that the unresolved resonances have the same properties as the resolved ones.

For the following parameters of the resolved resonances statistical distributions are determined:

$\bar{D}$	mean distance between resonances of the same type
$\bar{\Gamma}_x$	mean halfwidths ($x=n,\gamma,f$)

These parameters are extrapolated to the region with unresolved resonances. Generally, the resonance parameters still have considerable uncertainties.

4.4.2. Group constants and self-shielding factors

In the SNEAK set the group constants are arranged as described in chapter 3.2.

In the region of the unresolved resonances the group cross-section constants ${}^{K}\sigma_x^i(\infty,o)$ are calculated from microscopic nuclear data, while the self-shielding factors ${}^{K}f_x^i(\sigma_o,T)$ are calculated from the resonance parameters.

In the region of resolved resonances both factors are calculated from the resonance parameters.

The uncertainties in the group constants are dependent on

a) approximations of the calculation method
b) uncertainties of the nuclear data
   - microscopic data
   - resonance parameters

Generally, uncertainties due to approximation methods have to be small with respect to the uncertainties caused by the nuclear data.

On the dependence of group constants and selfshielding factors on the resonance parameter uncertainties only few publications are available.

In the region of resolved resonances it is possible to estimate the influence of the uncertainties with the help of the unshielded mean group cross-section

$$\langle\sigma_x\rangle^i = \frac{1}{\Delta E_i}\int_{\Delta E_i}\sigma_x(E)dE \qquad x=\gamma,f \qquad (4.2)$$

using in $\sigma_x(E)$ the single level Breit-Wigner formula (4.1) for the resonances.

However, in the more important region of the statistical resonances the situation is more complicated. Uncertainties may be introduced in 2 ways:

a) due to the standard deviations of the statistical distributions
b) due to the uncertainties in the parameters of these distributions.

Recently, Müller [29] did some investigations on this matter. He calculated the effect of some resonance parameter variations of U^{238} on the group constant $\langle\sigma_\gamma\rangle$. His estimations of the uncertainties vary from 10% at 1 keV to 20% at 100 keV. Here, in accordance with estimations of J.J. Schmidt [21] 20% uncertainty is assumed for all energies.

4.5. Evaluation of the cross section uncertainties

4.5.1. Pu^{239}

Pu^{239} is the main fissile material of the D-1 design. However, due to lack of measurements and to systematic deviations in available data the cross sections of this material still have rather large uncertainties. Moreover, recently some experimental data were reported considerably deviating from the formerly recommended values

a) Arnold et al. [30] reported for a steam cooled fast reactor lattice, with an energy spectrum similar to the spectrum of the D-1 design (figure 9) a mean value for α

$$\bar{\bar{\alpha}} = \frac{\langle\sigma_\gamma\rangle}{\langle\sigma_f\rangle} = 0.57 \pm 0.13$$

being significant larger than the calculated value $\bar{\bar{\alpha}} = 0.3873$.

As comparison, calculations for the D-1 design give

- with the ABN set $\bar{\bar{\alpha}} = 0.329$
- " " KFK-SNEAK set $\bar{\bar{\alpha}} = 0.325$

b) Schomberg et al. [25] found with a new experimental method much larger values of α in the energy region 0.5 keV to 50 keV (preliminary results not corrected for multiple scattering).

The results of Schomberg et al. are taken into account in the following way (figure 10):

Because these preliminary results are probably too high as upper limit in α an average curve through the experimental values is chosen instead of a curve through the upper uncertainty limits of the measurements.

Since the true α-values in this energy region are very probably higher than the α-values of the KFK-SNEAK set the latter are chosen as lower limits.

The uncertainty of σ_γ is obtained by combining the uncertainties of σ_f and α because σ_γ is to be calculated indirectly from σ_f and α-measurements. Large uncertainties result in the energy region 0.5 keV to 5o keV.

The uncertainties of σ_f are mainly taken from KFK 120/I with one complication in the energy region 30 keV to 500 keV.
In this region the SNEAK set contains the data of White et al. [27] being considerably lower than the recommended values in KFK 120/I. As upper uncertainty limit the upper limits of σ_f in KFK 120/I are chosen. The lower limit of the uncertainties is obtained by the following renormalization of the White data:

The σ_f measurement for Pu^{239} of White is relative to the σ_f of U^{235}. White has calculated ${}^{49}\sigma_f$ *) with the help of his values for ${}^{25}\sigma_f$. Recently, Beckurts [26] has recommended new, smaller values of ${}^{25}\sigma_f$. These smaller values lead to smaller values of ${}^{49}\sigma_f$.

For energy regions not mentioned, the uncertainty estimations of KFK 120/I are taken. This also was done for the inelastic cross section.

The estimated uncertainties are collected in tables 4.1 and 4.2.

4.5.2. U^{238}

U^{238} is the main fertile material in the reactor. As may be seen in figure 6 an important part of the captures is due to U^{238}. Moreover, in the energy region above 1.4 MeV the number of fissions of U^{238} is relatively large (figure 7).

The SNEAK set group constants are calculated with the last recommended data of KFK 120/I. In estimating the uncertainties only one more recent measurement of σ_γ by Pönitz et al. [28] in the energy region 25 keV - 500 keV had to be considered.

Between 40 keV and 200 keV KFK 120/I ascribes an uncertainty range of 20-30% for σ_γ. The Pönitz measurements are altogether within the lower uncertainty limit of 20%. Therefore, it appears to be reasonable to assume an uncertainty of 20% in this region.

For other energies the (mean) values of the KFK 120/I uncertainties are taken. The uncertainties collected are given in table 4.3.

*) The left upper index 49 comes from ${}_{94}Pu^{239}$, 25 from ${}_{92}U^{235}$ etc.

4.5.3. Structural materials

Figure 5 shows the capture rates for the structural materials. The latter are of the order of 1-10% of the U^{238} capture rates except for Fe with smaller values. However, Ni has more dominating capture rates in the upper and lower energy regions.

The SNEAK group constants are obtained in the following way.
- Cr, Fe and Ni are calculated with the data of KFK 120/I
- Mo and Nb have the existing group constants of the ABN set.

For the structural materials no more important recent measurements became available in excess of those already considered in KFK 120/I.

So, the given uncertainty values of KFK 120/I are taken over unchanged for Ni, Fe and Cr. For Mo and Nb the ABN data are compared with the data of KFK 120/I.

The missing uncertainty estimates for Fe in the energy range 2 keV to 100 keV and for Ni in the region 1 keV to 200 keV are obtained by crude estimation from available data in KFK 120/I.

Above 1 MeV the capture of Ni and Fe is mainly due to (n,p) processes. So, the tabulated uncertainty values are those of $\sigma(n,p)$. For Cr the $\sigma(n,p)$ and σ_γ have about the same order of magnitude above 1 MeV. However, only a few information about $\sigma(n,p)$ is available. Therefore, the expected maximum uncertainty values for σ_γ are tabulated.

For Nb the uncertainties are determined by comparing the ABN and BNL 325 data.

Capture Nb

Above 1 MeV only few BNL 325 data are given. However, the capture cross-sections in this region are very small. An arbitrary uncertainty of 20% is tabulated.

In the energy region 10 keV - 1 MeV comparison between ABN and BNL 325 data is possible. The ABN data are systematically somewhat higher. The upper and lower limits for the BNL 325 data are obtained by curves through the extreme values of the plotted measurements.

Below 1 keV a comparison between ABN and BNL 325 data is difficult because BNL 325 gives resolved resonance parameters and the ABN data are group constants. Again, an arbitrary uncertainty of 15% is chosen.

Below the first resonance at 35.8 eV the uncertainty is equal to the uncertainty at thermal energy being ±5%.

Inelastic scattering Nb

Comparison of BNL 325 and ABN data in the energy region below 2.5 MeV only shows a significant deviation in group 4 (1.4 MeV to 2.5 MeV). The ±15% uncertainty of BNL 325 in this region is tabulated. In group 4 the ABN value is compared with the BNL 325 limits.

Above 2.5 MeV no comparison is possible. An arbitrary uncertainty of 10% is tabulated because at these high energies the inelastic scattering cross-sections generally are rather accurate.

The uncertainties collected for the structural materials are given in tables 4.4, 4.5 and 4.6

4.5.4. Higher Pu isotopes

In KFK 120/I no data for the higher Pu isotopes were considered. The SNEAK set contains the same group constants as the ABN set.

The uncertainty evaluation is done with the help of BNL 325 [22] and of evaluations of Yiftah et al. [23] and Pitterle et al. [24]

For energies below 1 keV only resonance parameters with uncertainties are available what means that comparison of the recommended data with the ABN data is difficult.

Above 1 keV in the papers of Yiftah and Pitterle curves for fission and capture cross-sections are given. Here the comparison between these data and the ABN data is easier to do.

The uncertainty of group constants calculated from resonance data is described already in chapter 4.4.2. Because there are less measurements for the higher Pu isotopes a reasonable estimation for the uncertainties seems to be

±15% below 1 keV
±25% for group constants calculated with resonance parameters for energies above 1 keV

For energies above 1 keV, the evaluation is done per isotope.

4.5.4.1. Pu^{240}

Pu^{240} may be considered to be the most important higher Pu isotope. Several studies indicate its influence on safety coefficients, e.g. the recent studies of Kiefhaber[17] and Jirlow [18].

Yet, the difference between the ABN data and the recent evaluations of Yiftah et al. and Pitterle et al. are considerable.

Figure 11 shows the evaluations of Yiftah, Pitterle and the ABN group constants.

As upper and lower limits for the group constants are determined

a) Capture

In the energy region E>1 keV
upper limit: the ABN data
lower limit: the modified ENDF/B data of Pitterle

In the energy region below 1 keV
upper limit: the ABN data
lower limit: the ABN data minus 30%

The latter is chosen since at 1 keV the modified ENDF/B value is about 30% smaller than the ABN value.

b) Fission

Above 465 keV the uncertainty bars in the paper of Yiftah are used for the determination of the upper and lower limits for the uncertainty.
In the energy region 10 keV<E<465 keV ±20% uncertainty in the data of Yiftah is assumed. Below 10 keV the modified ENDF/B and the ENDF/B data of Pitterle are used as upper and lower limits respectively.
For the average number of neutrons per fission $\bar{\nu}$ the expression of Yiftah was used

$$\bar{\nu} = 3.00 + 0.101\ E \qquad E \text{ in MeV}$$

The upper and lower limits for the group constants are tabulated in table 4.7.

4.5.4.2. Pu^{241}

a) Capture

The capture cross-section data of Yiftah are partly (1 keV<E<50 keV) calculated from resonance parameters and partly taken equal to σ_γ of Pu^{239} (E>50 keV) because of the convergence of $^{49}\sigma_\gamma$ and $^{41}\sigma_\gamma$ below 50 keV.

However, it is very difficult to estimate reliable uncertainties for this evaluation particularly because of the large uncertainties of $^{49}\sigma_\gamma$.

The differences between ABN and Yiftah data are not significant. Only at the highest energies (the first energy groups) the cross-sections differ by a factor of about 2 (ABN larger). However, here the cross-sections are very small.

The uncertainty of the Yiftah data is estimated to be 30%. The uncertainties of the ABN data are obtained by comparing with the Yiftah limits.

b) Fission

The fission cross-section data of Yiftah are based on the evaluation of Davey[31]. The uncertainties estimated by Davey are

1 keV<E<40 keV	15%
40 keV<E<10 MeV	10%

These values were considered as upper and lower limits for the Yiftah data. The uncertainty of the ABN data is obtained by comparing the latter with the limits of the Yiftah data.

Rather large deviations exist between ABN and Yiftah data.

1 keV<E<100 keV	ABN data	20-30% larger
500 keV<E< 10 MeV	" "	20-30% smaller

The estimated uncertainties are collected in Table 4.7.

4.5.4.3. Pu^{242}

a) Capture

The capture data of Yiftah in the energy region 1 keV<E<1 MeV are calculated from the resonance parameters. This curve converges with increasing energy to the $^{28}\sigma_\gamma$ curve.

Above 1 MeV, $^{42}\sigma_\gamma$ is taken equal to $^{28}\sigma_\gamma$.

An arbitrary uncertainty of 25% is estimated for the Yiftah data.

The uncertainty limits of the ABN data are obtained with the help of comparison of the ABN data with the Yiftah limits.

b) Fission

The fission cross section data of Yiftah are taken from Davey (31) in the energy region 1 keV<E<1.7 MeV. This evaluation of Davey is only based on one measurement with a claimed accuracy of about 10%.

Above 2 MeV the fission cross-section of Pu^{242} is chosen equally to those of Pu^{240}. In this region an arbitrary uncertainty of 20% is assumed. This means that the ABN data are about equal to the lower Yiftah limits.

The estimated uncertainties are collected in table 4.8.

4.5.5. Hydrogen and oxigen

For hydrogen all nuclear data uncertainties are 1-2% or smaller.

For oxigen σ_γ is negligible. Cross-sections for other capture processes, e.g. (n,α), are only important at high neutron energies. The uncertainty is about ±20%.

The inelastic scattering of oxigen occurs only above 6.5 MeV and has an uncertainty of about ±30%.

4.5.6. The fission products of Pu^{239}

For the fission products the KFK-SNEAK set still contains the ABN data. For every fissionable material one pseudo fission product is available.

At Kernforschungszentrum Karlsruhe, Hakansson [32] has determined 2 pseudo fission products for Pu^{239}. The first one collects the fission products with relative fast removal by decay or neutron capture while the second one collects the other fission products. This division into 2 classes is made in order to be able to study the effect of"fission product burn-up" being only significant for the first class. Moreover, Hakansson has calculated his group constants with the help of the neutron energy spectrum both of a steam-cooled and a sodium-cooled fast breeder reactor instead of the Fermi spectrum for the ABN set.

Table 4.9 shows the comparison of the ABN data with the data of Hakansson combined in one pseudo fission product. Above 100 eV the data of Hakansson are considerably smaller, below 100 eV much larger than the ABN data.

The effect of fission product cross-section uncertainties may be studied by changing the ABN data by the Hakansson data.

Table 4.1: Data uncertainties of Pu^{239}

Group	Energy range	Fission +%	Fission -%	$\alpha = \sigma_c/\sigma_f$ +%	$\alpha = \sigma_c/\sigma_f$ -%	Capture +%	Capture -%	$\bar{\nu}$ +%	$\bar{\nu}$ -%
1	6.5-10.5MeV	7	7	20	20	20	20	2	2
2	4.0-6.5	7	7	20	20	20	20	2	2
3	2.5-4.0	7	7	20	20	20	20	2	2
4	1.4-2.5	7	7	20	20	20	20	2	2
5	0.8-1.4	7	10	10	10	12	15	2	2
6	0.4-0.8	10	10	10	10	15	15	1	1
7	0.2-0.4	10	10	10	10	15	15		
8	0.1-0.2	15	10	10	10	20	15		
9	46.5-100keV	20	7	15	15	25	20		
10	21.5-46.5	20	7	30	0	40	10		
11	10.0-21.5	10	10	80	0	80	10		
12	4.65-10.0	20	20	100	0	100	20		
13	2.15-4.65	20	20	100	0	100	20		
14	1.0-2.15	20	20	80	0	80	20		
15	0.465-1.0	20	20	70	0	75	20		
16	215-465eV	20	20	40	0	45	20		
17	100-215	20	20	25	0	30	20		
18	46.5-100	20	20	20	20	30	30		
19	21.5-46.5	20	20	20	20	30	30		
20	10.0-21.5	20	20	20	20	30	30		
21	4.65-10.0	15	15	20	20	25	25		
22	2.15-4.65	15	15	20	20	25	25		
23	1.0-2.15	15	15	20	20	25	25		
24	0.465-1.0	7	7	20	20	20	20		
25	0.215-0.465	7	7	10	10	15	15		
26	0.0252	2	2	3	3	3	3	1	1

Table 4.2: Inelastic scattering cross-section uncertainty of Pu^{239}

Group	Energy range	inelastic scattering +%	inelastic scattering -%
1	6.5MeV-10.5MeV	20	20
2	4.0 - 6.5	20	20
3	2.5 - 4.0	20	20
4	1.4 - 2.5	20	20
5	0.8 - 1.4	20	20
6	0.4 - 0.8	20	20
7	0.2 -0.4	50	50
8	0.1 - 0.2	50	50
9	46.5keV- 100keV	50	50
10	21.5 - 46.5	50	50
11	10.0 - 21.5	50	50

Table 4.3: Data uncertainties of U^{238}

Group	Energy range	Capture +%	Capture -%	Fission +%	Fission -%	inelastic scattering +%	inelastic scattering -%
1	6.5MeV-10.5MeV	10	10	10	10	15	15
2	4.0 -6.5	10	10	10	10	15	15
3	2.5 -4.0	10	10	15	15	15	15
4	1.4 -2.5	10	10	7	7	20	20
5	0.8 -1.4	10	10	7	7	15	15
6	0.4 -0.8	10	10	7	7	15	15
7	0.2 -0.4	20	20	7	7	15	15
8	0.1 -0.2	20	20			15	15
9	46.5keV-100keV	20	20			15	15
10	21.5 -46.5	20	20				
11	10.0 -21.5	20	20				
12	4.65 -10	20	20				
13	2.15 -4.65	20	20				
14	1.0 -2.15	20	20				
15	0.465 -1.0	15	15				
16	215 eV-465eV	|	|				
17	100 -215	|	|				
18	46.5 -100	|	|				
19	21.5 -46.5	|	|				
20	10.0 -21.5	|	|				
21	4.65 -10.0	|	|				
22	2.15 -4.65	|	|				
23	1.0 -2.15	15	15				
24	0.465 -1.0	2	2				
25	0.215 -0.465	2	2				
26	0.0252	1	1				

Table 4.4: Data uncertainties of Fe and Ni

Group	Energy range	Iron				Nickel			
		Capture		inelastic scattering		Capture		inelastic scattering	
		+%	-%	+%	-%	+%	-%	+%	-%
1	6.5MeV-0.5MeV	15	15	10	10	10	10	20	20
2	4.0 -6.5	15	15	20	20	20	20	20	20
3	2.5 -4.0	15	15	30	30	20	20	20	20
4	1.4 -2.5	25	25	25	25	10	10	20	20
5	0.8 -1.4	20	20	10	10	10	10		
6	0.4 -0.8	15	15			15	15		
7	0.2 -0.4	15	15			15	15		
8	0.1 -0.2	15	15			30	30		
9	46.5keV-100keV	100	70			100	40		
10	21.5 -46.5	100	70			150	10		
11	10.0 -21.5	100	70			∞	85		
12	4.65 -10.0	100	70			200	15		
13	2.15 -4.65	100	70			100	40		
14	1.0 -2.15	15	15			20	20		
15	0.465 -1.0	10	10			5	5		
16	215 eV-465eV	4	4						
17	100 -215								
18	46.5 -100								
19	21.5 -46.5								
20	10.0 -21.5								
21	4.65 -10.0								
22	2.15 -4.65								
23	1.0 -2.15								
24	0.465 -1.0								
25	0.215 -0.465								
26	0.0252	4	4			5	5		

Table 4.5: Data uncertainties of Mo and Cr

Group	Energy range	Molybdenum				Chromium			
		Capture		Inelastic scattering		Capture		Inelastic scattering	
		+%	-%	+%	-%	+%	-%	+%	-%
1	6.5MeV-10.5MeV	30	30	25	10	30	30	10	10
2	4.0 -6.5	25	25	30	0	25	25	10	10
3	2.5 -4.0	0	40	30	10	25	25	10	10
4	1.4 -2.5	0	30	25	25	25	25	20	20
5	0.8 -1.4	20	20	50	0	20	20	25	25
6	0.4 -0.8	20	20	50	0	20	20	25	25
7	0.2 -0.4	20	20	30	30	20	20		
8	0.1 -0.2	20	25			20	20		
9	46.5keV-100keV	30	30			30	30		
10	21.5 -46.5	50	0			30	30		
11	10.0 -21.5	60	0			30	30		
12	4.65 -10.0	60	0			20	20		
13	2.15 -4.65	50	0			20	20		
14	1.0 -2.15	40	0			20	20		
15	0.465 -1.0	15	15			20	20		
16	2.15eV-4.65eV	|	|			7	7		
17	100 -215	|	|			|	|		
18	46.5 -100	|	|			|	|		
19	21.5 -46.5	|	|			|	|		
20	10.0 -21.5	15	15			|	|		
21	4.65 -10.0	5	5			|	|		
22	2.15 -4.65	|	|			|	|		
23	1.0 -2.15	|	|			|	|		
24	0.465 -1.0	|	|			|	|		
25	0.215 -0.465	|	|			|	|		
26	0.0252	5	5			7	7		

Table 4.6: Data uncertainties of Nb

Group	Energy range	Capture +%	Capture -%	Inelastic scattering +%	Inelastic scattering -%
1	6.5MeV-10.5MeV	20	20	10	10
2	4.0 -6.5	20	20	10	10
3	2.5 -4.0	20	20	10	10
4	1.4 -2.5	20	20	30	0
5	0.8 -1.4	20	20	15	15
6	0.4 -0.8	10	25	15	15
7	0.2 -0.4	10	30	15	15
8	0.1 -0.2	10	40		
9	46.5keV-100keV	10	25		
10	21.5 -46.5	10	25		
11	10.0 -21.5	10	10		
12	4.65 -10.0	15	15		
13	2.15 -4.65	|	|		
14	1.0 -2.15	|	|		
15	0.465 -1.0	|	|		
16	215eV -465eV	|	|		
17	100 -215	|	|		
18	46.5 -100	|	|		
19	21.5 -46.5	15	15		
20	10.0 -21.5	5	5		
21	4.65 -10.0	|	|		
22	2.15 -4.65	|	|		
23	1.0 -2.15	|	|		
24	0.465 -1.0	|	|		
25	0.215 -0.465	|	|		
26	0.0215	5	5		

Table 4.7: Data uncertainties of Pu^{240} and Pu^{241}

Group	Energy range	Pu^{240} Capture MAX (barn)	Pu^{240} Capture MIN (barn)	Pu^{240} Fission MAX (barn)	Pu^{240} Fission MIN (barn)	Pu^{241} Capture +%	Pu^{241} Capture -%	Pu^{241} Fission +%	Pu^{241} Fission -%
1	6.5MeV-10.5MeV	0.01	0.005	2.2	1.8	0.003b	-	50	-
2	4.0 -6.5	0.02	0.01	1.6	1.4	-	50	30	-
3	2.5 -4.0	0.04	0.02	1.6	1.4	-	50	30	-
4	1.4 -2.5	0.09	0.05	1.6	1.4	-	50	30	-
5	0.8 -1.4	0.24	0.1	1.6	1.4	-	40	10	10
6	0.4 -0.8	0.26	0.1	0.7	0.5	100	10	20	10
7	0.2 -0.4	0.34	0.12	0.17	0.13	50	10	10	10
8	0.1 -0.2	0.45	0.15	0.12	0.08	50	10	10	10
9	46.5keV-100keV	0.65	0.26	0.09	0.07	100	-	-	20
10	21.5 -46.5	0.90	0.42	0.12	0.09	80	-	-	30
11	10.0 -21.5	1.30	0.60	0.11	0.09	50	20	-	40
12	4.65 -10.0	1.80	0.85	0.12	0.08	50	20	-	30
13	2.15 -4.65	2.70	1.3	0.20	0.07	30	30	-	30
14	1.0 -2.15	4.50	3.0	0.30	0.06	15	15	-	20
15	465eV -1000eV	6.50	4.5	0.40	0.06			15	15
16	215 -465	12.0	8.0						
17	100 -215	18.0	12.0						
18	46.5 -100	49.0	33.0						
19	21.5 -46.5	44.0	30.0						
20	10.0 -21.5	28.0	19.0						
21	4.65 -10.0	0.6	0.4						
22	2.15 -4.65	6.0	4.0	0.40	0.06				
23	1.0 -2.15	14250	10600	3.0	2.0				
24	0.465-1.0	1110	780	0.4	0.1				
25	0.215-0.465	160	120	0.05	0.02	15	15	15	15
26	0.0252	295	270	0.06	0.04	20	20	3	3

Table 4.8: Data uncertainties of Pu^{242}

Group	Energy range	Capture +%	Capture -%	Fission +%	Fission -%
1	6.5MeV-10.5MeV	0.01b	-	60	-
2	4.0 -6.5	30%	30%	60	10
3	2.5 -4.0	30	30	60	-
4	1.4 -2.5	30	30	50	-
5	0.8 -1.4	40	10	10	10
6	0.4 -0.8	70	10	10	10
7	0.2 -0.4	50	10	10	10
8	0.1 -0.2	40	20	10	10
9	46.5keV-100keV	50	20	10	10
10	21.5 -46.5	100	-	10	10
11	10.0 -21.5	100	-	10	10
12	4.65 -10.0	100	-	10	10
13	2.15 -4.65	70	20		
14	1.0 -2.15	15	15		
15	0.465 -1.0				
16	215eV -465eV				
17	100 -215				
18	46.5 -100				
19	21.5 -46.5				
20	10.0 -21.5				
21	4.65 -10.0				
22	2.15 -4.65				
23	1.0 -2.15				
24	0.465 -1.0				
25	0.215 -0.465	15	15		
26	0.0252	20	-		

Table 4.9: Comparison of the data by Hakansson with the ABN data for the fission products of Pu^{239}

Group	Energy range	σ^1_x HAKANSSON / σ^1_x ABN			
		σ_{TOT}	σ_γ	σ_{el}	σ_{in}
1	6.5MeV-10.5MeV	0.77	0.37	0.84	0.69
2	4.0 -6.5	0.75	0.37	0.78	0.70
3	2.5 -4.0	0.79	0.37	0.86	0.67
4	1.4 -2.5	0.84	0.41	0.93	0.64
5	0.8 -1.4	0.87	0.70	0.95	0.50
6	0.4 -0.8	0.90	0.83	0.95	0.37
7	0.2 -0.4	0.96	0.80	0.98	0.46
8	0.1 -0.2	0.99	0.89	0.98	0.51
9	46.5keV-100keV	1.03	0.86	1.03	
10	21.5 -46.5	1.01	0.96	1.01	
11	10.0 -21.5	1.11	0.90	1.12	
12	4.65 -10.0	0.96	0.80	0.97	
13	2.15 -4.65	0.89	0.85	0.89	
14	1.0 -2.15	0.99	0.95	1.00	
15	0.465 -1.0	0.87	0.95	0.85	
16	215eV -465eV	0.94	0.93	0.94	
17	100 -215	0.72	1.03	0.58	
18	46.5 -100	0.64	0.78	0.50	
19	21.5 -46.5	1.65	1.25	2.01	
20	10.0 -21.5	1.40	1.14	1.49	
21	4.65 -10.0	1.11	0.91	1.64	
22	2.15 -4.65	1.12	1.24	1.01	
23	1.0 -2.15	0.92	0.90	1.03	
24	0.465 -1.0	2.52	3.74	1.03	
25	0.215 -0.465	1.93	2.81	1.04	
26	0.0252	15.4	19.75	1.22	

5. THE METHODS APPLIED AND THE COMPUTER PROGRAMS USED FOR THE INVESTIGATIONS

For the selection of the calculation methods the following considerations were important:

a) The influence of the data uncertainties on the reactor parameters should be calculated for critical reactors. After every cross-section variation the reactor should be made critical again.

b) The investigations should be done with existing programs if possible.

c) The computing times required should be as moderate as possible.

The calculations were performed with the IBM 7074 digital computer situated at Kernforschungszentrum Karlsruhe. For the investigations of the influence of the data uncertainties on the reactor parameters computer programs developed by members of the Institut für Neutronenphysik und Reaktortechnik were used. Most of these programs are collected in the "Nuclear code system NUSYS" (33). The influence of the parameter variations on the stability and dynamic behaviour of the reactor (described in chapter 7) was investigated with programs developed by members of the Institut für Reaktorentwicklung.

5.1. The methods applied for the calculations of the reactor parameters

5.1.1. The Doppler coefficient

The Doppler effect was investigated by calculation of the multiplication factor k of the system at 2 temperatures 900°K and 2100°K. The reasons for this selection are:

a) For the higher Pu isotopes the Karlsruhe grouco file only contains self-shielding factors at 2 temperatures. For the temperature dependence of the D.C. often the relation D.C. = a/T is used. In this case the D.C. may be calculated with the multiplication factor at 2 temperatures and formula (3.37) (chapter 3.4.1.2.).

b) With the method selected effects of the whole energy region are considered. This is not the case with the method by Froelich (chapter 3.4.1.1.).

c) It is expected that the errors introduced by the fact that resonance parameters should be changed if the group cross sections are

varied in the resonance energy region will be smaller with the method selected than with the method of Froelich because the temperature dependence of the self-shielding factors $f(\sigma_o,T)$ is less dependent on the resonance parameters than the temperature derivatives $\frac{d\Sigma_x}{dT}$.

In chapter 7 a short comparison of results with the Doppler coefficient calculations described in chapter 3.4.1.1, 3.4.1.2 and 3.4.1.3 is given.

5.1.2. The reduced steam-density coefficient R.S.D.C.

The R.S.D.C. was determined with the help of the calculation of the multiplication factor k of the system for the steam-densities $(\rho_N-\delta\rho)$ and $(\rho_N+\delta\rho)$ (see chapter 3.4.2.). The R.S.D.C. is equal to

$$R.S.D.C. = \frac{\rho_N}{k} \frac{\{k(\rho_N+\delta\rho)-k(\rho_N-\delta\rho)\}}{2\delta\rho} \qquad (5.1)$$

For $\delta\rho$ was selected $\delta\rho = 0.01\ \rho_N$

The linearity in the interval $0.99\rho_N<\rho<1.01<_N$ is satisfactory. The value of $\hat{\rho}$ of formula (3.40) was about 1.01 in most cases.

The truncation error in the calculation of the multiplication factor was $\pm 1.10^{-6}$. For the basic group constant set the relative error in

$$\Delta k = k\ (1.01\rho_N) - k\ (0.99\rho_N)$$

is about 0.5%.

For the calculation of the R.S.D.C. no perturbation code was selected because in the NUSYS system only a one-dimensional code was available. The latter requires toomuch computing time. This code was only used for the investigation of the energy dependence of the R.S.D.C.

5.1.3. The loss of coolant reactivity Δk_L

As described in chapter 3.4.3., Δk_L was determined with the help of the calculation of the multiplication factor for the steam-densities $\rho=o$ and $\rho=\rho_N$. For this calculation only one group constant set was used.

5.1.4. The conversion ratio of the core

The calculation of the C.R. of the core was approximated with the help of formula (3.44) and fundamental mode calculations for the flux.

5.2. Subdivision of the energy region

The effects of variation of several cross-sections of several materials have to be considered. The calculations are performed with multi-group calculations using 26 groups.

Each of the group constants has an uncertainty and also a certain effect on the parameters considered. With the calculation methods applied it was impossible to consider the effect of each group constant separately. So a suitable subdivision of the energy region was necessary.

This subdivision of the energy spectrum was based on properties of the nuclear data and of the system observed. Moreover, during the calculations it seemed that some subdivisions should be performed or could be omitted.

The following properties were considered:

5.2.1. Nuclear data

5.2.1.1. In different energy regions certain processes are dominant. For an isotope with resonances, for example

a) region below resonances
b) region with resolved resonances
c) region with unresolved (statistical) resonances
   - weakly overlapping resonances
   - considerably overlapping resonances
   - strongly overlapping resonances
d) region above resonances
   (the resonance effect is not noticeable any more)

5.2.1.2. In different energy regions the nuclear data are determined by different methods or experimental groups or laboratories. In this case attention should be paid to determine systematical errors.

5.2.2. The system observed

With respect to the energy spectrum subdivision important properties of the system are:

a) The energy spectrum of the flux and of the adjoint flux (figures 3,4).

b) The energy dependence of the most important reaction rates (figures 5,6,7).

Since the energy dependence of the flux is much stronger than of the adjoint flux, the flux energy dependence is most siginificant.

In this study most attention is paid to the D.C. and to the R.S.D.C. So, analyses of these parameters may give important information too. Figures 12 and 13 show the energy dependence of these parameters.

The investigations have started with the following energy spectrum subdivision:

1) 1.4 MeV<E<10.5 MeV or group 1 to 4,
   because
   a) energy region above resonances
   b) main energy region of the fission neutrons
   c) decreasing flux and reaction rates

2) 46.5 keV<E<1.4 MeV or group 5 to 9,
   because
   a) flux and reaction rates at maximum
   b) most influence on the Doppler effect below 46.5 keV
   c) energy dependent contributions to the R.S.D.C. change sign between group 9 and 10 (figure 13).

3) 46.5 eV<E<46.5 keV or group 10 to 18,
   because
   a) main energy region for the Doppler effect
   b) region with large uncertainties in σ_γ of Pu^{239}
   c) flux and reaction rates still large
   More detailed calculations showed that in this energy range the groups 15 to 18 were dominant for the influence on the R.S.D.C.

Therefore, this region was further divided.

3-A 1 keV<E<46.5keV or group 10 to 14
3-B 46.5 eV<E< 1 keV of group 15 to 18

4) E<46.5 eV or group 19 to 26,
because
a) below main region for the Doppler effect
b) in this energy range the flux and reaction rates are relatively small.

For the materials U^{238} and Pu^{239} the energy region 46.5 eV to 46.5 keV (group 10 to 18) was examined more extensively. For the less important materials the subdivision of the energy spectrum was kept less detailed.

5.3. The computer programs used

5.3.1. The calculation of the reactor parameters

For the investigation of the influence of the cross-section uncertainties on the reactor parameters mainly the multiplication factor k for different states of the reactor is to be calculated. The latter was done with programs of the NUSYS system.

Program 446 by Sanitz enables the calculation of the macroscopic cross-sections of the system taking into account the self-shielding effect. The multiplication factor in the fundamental mode approximation was calculated with program 352 by Ferranti and Kraetsch giving k with a truncation error of 10^{-6}.

Some calculations with one-dimensional approximation of the diffusion equation were done with program 6731 by Sanitz and Woll.

After each variation in the group constant set the reactor was made critical by variation of the ratio y (fertile to fissile material). This was done with the iteration program 2210 by Bachmann.

For the determination of the conversion ratio of the core the components of formula (3.44) were calculated with the evaluation program 447 by Sanitz.

5.3.2. The variation of the group constant set

If a group cross-section changes several other group constants may change too (e.g. Σ_f^i variation influences also $\nu\Sigma_f^i$, Σ_{rem}^i and Σ_{tr}^i). In order to maintain the relations between the group constants 2 programs were available:

a) NUSYS program 4840 by Langner.
In this program all group constants for infinite dilution are modified except for ${}^K\Sigma_{tr}$. The possibility for changing the latter is available separately.

For each NUSYS run the group constants have to be modified again.

b) Program 2229 by Bachmann
With this program a new tape with group constants is arranged. Both group constants for infinite dilution and self-shielding factors for the removal and transport cross-sections are modified.

The main difference between the 2 programs is the treatment of Σ_{tr}. Indeed, the determination of Σ_{tr} for the multi-group diffusion calculations is not well defined because of the weighting procedure. Moreover, variation of Σ_f and Σ_γ between extreme limits may introduce Σ_t variations out of the uncertainty range of the latter if the balance

$$\Sigma_t = \Sigma_\gamma + \Sigma_f + \Sigma_{in} + \Sigma_e$$

is maintained.
Comparison of the methods showed only very small differences in the parameters considered.

Mainly for reasons of computing time required the second method by Bachmann is being used for most calculations.

The variation of the total macroscopic cross-sections was done with NUSYS program 4837 by Langner. The latter has the same features as program 4840.

6. THE INFLUENCE OF THE DATA UNCERTAINTIES ON THE REACTOR PARAMETERS

6.1. Macroscopic cross-section variations

In order to obtain some general information about the influence of cross-section uncertainties on the reduced steam-density coefficient (R.S.D.C.) and the Doppler coefficient (D.C.) the effect of 10% increase of the macroscopic cross-sections for capture and fission was considered. Only, fundamental mode calculations were made and the variations were performed in several energy regions. Table 6.1 shows the effects calculated. Presented are relative deviations determined with the formula

$$\frac{\delta X}{X} = \frac{|X_{new}| - |X_{normal}|}{|X_{normal}|} \cdot 100\% \; ; \quad X \equiv \begin{cases} Y \\ \Delta k(\Delta T) \text{ (D.C.)} \\ \text{R.S.D.C.} \end{cases} \qquad (6.1)$$

$\frac{\delta X}{X} = +1\%$ for the negative D.C. and R.S.D.C., means that the new calculated value of $|X|$ is 1% larger. The D.C. and R.S.D.C. are more negative.

Variation in the group	Relative deviations determined with form.(6.1)					
	Macrosc.capt.cross-sect.+10%			Macrosc.fiss.cross-sect.+10%		
	Y (%)	RSDC(%)	$\delta\Delta k(\Delta T)$(%)	Y (%)	RSDC(%)	$\delta\Delta k(\Delta T)$(%)
1-9	-2.7	-9.1	-2.9	+8.7	+14.6	+1.1
5-9	-2.2	-9.5	-2.5	+5.6	+19.2	+0.7
10-18	-5.8	+31.9	-6.3	+5.8	-27.5	+5.2
10-14	-3.9	+1.3	-4.2	+3.6	+4.4	+0.9
15-18	-2.1	+30.3	-2.3	+2.3	-32.7	+4.3
18-26	-0.3	+11.0	-1.8	+0.3	-10.9	+1.7
1-26	-8.5	+32.3	-9.4	+15.2	-22.5	+8.0

Table 6.1

From these calculations follows

a) The influence of group cross-section variations is larger for the R.S.D.C. than for the D.C.

b) The effects due to capture and fission cross-section variations are of the same order of magnitude. However, with opposite sign.

c) The effect of variations of a cross-section over the whole energy region is in rather good agreement with the sum of the effects of variations in parts of it (the effects are rather well additional over the energy region).

d) Cross-section variations at high and low energies have effects with opposite sign on the R.S.D.C. and with the same sign on the D.C.

e) The influence on the R.S.D.C. of variations in the energy regions 50 eV to 1 keV (group 15 to 18)and 50 keV to 1 MeV (group 5 to 9) is remarkable.

In order to explain these effects qualitatively we have to examine the following aspects:

a) The effects due to cross-section variations.

b) The origin of the R.S.D.C. and the D.C. and the way the latter are influenced by the effects due to cross-section variations.

6.1.1. The effects due to cross-section variations. The main effects are:

a) Change of the quantity of fissile material required.

b) Changes in the flux and adjoint flux spectrum.

Since in this study mainly the influences of capture and fission cross-section variations are considered, here, only the effect of variations of these cross-sections is examined.

If in a just critical reactor the capture cross-section increases or if the fission one decreases at some energy, the reactor will become sub-critical because less neutrons are available for the multiplication process. In order to keep the reactor critical the amount of fissile material is increased (the ratio y between fertile and fissile material decreases).
For decreasing of the capture or increasing of the fission cross-section the effect is just inverse (increasing of y).

The flux $\phi(E)$ is a measure for the mean number of neutrons with energy E in the reactor.
The adjoint flux $\phi^*(E)$ may be considered to be the number of daughter neutrons of the neutron distribution due to a neutron put in the reactor with energy E.

The flux and adjoint flux spectrum are influenced by 2 effects:

a) The initial variation of the cross-sections

b) The variation of y (to keep the reactor critical) will influence the spectra considered because the energy dependence of the cross-sections of the different fuel materials (e.g. U^{238} and Pu^{239}) is not identical.

In a first approximation the flux in group i may be considered inverse proportional to the removal cross-section of this energy group and the adjoint flux proportional to the number of fission neutrons per absorption in group i.

$$\eta_i = \frac{\nu\Sigma_f^i}{\Sigma_f^i+\Sigma_\gamma^i}$$

Influence on the flux.

If the capture or fission cross section in group i increases the flux in this group will decrease relatively. The same occurs in groups with smaller energy because less neutrons come from group i. The relative decreasing of the flux in the latter groups is smaller than in group i because the hydrogen in the reactor enables "overscattering" (neutrons of group j with energy larger than group i ($j<i$) may be scattered to group $j+k$ with $j+k>i$).

Generally, variation of the cross section in group i mainly has influence on the flux in this group i and in groups with energy smaller than the energy in group i.

The dependence of the flux spectrum on the variation of y may be shown with the help of $\frac{\partial \Sigma_{rem}}{\Sigma_{rem}} / \frac{\partial y}{y}$, that is the relative variation of the removal cross-section with y variation. Figure 14 shows the energy dependence of $\frac{\partial \Sigma_{rem}}{\Sigma_{rem}} / \frac{\partial y}{y}$ for the D-1 design. With increasing y, Σ_{rem} decreases more for low energies than for the high ones. This means that for increasing y the neutron flux spectrum will become softer.

Influence on the adjoint flux.

If the capture cross section in group i increases the adjoint flux in this group will decrease (less daughter neutrons are produced by neutrons put in the reactor with energies of group i). Increasing of the fission cross-section has the opposite effect: more daughter neutrons and larger adjoint flux in group i. These effects described are also noticeable in the energy groups with larger energy than group i because neutrons put in the reactor with energies larger than group i result in a neutron spectrum with neutrons in group i. In the energy groups with smaller energies the adjoint flux is hardly influenced.

Analyses of the dependence of η on the variation of y did not show significant energy dependence of $\frac{\partial \eta}{\partial y}$. So, in a first approximation we may assume that the adjoint flux spectrum is not influenced significantly by the variation of y.

6.1.2. The origin of the D.C. and R.S.D.C. and the way the latter are influenced by the effects due to cross-section variations.

6.1.2.1. The Doppler coefficient D.C.

The Doppler effect is the reactivity effect caused by the temperature dependent variations of the cross-sections in the resonance region. The D.C. is dependent on the ratio between the capture and fission cross-section variations and on the relative magnitude of the flux and adjoint flux in the energy region where the cross-section temperature dependence

is significant. Since U^{238} has negative Doppler effect and Pu^{239} has none or a small positive one the total effect is dependent on the ratio between these materials (the ratio y).

In table 6.1 the variation of $\delta\Delta k(T=900\rightarrow2100)$ is identical with the variation of the D.C. We may observe that the D.C. variations have the same sign as the y variations in all calculated cases. This means that increasing of y results in a more negative D.C.

Dependent on other influences due to the cross-section variations, the change of the D.C. is larger or smaller than the change in y.

For variations in the energy region above 50 keV (group 1 to 9) the most significant second effect is the variation of the flux spectrum. Increasing of the capture and fission cross-sections in this energy region causes a relative decreasing of the flux in the resonance region, resulting in a less negative D.C. Both for the capture and fission cross-section variations this effect may be observed.

For variations in the energy region below 50 eV (group 19 to 26) the most significant second effect is the variation of the adjoint flux spectrum in the resonance region. Increasing of the capture cross-section below 50 eV results in decreasing of the adjoint flux above 50 eV (also in the important resonance region) and in a less negative D.C. Increasing of the fission cross section results in increasing of the adjoint flux in the resonance region and in a more negative D.C. Both effects may be observed.

In the energy region $50eV<E<50keV$ both effects due to flux and adjoint flux variations occur. A further significant effect in this region is the influence of the cross-section variation itself. In the calculation method applied the temperature dependence of the self-shielding factors is independent of the group cross-section variations. This means that in the case of increasing of the capture cross-section in the resonance region the D.C. will be more negative due to the larger difference between the cross-sections at $900^{\circ}K$ and $2100^{\circ}K$. The same holds for variations of the fission cross-sections in this region. However, now the D.C. will be less negative.

This effect may be observed in the case of variations in group 15 to 18.

6.1.2.2. Reduced steam-density coefficient R.S.D.C.

The R.S.D.C. is a measure for the reactivity effect due to variation of the steam-density. As for steam the absorption may be neglected practically the R.S.D.C. is mainly caused by the variation in the spectral distribution of the flux and adjoint flux due to the moderation changed. It may be noticed that the R.S.D.C. would be zero in the case of a constant adjoint flux over the whole energy region. In this case variation of the flux energy spectrum does not result in a reactivity effect.

Increasing of the steam-density has the consequence that the neutrons are moderated stronger. In the case where the adjoint flux decreases with decreasing energy the reactivity effect is negative (less neutrons are produced) while in the case of increasing adjoint flux with decreasing energy the reactivity effect will be positive. Moreover, the reactivity effect is proportional to the flux.

A good measure for the adjoint flux spectrum is the energy dependence of $\eta = \frac{\nu\Sigma_f}{\Sigma_f+\Sigma_\gamma}$. In figure 15 η and ϕ^+ are plotted as a function of the energy (for die D-1 design). For energies 10keV<E<10MeV η is decreasing with decreasing energy. This means that in this region for increased steam-density a negative reactivity effect may be expected.

In the energy region 100eV<E<10keV η increases with decreasing energy. The reactivity effect is expected to be inverse to the effect for energies E>10keV.

For energies below 100 eV η is fluctuating. However, in this region the flux has decreased considerably and the expected reactivity effect will be small. These qualitative considerations are in good agreement with results from perturbation calculations (see figure 13).

The influence of cross-section variations on the R.S.D.C. is dependent on the way its negative and positive components are changing:

These components may be changed mainly by:

a) Hardening of the neutron spectrum:
The negative component gets more importance and the R.S.D.C. will become more negative.

b) Variation of the course of the adjoint flux at energies above 10 keV:
Flattening results in a smaller negative component and the R.S.D.C. will be less negative.

c) Variation of the course of the adjoint flux at energies below 10 keV:
In this case flattening results in a smaller positive component and the R.S.D.C. will become less positive (or more negative).

d) Variation of the relative difference of the adjoint flux at energies above and below 10 keV:
If this difference decreases the R.S.D.C. will become less negative (or more positive).

With the help of these considerations the effect of cross-section variations on the R.S.D.C. may be explained qualitatively. Significant for the effects are the variations of the adjoint flux.

For one case the effect will be analysed in more detail.

10% increase of Σ_γ in the groups 5 to 9

The following effects occur:

a) γ decreases. The neutron flux spectrum becomes harder. The R.S.D.C. becomes more negative.

b) Due to the Σ_γ variations in the groups 5 to 9 the neutron flux spectrum becomes softer. The R.S.D.C. will become less negative.

c) Due to the Σ_γ variations the course of the adjoint flux in the energy range above 10 keV will become steeper. The R.S.D.C. becomes more negative.

d) Due to the Σ_γ variations the differences between the adjoint flux below and above 10 keV decrease. This effect results in a less negative R.S.D.C.

The points a) through d) show influences with opposite sign on the R.S.D.C. Namely, a negative variation of the R.S.D.C. due to the points a) and c) and a positive variation due to the points b) and d).

The calculations in table 6.1 give a positive change of the R.S.D.C.

Further analyses of the influence of the points a) through d) show that the main effect comes from the point d): the variation of the difference between the adjoint flux above and below 10 keV.

Some general remarks with respect to the influence of the cross-section variations on the R.S.D.C.:

a) Variations of the capture and fission cross-sections generally have opposite influence because the effects of these variations on the adjoint flux are opposite.

b) Variations in the groups 10 to 14 only have small not well defined influence for 2 reasons:
   - The relative variations in the adjoint flux are not very large. Moreover, both the positive and the negative components are influenced simultaneously. These effects counterbalance each other partly.
   - More extensive investigations of this energy region for material dependent cross-section variations showed that changes in the groups 10 to 12 have opposite effect with respect to variations in the groups 13 and 14.

c) Variations in the groups 5 to 9 have large influence since the effect on the negative component of the R.S.D.C. due to the changing difference between the adjoint flux above and below 10 keV is relatively large.

d) Variations in the groups 15 to 18 have large influence because the effect on the positive component of the R.S.D.C. due to the variation of the course of the adjoint flux below 10 keV is relatively large.

6.1.3. The maximum variation of the R.S.D.C. obtained by 10% changes of the macroscopic capture and fission cross-sections.

Finally, some group constants for capture and fission were changed by 10% in a way that

a) the variation of y was small

b) the R.S.D.C. became most positive and most negative.

Table 6.2 shows the variations performed. The calculated parameters with the variations of table 6.2 shows table 6.3.

Group		5-9	10-14	15-18
Most positive R.S.D.C.	Σ_γ^i	+10%	-	-10%
	Σ_f^i	-10%	+10%	+10%
Most negative R.S.D.C.	Σ_γ^i	-10%	-	+10%
	Σ_f^i	+10%	-10%	-10%

Table 6.2

	$\frac{\delta y}{y}$ (%)	$\frac{\delta \lvert RSDC \rvert}{\lvert RSDC \rvert}$ (%)	$\frac{\delta \lvert \Delta k(\Delta T) \rvert}{\lvert \Delta k(\Delta T) \rvert}$ (%)
Most positive R.S.D.C.	+0.44	-91.6	+3.7
Most negative R.S.D.C.	-0.37	+88.0	-4.7

Table 6.3

The influences appeared to be rather well additional.

Already from these calculations follows that the R.S.D.C. is very sensitive to cross-section uncertainties and may vary over a wide range.

6.2. The influence of the data uncertainties of the reactor materials

As described in chapter 2 the parameters considered are D.C., R.S.D.C., Δk_L, y and C.R.

The investigations of the influence of macroscopic cross-section variations (chapter 6.1.) showed that the R.S.D.C. is very sensitive to cross-section variations in the energy range where the Doppler effect is dominant. Therefore, the temperature dependence of the R.S.D.C. and the Δk_L is investigated too. The values calculated at 900°K and 2100°K with the KFK-SNEAK set are given in table 6.4.

T °K	R.S.D.C.	Δk_L
900	$-2.14 \cdot 10^{-2}$	$3.6384 \cdot 10^{-2}$
2100	$-2.58 \cdot 10^{-2}$	$4.3842 \cdot 10^{-2}$

Table 6.4

Evidently, the differences are rather large. The reason that the R.S.D.C. becomes more negative with increasing temperature may be explained by the influence of a temperature change on the adjoint flux spectrum. Increasing of the temperature causes increasing of the effective cross sections for capture and fission in the resonance energy range. Since the D.C. is negative the increasing of the effective capture cross-section is dominant. This means that in this energy region the adjoint flux decreases, resulting in a smaller positive component of the R.S.D.C. (see chapter 6.1.2.2.). At the time where the investigations of the influence of the data uncertainties were started the preparation of the KFK-SNEAK set was not yet completed entirely. The self-shielding factors of Pu^{239} were still taken from the ABN set. That is why most influences of group constant variations are calculated with respect to the KFK-SNEAK set with old f-factors for Pu^{239}.

In table 6.5 the parameters calculated with the old and new f-factors for Pu^{239} are given.

KFK-SNEAK set with	y	C.R.	Δk_L $ [m]		R.S.D.C.·10²		$A_D \cdot 10^{2}$ [mm]
			T=900°K	T=2100°K	T=900°K	T=2100°K	
Old f-factors for Pu^{239}	7.40758	0.9952	+12.96	+14.55	-2.52	-2.74	-1.0662
New f-factors for Pu^{239}	7.39310	0.9857	+11.30	+13.61	-2.14	-2.58	-1.3857

Table 6.5

[m] 1 $ \hat{=} 0.00322

[mm] A_D is the Doppler constant, assuming the temperature dependence D.C. = $\frac{A_D}{T}$

For the important parameters the differences are remarkable.

Since not all calculations could be done with the help of the final KFK-SNEAK set the results will be presented as absolute parameter variations. Only for the ratio y the relative deviation $\frac{\partial y}{y}$ is given.

The uncertainties of the most important cross-sections of the reactor materials are collected in the tables 4.1 to 4.9.

In the cases the upper and lower limits have the same deviation from the data of the KFK-SNEAK set usually only the effect of the upper limit is calculated.

Some comparison calculations showed that the absolute value of the effects due to equal positive and negative variations of the group constants are not the same exactly. However, the differences observed are relatively small.

For the inelastic cross section only the total value was varied. The transfer probabilities were kept constant. This means that with

$$\Sigma^i_{IN} = \sum_j \Sigma_{i \to j}$$

Σ^i_{IN} and $\Sigma_{i \to j}$ were varied in the same way.

The influence of the data uncertainties of Pu^{239} and U^{238} is investigated most extensively because the latter have the largest atom density of the materials with considerable data uncertainties.

The variations of the parameters D.C. and R.S.D.C. due to the data uncertainties show the same behaviour as the effects due to the macroscopic cross-section variations described in chapter 6.1.

6.2.1. Pu^{239}

The variations caused by the data uncertainties of Pu^{239} are collected in table 6.8. These deviations may be compared with the parameters of table 6.5.

The main influence on the parameters considered is due to the fission and capture cross section uncertainties in the energy range 50 eV to 10 keV. It also may be observed that the measurements of Schomberg et al. [25] influence the C.R. and the R.S.D.C. very unfavourably (see also chapter 7). The influence of the inelastic scattering uncertainties is small. Since the R.S.D.C. is important for the stability and the dynamic behaviour of the reactor and also very sensitive to cross-section variations the maximal expected influence on this parameter due to the data uncertainties of Pu^{239} is calculated (table 6.6).

Variations of σ_γ and σ_f of Pu^{239} in a way that	y	C.R.	Δk_L \$		RSDC·10^2		$A_D \cdot 10^2$
			T=900°K	T=2100°K	T=900°K	T=2100°K	
RSDC most positive	7.33667	0.9707	- 3.65	- 1.00	+1.365	+0.86	-1.6697
RSDC most negative	7.33477	0.8931	+31.57	+33.39	-6.455	-6.82	-1.0704

Table 6.6

6.2.2. U^{238}

Table 6.9 gives the variations due to the data uncertainties of U^{238}. The largest influences come from the capture cross-section uncertainties in the groups 5 to 9 and 15 to 18. It may be observed that for the variation in the groups 15 to 18 the influence on the D.C. by the variation of the ratio y is overcompensated by the increasing of the capture cross-section in the resonance region of U^{238} (compare with chapter 6.1.2.1.).

The influence of the inelastic cross-section uncertainties of U^{238} is small. For the other reactor materials the influence of the inelastic cross-section uncertainties will not be calculated.

The most negative R.S.D.C. caused by the data uncertainties of U^{238} is given in table 6.7.

Variation	y	C.R.	Δk_L, $		RSDC.10^2		$A_D \cdot 10^2$
			T=900°K	T=2100°K	T=900°K	T=2100°K	
For U^{238} σ_γ Min Gr. 1 to 11 Max Gr. 12 to 26	7.44384	0.9857	+18.14	+20.67	-3.36	-3.76	-1.5053

Table 6.7

6.2.3. The higher Pu isotopes

For the higher Pu isotopes less calculations are performed.
For the Pu^{240} the parameters are calculated for 3 cases.

a) With the data recommended by Yiftah (23)
b) With the minimum expected capture cross sections
c) With the data recommended by Pitterle (24) (MOD-ENDF/B)

With the data of Yiftah the D.C. and R.S.D.C. become slightly more unfavourable. Due to the smaller capture cross-sections the data of Pitterle give parameters conciderably more favourable.

For Pu^{241} the influences on the parameters are still considerably smaller. In some energy regions the influence of the largest data uncertainties is calculated. The same was done for Pu^{242}.

The results are collected in table 6.10.

6.2.4. The structural materials, the fission products and oxigen

The influence of the data uncertainties of Ni is examined in detail. For the other materials only one calculation is made. The influences observed are small. The results are collected in table 6.11.

Table 6.8

Variations	$\partial y/y$ (%) *)	$\delta C.R. \cdot 10^2$ *)	$\delta \Delta k_L$ % *)		$\delta RSDC \cdot 10^2$ *)		$\delta \Lambda_D \cdot 10^2$ *)
			T=900°K	T=2100°K	T=900°K	T=2100°K	
σ_γ MAX ALL GROUPS	-7.36	-6.98	+6.18	+6.00	-1.17	-1.15	+0.1846
σ_γ MAX GR 1- 4	-0.01	-0.01	0.0	+0.09	0.0	-0.01	0.0
σ_γ MAX GR 5- 9	-0.38	-0.97	-0.40	-0.25	+0.045	+0.05	+0.0049
σ_γ MAX GR 10-14	-4.12	-10.39	+2.07	+2.01	-0.155	-0.16	+0.1019
σ_γ MAX GR 10-11	-1.05	-2.96	-0.32	-0.32	+0.075	+0.07	+0.0185
σ_γ MAX GR 12-14	-3.11	-7.75	+2.34	+2.29	-0.225	-0.23	+0.0840
σ_γ MAX GR 15-18	-2.65	-5.34	+3.93	+3.83	-0.87	-0.86	+0.0692
σ_γ MAX GR 19-26	-0.28	-0.63	+0.47	+0.45	-0.205	-0.19	+0.0099
σ_γ MIN GR 12-18	+2.14	+4.86	-2.67	-2.61	+0.575	+0.59	-0.0517
σ_γ MIN GR 5-11	+0.49	+1.33	+0.27	+0.28	-0.055	-0.05	-0.0071
σ_f MAX ALL GROUPS	+5.08	+4.27	-3.56	-3.37	+0.91	+0.88	-0.1621
σ_f MAX GR 1- 4	+0.77	+0.23	-0.13	-0.13	+0.02	+0.02	-0.0018
σ_f MAX GR 5- 9	+6.89	+1.44	+3.85	+3.87	-0.735	-0.73	-0.0082
σ_f MAX GR 10-14	+5.91	+1.36	-0.56	-0.57	-0.14	-0.13	-0.0161
σ_f MAX GR 10-12	+3.35	+0.72	+1.29	+1.29	-0.285	-0.28	-0.0043
σ_f MAX GR 13-14	+2.56	+0.50	-1.89	-1.90	+0.145	+0.15	-0.0120
σ_f MAX GR 15-18	+4.15	+1.32	-6.07	-5.95	+1.43	+0.24	-0.0779
σ_f MAX GR 19-26	+0.51	+0.05	-0.86	-0.81	+0.375	+0.36	-0.0232
σ_f MIN GR 5-12	-6.00	-1.37	-2.90	-2.92	+0.575	+0.58	+0.0092
σ_{IN} MAX GR 1-11	-0.16	-0.12	-0.05	-0.05	+0.01	+0.01	-0.0011

*) For the values of the parameters see table 6.5
Influence of cross-section uncertainties of Pu^{239}

Table 6.9

Variation	$\partial y/y$ (%) *)	$\partial C.R. \cdot 10^2$ *)	$\delta\Delta K_L$, % *)		$\delta RSDC \cdot 10^2$ *)		$\delta A_D \cdot 10^2$ *)
			T=900°K	T=2100°K	T=900°K	T=2100°K	
σ_f MAX GR 1- 7	+1.73	+1.47	-0.42	-0.31	+0.06	+0.05	-0.0041
σ_γ MAX ALL GROUPS	-8.32	+7.16	+1.71	+1.75	-0.29	-0.34	+0.0285
σ_γ MAX GR 1- 4	-0.10	+0.03	+0.01	+0.01	0.0	0.0	+0.0009
σ_γ MAX GR 1- 9	-2.68	+1.44	-1.58	-1.63	+0.285	+0.28	+0.0383
σ_γ MAX GR 5- 9	-2.60	+1.82	-1.59	-1.63	+0.29	+0.28	+0.0375
σ_γ MAX GR 10-14	-4.72	+1.63	+1.30	+1.32	-0.055	-0.07	+0.0260
σ_γ MAX GR 15-18	-1.27	+1.14	+1.87	+1.99	-0.415	-0.46	-0.0762
σ_γ MAX GR 19-26	-0.13	+0.18	+0.29	+0.28	-0.125	-0.23	+0.0032
σ_{IN} MAX GR 1- 4	-1.48	-0.86	+0.16	+0.16	-0.015	-0.02	-0.0021
σ_{IN} MAX GR 1- 9	-1.79	-0.94	-0.22	-0.22	+0.05	+0.05	-0.0069

*) For the values of the parameters see table 6.5

Influence of cross-section uncertainties of U^{238}

Table 6.10

Material	Variation	$\partial y/y$ (%) a)	$\partial C_o R_o \cdot 10^2$ a)	$\delta\Delta k_L$ %		$\delta RSDC \cdot 10^2$ a)		$\delta A_D \cdot 10^2$ a)
				T=900°K	T=2100°K	T=900°K	T=2100°K	
Pu^{240}	DATA BY YIFTAH	+1.18	+0.99	+0.11	+0.12	-0.035	-0.04	-0.0093
	σ_γ MIN ALL GROUPS	+3.15	-2.56	-1.19	-1.13	+0.29	+0.29	-0.0663
	MOD.ENDF/B by Pitterle	+5.30	-0.77	-1.32	-1.23	+0.295	+0.30	-0.0856
Pu^{241}	σ_γ GR 1-9 MAX GR 10-26 MIN	-1.45	-0.42	+0.83	+0.78	-0.15	-0.13	+0.0316
	σ_f GR 1- 5 MAX	+0.10	0.0	-0.02	-0.02	-0.01	0.0	-0.0001
	σ_f GR 6-10 MIN	-0.42	-0.10	-0.33	-0.33	+0.055	+0.06	+0.0006
	σ_f GR 11-14 MIN	-0.74	-0.20	+0.14	+0.14	-0.15	-0.19	+0.0034
	σ_f GR 15-18 MAX	+0.20	+0.07	-0.30	-0.28	+0.065	+0.07	-0.0457
	σ_γ GR 1-26 MAX	-0.38	-0.93	+0.43	+0.37	-0.175	-0.14	+0.0237
	σ_γ GR 6-11 MAX	-0.08	-0.21	-0.05	-0.05	+0.01	+0.01	+0.0010
	σ_γ GR 12-26 MAX	-0.30	-0.36	+0.48	+0.45	-0.18	-0.16	+0.0238
Pu^{241}	σ_γ GR 1-11 MAX	-0.04	-0.04	-0.02	-0.02	+0.005	0.0	+0.0007
	σ_γ GR 12-26 MAX	-0.04	-0.03	+0.04	+0.04	-0.005	0.0	+0.0016
	σ_f GR 1- 6 MAX	+0.06	+0.05	-0.01	-0.01	0.0	+0.01	-0.0001

a) For the values of the parameters see table 6.5

Influence of the cross-section uncertainties of the higher Pu isotopes.

Table 6.11

Material	Variation	$\delta y/y$ (%) *)	$\delta C_e \cdot 10^2$ *)	$\delta\Delta K_L$, % *)		$\delta RSDC \cdot 10^2$ *)		$\delta A_D \cdot 10^2$ *)
				T=900°K	T=2100°K	T=900°K	T=2100°K	
Ni	σ_γ MAX GR 1-18	-1.68	-1.52	+0.04	+0.02	+0.02	+0.02	+0.0279
	σ_γ MAX GR 1- 4	-0.56	-0.46	+0.06	+0.05	-0.015	0.0	+0.0046
	σ_γ MAX GR 5- 9	-0.35	-0.34	-0.25	-0.26	+0.045	+0.05	+0.0047
	σ_γ MAX GR 10-14	-0.77	-0.72	+0.21	+0.20	-0.05	-0.01	+0.0175
	σ_γ MAX GR 15-18	-0.02	-0.01	+0.02	+0.02	+0.01	0.0	+0.0011
Nb	σ_γ MAX GR 1-17	-0.44	-0.36	+0.28	+0.27	+0.04	+0.04	+0.0148
Cr	σ_γ MAX GR 1-18	-0.15	-0.14	+0.02	+0.02	0.0	0.0	+0.0036
Fe	σ_γ MAX GR 1-18	-0.10	-0.09	-0.02	-0.02	+0.005	+0.01	+0.0019
Mo	σ_γ MIN GR 1-10 MAX GR 11-20	-0.69	-0.56	+0.74	+0.70	-0.12	-0.11	+0.0292
F.P.	DATA OF HAKANSSON	+0.75	+0.55	-0.17	-0.16	0.0	0.0	-0.0144
O	σ_γ MAX GR 1- 3 σ_{IN} MAX GR 1	-0.16	-0.16	+0.02	+0.02	-0.01	0.0	+0.0008

*) For the values of the parameters see table 6.5

Influence of the cross-section uncertainties of the structural materials, the fission products (F.P.) and oxigen.

7. THE INFLUENCE OF THE DATA UNCERTAINTIES ON THE SAFETY, STABILITY AND DYNAMIC BEHAVIOUR OF THE D-1 DESIGN

7.1. The safety, stability and dynamic behaviour of the D-1 design

At the Kernforschungszentrum Karlsruhe several extensive studies on these subjects were performed [34,35,36,37,38,39,40]. The most important aspects for this study are summarized here.

7.1.1. Safety

For the safety the Doppler effect and the loss of coolant reactivity are the most important parameters.
The Doppler effect is a relative large prompt negative reactivity effect. In the case of a reactor accident the energy released in an excursion depends strongly on the Doppler constant $T\frac{dk}{dT}$.
The loss of coolant reactivity Δk_L is one of the significant measures for the steepness of a reactivity ramp after a large disturbance in the cooling circuit (e.g. pipe ruptures).

7.1.2. Stability

The stability of the core and of the reactor plant (core with cooling circuit) are investigated separately.

Stability of the core

The core stability of a steam-cooled fast breeder reactor was studied extensively by Frisch [34].
If one considers the stability of the core the quantities dependent on the cooling loop are assumed to be constant. These quantities are coolant inlet temperature, coolant pressure and mass flow through the core.
The behaviour of the core after a reactivity variation is mainly defined by the reactivity effect caused by this variation (reactivity feedback).
The core may be

a) stable

After a positive reactivity disturbance in the core the power is increasing as long as the total reactivity effect becomes zero due to the negative reactivity feedback.

This means that the transfer function of the core only has poles in the left half of the complex plane. After a limited reactivity disturbance a new stable state may be reached without control.

b) Monotonic unstable

This occurs if the feedback is positive. After a positive reactivity disturbance the power increasing is intensified by the feedback. The transfer function has one pole in the right complex half plane After a step disturbance in the reactivity, without control no stable state is reached.

c) Oscillatory unstable

This may occur if the feedback is large, negative and delayed. A positive reactivity disturbance is overcompensated by the feedback and the power level keeps swinging. The transfer function has a complex pair of poles in the right complex half plane.

Investigations of the D-1 core have shown that oscillatory instability of the core only could be reached if the coolant density coefficient would be positive with an absolute value more than 10 times larger than the value usually assumed.

For the investigations of the core stability approximation models are used for:

- neutron kinetics
- thermo dynamics of the core
- reactivity feedback

Neutron kinetics

The neutron kinetics are described by the point model with 6 groups delayed neutrons. The spatial dependence of the neutron kinetics may be neglected if the flux profile in the reactor does not change significantly as a function of the time.

Thermodynamics of the core

The heat exchange from the fuel to the coolant is simulated by the exchange from one fuel rod with mean power density to its corresponding coolant. The D-1 core is designed in a way that all cooling channels have the same coolant outlet temperature and therefore nearly the same axial temperature and density distribution. That is why the approximation applied does not introduce large errors.

Reactivity feedback

The following feedback coefficients are considered

- the Doppler coefficient α_D
- the steam-density coefficient α_ρ
- the fuel temperature coefficient α_F giving the reactivity effect due to fuel expansion
- the canning material coefficient α_c for the reactivity effect due to geometrical and density variations of the canning
- the structure material temperature coefficient α_s for the reactivity effect due to geometrical and density variations of the structure.

The negative Doppler coefficient causes a negative feedback reactivity. A negative steam-density coefficient gives a positive feedback reactivity because $\frac{d\rho}{dT} < 0$. The other feedback effects are considerably smaller.

Due to α_F a negative feedback reactivity
" " α_c a positive " "
" " α_S a negative " "

Investigations with linearized models showed that the D-1 core is near to the boundary for monotonic instability.

Therefore, a digital computer program was developed for the calculation of the feedback reactivity taking into account the following non-linearities:

- temperature dependence of the Doppler coefficient:
  D.C. = $\alpha_D = \frac{A_D}{T}$ T in degrees Kelvin
- dependence of the heat exchange constants on the canning and coolant temperature, steam pressure and mass flow
- dependence of the steam-density and the specific heat of steam on the steam pressure and temperature.

This computer program allows the calculation of the relative power coefficient in dollar:

$$A = \frac{\delta k_f}{\Delta P/P} \cdot \frac{1}{\beta} \$ \qquad (7.1)$$

δk_f feedback reactivity

$\frac{\Delta P}{P}$ relative variation of the power

β fraction delayed neutrons, being about equivalent with 1 $

The feedback reactivity is equal to:

$$\delta k_f = \frac{1}{H} \int_o^H dz \left[W_D(z)\, A_D \ln \frac{\theta_F^{\mathbb{K}}(P,z)}{\theta_{Fo}^{\mathbb{K}}(z)} + \right.$$

$$W_\rho(z)\alpha_\rho \{\rho_k(P,z) - \rho_{ko}(z)\} +$$

$$W_F(z)\alpha_F \{\theta_F(P,z) - \theta_{Fo}(z)\} +$$

$$W_C(z)\alpha_C \{\theta_C(P,z) - \theta_{Co}(z)\} +$$

$$\left. W_S(z)\alpha_S \{\theta_k(P,z) - \theta_{ko}(z)\} \right] \qquad (7.2)$$

$W(z)$ axial weighting function

$\theta^{\mathbb{K}}$ temperature in degrees Kelvin

θ " " " centigrade

indices

D Doppler effect

k coolant

F fuel

C canning

S structure

o stationary values

A relative power coefficient $A = -1$ $ means that for a relative power variation $\frac{\Delta P}{P} = 0.01$ a negative feedback reactivity $\delta k_f = -0.01$ $ will arise.

The analysis of A showed that its main components are due to the coefficients A_D and α_ρ. Therefore, the boundary for A=0 as a function of these coefficients A_D and α_ρ was calculated for several values of the power level P and for several relative deviations $\frac{\Delta P}{P}$.

These graphs published in [34] are very suitable to show the effect of the data uncertainties on the core stability.

Also the variation of the power coefficient A due to cross section uncertainties gives important information.

Stability of the reactor plant

In[34] Frisch proved with the help of a linearized model that it is impossible to obtain an inherent stable reactor with an inherent unstable core. From this analysis also follows that the reactor will be unstable if the steam-density coefficient is positive.
Simulation of the reactor plant on an analog computer confirmed these results. Moreover, followed from this simulation that for large negative steam-density coefficients the plant may become unstable if the core is still stable.

The stability of the reactor plant is strongly dependent on the delay times of the cooling circuit. In [38] it is pointed out that oscillations of the reactor power are prevented if:

$$k_k \cdot \alpha_\rho \cdot \frac{d\rho}{dp} \cdot \frac{X \cdot P}{C} \cdot T_u < A_{crit} \qquad (7.3)$$

with

$k_k = \frac{\Delta P/P}{\Delta k}$: reactivity gain. After a reactivity disturbance Δk, the power level increases from p to $p+\Delta p$.

α_ρ steam-density coefficient

ρ steam-density

p steam-pressure

X ratio of the quantity of superheated steam flowing to the evaporators to the total quantity of steam flowing through the core.

C energy storage capacity of the coolant system

T_u delay time

A_{crit} depends on the composition of the delay time T_u and has a minimum of $\frac{\pi}{2}$ under the assumption of a pure dead time. In the case of 2 delay times of equal length A_{crit} becomes 4. In [40] it is shown that in the case of several time constants of the same order of magnitude (as in the D-1 design) A_{crit} lies between:

$$\frac{\pi}{2} < A_{crit} < 4 \qquad (7.4)$$

The left hand side component of formula (7.3)

$$B = k_k \cdot \alpha_\rho \cdot \frac{d\rho}{dp} \cdot \frac{X \cdot P}{C} \cdot T_u \qquad (7.5)$$

may be calculated with the help of a digital computer code. Comparison of the value of B with the boundaries of A_{crit} gives information about the stability of the reactor plant.

However, a large steam-cooled fast breeder reactor very probably will be equiped with a control system, that stabilizes the core outlet temperature. In this case the influence of the coolant loop on the plant stability will be small.

7.1.3. Dynamic behaviour

Particularly the behaviour of a reactor plant after a credible severe failure is important for its safety and serviceability. The most severe credible failure of the D-1 design is the rupture of a single main coolant pipe in the region of the coolant inlet [35] (point A in fig. 1). The behaviour of the plant after this failure may be investigated both by simulation on an analog computer and by the calculation of the transients with the help of a digital computer program.
The influence of the data uncertainties on the behaviour of the core after the failure just mentioned was examined with the help of a digital computer program developed by Hornyik [41]. In this program the behaviour of the core and the coolant loop are separated in the following way:
The time dependent effect on the coolant properties due to the pipe rupture is calculated for a constant reactor power. With the help of these time dependent coolant properties the behaviour of the core is calculated. This separation does not lead to large errors as long as

the transients considered are so short that due to the delay in the heat exchange from fuel to coolant, the coolant properties are not influenced significantly by the changed thermal power of the core.

The most important features calculated for the core are the time dependent behaviour of:

- the temperature of the fuel and of the can material in a coolant channel with mean power density and in the hot channel.
- the thermal power
- the feedback reactivity components.

The transients may be calculated with and without a scram.

7.2. The uncertainty of the most important parameters

7.2.1. The uncertainty of the R.S.D.C. and Δk_L.

The investigations have shown that the influence of the data uncertainties on these parameters is very large. The outside values caused by the uncertainties of Pu^{239} and U^{238} are given in table 7.1. The influence of the other materials is relatively small.

Variation of Pu^{239} + U^{238} data in a way that	Y	C.R.	Δk_L $		RSDC·10^2		$A_D \cdot 10^2$
			T=900°K	T=2100°K	T=900°K	T=2100°K	
RSDC most positive	7.62523	0.9529	-11.90	-9.37	+3.555	+2.65	-1.5192
RSDC most negative	7.38024	0.8954	+38.70	+40.44	-7.80	-8.11	-1.0509

Table 7.1

The difference between fundamental mode and more detailed calculations is small. E.g. the difference between the R.S.D.C. determined at 900°K with a fundamental mode calculation and with a 1-dimensional multi-group calculation taking into account the axial variation of the steam-density is considerably smaller than the difference between the R.S.D.C. calculated at 900°K and 2100°K with fundamental mode calculations.

7.2.2. The uncertainties of the D.C.

The D.C. is not very sensitive to the nuclear data uncertainties. The influences observed are smaller than 20%.
However, the uncertainty of the D.C. caused by the discrepancy between the different calculation methods is important too.
Comparison calculations showed that the method of Froelich systematically gives a D.C. about 15% more negative than the method of successive k-calculation.

7.3. Influence on the safety

The influence of the D.C. variations on the energy released in a reactor excursion is difficult to determine. Some preliminary calculations for the D-1 design showed a nearly inverse proportionality between the Doppler constant and the energy released [42]. The influence of the Δk_L variations on the safety may be observed in chapter 7.5 because the influence of the R.S.D.C. variations on the safety aspects of the dynamic behaviour is about equivalent with the influence of the Δk_L variations on the safety. In figure 20 may be observed the differences in the reactivity ramp after a severe failure. These differences are mainly caused by the variations in the R.S.D.C.

7.4. Influence on stability

The regions for inherent stability of the D-1 core as determined by Frisch [34] are given in figure 16. In this R.S.D.C.-D.C. plane some significant results of the investigation of the influence of the data uncertainties are plotted. It is assumed that the other reactivity effects are not influenced by the data uncertainties. In figure 16 also are plotted the uncertainties of the D.C. caused by the discrepancy between the calculation methods and the variation of the R.S.D.C. caused by a temperature change of T=900°K to T=2100°K.

With the nuclear data of the KFK-SNEAK set the reactor is inherent stable.
The new α-measurements for Pu^{239} by Schomberg et al [25] are very unfavourable for the stability.
The most recent evaluation of the data for Pu^{240} (the mod. ENDF/B data by Pitterle [24]) has a favourable influence on the stability.

Due to the possible data uncertainties of Pu^{239} and U^{238} the R.S.D.C. may become so far negative that the reactor is unstable. The R.S.D.C. also may become positive. In this case the reactor plant will be unstable without a control system. However, it may be expected that the R.S.D.C. will not become so much positive that oscillatory instability of the core will occur.

For some cases the power coefficient A of equation (7.1) is calculated and tabulated in table 7.2.

Description	A $
KFK-SNEAK SET	-1.253
σ_f of Pu^{239} MAX in GR. 5- 9	-0.770
σ_f of Pu^{239} MAX in GR. 15-18	-2.385
σ_γ of Pu^{239} MAX in GR. 5- 9	-1.287
σ_γ of Pu^{239} MAX in GR. 15-18	-0.516
σ_γ of U^{238} MAX in GR. 5- 9	-1.401
σ_γ of U^{238} MAX in GR. 15-18	-1.083
DATA of Pu^{239} FAVOURABLE	-4.307
DATA of Pu^{239} UNFAVOURABLE	+1.858
DATA of U^{238} FAVOURABLE	-2.086
DATA of U^{238} UNFAVOURABLE	-0.447
FOR Pu^{240} MOD. ENDF/B DATA	-1.638
FOR Pu^{239} DATA OF SCHOMBERG	-0.163

Table 7.2

The plant will be inherent unstable if the core is inherent unstable and if the steam-density coefficient is positive.
With the help of the formulae (7.3) to (7.5) the stability of the plant may be examined for the cases where the core is inherent stable and the R.S.D.C. is negative. For 3 cases of an inherent stable core the value B of formula (7.5) is calculated (table 7.3). The following realistic quantities for the D-1 design are used:

$X = 0.64$

$P = 2500$ MWth

$C = 500 \frac{MWs}{ata}$

$T_u = 4.2$ sec (T_u is composed by a dead time 0.7 sec, a delay time of 1.5 sec for the heating of the structure material and the pipes and a delay time of 2 sec for the heat exchange between the fuel and the coolant.)

	Description	B (form. 7.5)	Comment
1	KFK-SNEAK SET	0.629	$< A_{crit}$
2	MOD. ENDF/B DATA for Pu^{240}	0.166	$< A_{crit}$
3	σ_γ of Pu^{239} DATA by SCHOMBERG	4.640	$> A_{crit}$

Table 7.3.

In the cases 1 and 2 the behaviour of the plant will be satisfactory. However, in the case 3 after a reactivity disturbancy power oscillations will occur.

7.5. Influence on the dynamic behaviour

The influence of the data uncertainties on the dynamic behaviour of the core is examined with the digital computer program of Hornyik (described in chapter 7.1.).

The behaviour of the core after a rupture of a single coolant pipe near the reactor inlet without scram is calculated for 3 cases. Namely with parameters determined with

- the KFK-SNEAK set
- the most favourable data for Pu^{239} (R.S.D.C. positive)
- the σ_γ data of Pu^{239} calculated with the mean α values by Schomberg et al. [25] (figure 10).

Table 7.4 shows the Doppler constant A_D and the R.S.D.C. for the cases calculated:

CASE	DESCRIPTION	$A_D \cdot 10^2$	RSDC$\cdot 10^2$
a	KFK-SNEAK SET	-1.386	-2.14
b	FAVOURABLE DATA Pu^{239}	-1.55	+1.365
c	σ_γ DATA SCHOMBERG	-1.30	-3.55

Table 7.4

In figure 17 the maximal fuel and can temperatures of the hot channel, the thermal power and the feedback reactivity are plotted as a function of the time after the pipe rupture.

The figures 18 to 20 show the differences for these quantities for the cases a, b and c of table 7.4.

For the positive R.S.D.C. no danger for the core occurs immediately after the failure. The can temperature increases slightly due to the fact that the cooling becomes worse.
For the data by Schomberg the fuel melting already occurs after 0.33 sec instead of 0.75 sec for the parameters calculated with the KFK-SNEAK set.

For the case where the R.S.D.C. is influenced most unfavourably by the data uncertainties of Pu^{239} it was examined if a scram could save the core from damage if a main pipe rupture near the reactor inlet occurs. It is assumed that the scram begins 0.1 sec after that where the power level has increased 25%. In figure 21 the reactivity effects are plotted and in figure 22 the can and fuel temperatures in the hot channel. In this case the core will be destored after the failure described.

8. CONCLUSIONS

The investigations of this study may be summarized with the following conclusions:

1) The Doppler coefficient D.C. is not very sensitive to the nuclear data uncertainties of the reactor materials. (The variations of the D.C. are smaller than 20%.) An important part of the variations of the D.C. due to group constant variations comes from the change of the ratio y (fertile to fissile material).

2) The reduced steam-density coefficient R.S.D.C. is very sensitive to the uncertainties of the capture and fission cross-sections and may vary over a wide range. The dependence of the R.S.D.C. on the cross-section variations may be explained qualitatively mainly with the influence of these cross-section variations on the adjoint flux (chapter 6.1.2.2.).

3) The uncertainties of the capture and fission cross-sections of Pu^{239} and U^{238} have most influence on the parameters considered. The influence of the data uncertainties of the higher Pu isotopes is considerable. The other materials only have small effects.

4) Since the R.S.D.C. may vary over a wide range the stability, safety and dynamic behaviour of the D-1 design is influenced strongly by the nuclear data uncertainties.
With the data of the KFK-SNEAK set the D-1 design is inherent stable. The most recent data for Pu^{240} by Pitterle [24] have a favourable effect on the D.C. and the R.S.D.C.
On the other hand these parameters D.C. and R.S.D.C. are influenced unfavourably by the recent measurements by Schomberg et al. [25] for $\alpha = \frac{\sigma_\gamma}{\sigma_f}$ of Pu^{239}.

5) The uncertainty of the D.C. and the R.S.D.C. of the D-1 design may be reduced significantly if:
   a) The discrepancy between the different calculation methods for the D.C. is removed.
   b) The uncertainties of the capture and fission cross-sections of Pu^{239} and U^{238} would be reduced, particularly in the energy ranges 50 eV to 1 keV and 10 keV to 1 MeV.

6) Very probably the investigation of the dynamic behaviour will be improved if the dependence of the steam-density coefficient on the fuel temperature will be considered. Particularly, in the cases the fuel temperature varies considerably.

ACKNOWLEDGEMENTS

I wish to express my gratitude to Professor Dr. M. Bogaardt and to Professor Dr. K. Wirtz for the opportunity to do the final part of my study in the Institut für Neutronenphysik und Reaktortechnik at the Kernforschungszentrum Karlsruhe.

All members of the I.N.R. I want to thank for their patience and willingness to help me with my problems. They have made my stay at Karlsruhe most instructive and pleasant. The following persons I wish to mention by name: Dr. H. Küsters for the providing of the theme of this study and for his interest for the progress of it, D.P. K.Schroeter for the many valuable discussions and advices and for the reading of the manuscript, Dr. J.J. Schmidt for his helpful advices and assistance during the evaluation of the data uncertainties of the reactor materials, Mr. H. Bachmann for the programming of some special codes for this study, Dr. W. Frisch for placing at my disposal a preliminary manuscript of his thesis and for the valuable discussions of the stability of the D-1 design, Dr. K. Hornyik for the valuable discussions of the dynamic behaviour problems and for the calculation of some significant cases with his computer programs.

Last but not least I wish to thank Mrs. U. Besch for the typing of the manuscript and Miss B. Betsche for the drawing of the figures.

List of symbols

All symbols used in this study are explained in the text. Only the symbols occurring several times are listed here.

A_D	Doppler constant
B_g^2	geometrical buckling
C	energy storage capacity of the cooling system
D	diffusion constant
E	energy
P	power level of the reactor
S_j	summation symbol
T	temperature
T_u	delay time
X	ratio of the quantity of superheated steam flowing to the evaporators to the total quantity of steam flowing through the core
f	self-shielding factor
k	multiplication factor
p	steam pressure
t	time
v	neutron velocity
$\bar{x}$	space vector
y	ratio of the fertile material to the fissile material
z	axial coordinate
Γ	resonance half width
Σ	macroscopic cross-section
ϕ	neutron flux
ϕ^+	adjoint flux or importance function
$\bar{\Omega}$	direction vector
α	ratio of σ_γ to σ_f
α	reactivity coefficients in chapter 7
β	fraction of delayed neutrons
η	number of fission neutrons per absorption
θ	temperature in chapter 7

μ	mean cosine of the scattering angle in the laboratory system
ν	number of fission neutrons per fission
ρ	steam density
σ	microscopic cross-section
σ_o	microscopic background cross-section
χ	number of fission neutrons

indices

C	canning material temperature
D	Doppler effect
F	fuel temperature
N	normal value
S	structural material temperature
a	absorption
be	elastic removal
bin	inelastic removal
f	fission
f	feedback in chapter 7
i,j	group numbers
rem	removal
s	scattering
t	total
tr	transport
γ	capture

The cross-sections and the self-shielding factors have the following identification:

$K\Sigma_x^i$ and Kf_x^i with

K material index
i group index
x nuclear process index

LIST OF FIGURES

REFERENCES

1 A. Müller et al.
Referenzstudie für den 1000 MWe dampfgekühlten schnellen Brutreaktor (D1)
KFK-Report 392 (1966), Kernforschungszentrum Karlsruhe

2 R.A. Müller, F. Hoffmann, E. Kiefhaber, D. Smidt
Design and evaluation of a steam-cooled fast breeder reactor of 1000 MWe
Proceedings of the London Conference on Fast Breeder Reactors, 1966

3 A. Jansen
The long-time behaviour of fast power reactors with Pu-recycling
Proceedings of the IAEA Symposium on Fast Reactor Physics and Related Safety Problems, Karlsruhe, 1967
SM 101/16; KFK 630; Eur 3674e

4 A. Jansen
Das Langzeitverhalten schneller Reaktoren mit Plutoniumrückführung (Thesis T.H. Karlsruhe)
External report No. INR-4/67-12 (1967), Kernforschungszentrum Karlsruhe

5 D. Braess, R. Froelich, A. Jansen, H. Küsters, K. Schroeter
The calculation of large fast reactors
KFK-Report 620 (1967), Kernforschungszentrum Karlsruhe

6 H. Bachmann et al.
The group cross-section set KFK-SNEAK. Preparation and results.
Proceedings of the IAEA Symposium on Fast Reactor Physics and Related Safety Problems, Karlsruhe, 1967
SM 101/12; KFK 628; Eur 3672e

7 H. Huschke
Gruppenkonstanten für dampf- und natriumgekühlte schnelle Reaktoren in einer 26-Gruppendarstellung
KFK-Report 770, Eur 3953d (1968), Kernforschungszentrum Karlsruhe

8 L.P. Abagjan et al.
Gruppenkonstanten schneller und intermediärer Neutronen für die Berechnung von Kernreaktoren
KFK-tr-144, Kernforschungszentrum Karlsruhe

9 J.J. Schmidt
Influence of nuclear data uncertainties on the theoretical prediction of Doppler coefficients in fast and intermediate reactors
EANDC-46 L (1963)

10 A. Weinberg and E. Wigner
The physical theory of neutron chain reactors
The University of Chicago Press (1958)

11 R.B. Nicholson
The Doppler effect in fast nuclear reactors. (Thesis Cornell University)
APDA 139 (1960)

12 R. Froelich
Theorie der Dopplerkoeffizienten schneller Reaktoren unter Berücksichtigung der gegenseitigen Abschirmung der Resonanzen
KFK-Report 367 (1964), Kernforschungszentrum Karlsruhe

13 W. Rothenstein and D. Naot
Monte Carlo code for calculating the Doppler effect in fast reactors
Proceedings of the IAEA Symposium on Fast Reactor Physics and Related Safety Problems, Karlsruhe, 1967
SM 101/19

14 R. Froelich
private communication

15 L. Dresner
Resonance absorption in nuclear reactors
Pergamon Press (1960)

16 E. Kiefhaber
Berechnung der durch große Systemänderungen bewirkten Kritikalitätsunterschiede mit Hilfe eines modifizierten Störungstheorie Formalismus
External report INR-4/66-9 (1966), Kernforschungszentrum Karlsruhe

17 E. Kiefhaber
Konfiguration und nukleare Kenngrößen eines Dampfgekühlten Schnellen Brutreaktors. (Thesis T.H. Karlsruhe)
External report INR-4/67-13 (1967), Kernforschungszentrum Karlsruhe

18 K. Jirlow
Reactivity dependence of coolant density in steam-cooled fast reactors
Proceedings of the IAEA Symposium on Fast Reactor Physics and Related Safety Problems, Karlsruhe, 1967
SM 101/52

19 P. Greebler et al.
Calculated nuclear reactor parameters and their uncertainties in a 1000 MWe fast ceramic reactor
GEAP 4471 and ANL 7120 (1965)

20 P. Greebler and B. Hutchins
User requirements for cross-sections in the energy range from 100 eV to 100 keV
GEAP 4472 (1966)

21 J.J. Schmidt
Neutron cross-sections for fast reactor materials
KFK-Report 120, part I, ed. 1966

22 J.Stehn et al.
Neutron cross-sections Vol. II-B and III
BNL 325, sec. ed., suppl. 2 (1965)

23 S. Yiftah, J.J. Schmidt, M. Caner, and M. Segev
Basic nuclear data for the higher Pu-isotopes
Proceedings of the IAEA Symposium on Fast Reactor
Physics and Related Safety Problems, Karlsruhe, 1967
SM 101/21

24 T.A. Pitterle and M. Yamamoto
A comparison of Pu^{240} cross-section evaluations by
calculations of ZPR III assemblies 48, 48B
Second Conference on Neutron Cross-Sections Technology,
Washington (1968), Paper H-8

25 W.G. Schomberg et al.
A new method of measuring $\alpha(E)$ for Pu^{239}
Proceedings of the IAEA Symposium on Fast Reactor Physics
and Related Safety Problems, Karlsruhe, 1967
SM 101/41

26 K.H. Beckurts and J.J. Schmidt
private communication

27 P.H. White et al.
Measurement of fission cross-sections for neutrons of
energy in the range 40-500 keV
Proceedings of the IAEA Symposium, Salzburg, 1965
SM 60/14

28 W.P. Pönitz et al.
Some new measurements and renormalizations of neutron
capture cross-section data in the keV energy range
Proceedings of the IAEA Symposium on Fast Reactor Physics
and Related Safety Problems, Karlsruhe, 1967
SM 101/9; KFK 635; Eur 3679e

29 A. Müller
On the calculation of temperature dependent effective
neutron cross sections
Proceedings of the IAEA Symposium on Fast Reactor Physics
and Related Safety Problems, Karlsruhe, 1967
SM 101/32

30 M.J. Arnold, W.N. Fox, C.F. George, R. Richmond
A comparison of experiment with prediction of the variation
of k-inf with coolant density for a Pu-fueled steam-cooled
fast reactor lattice
Proceedings of the IAEA Symposium on Fast Reactor Physics
and Related Safety Problems, Karlsruhe, 1967
SM 101/43

31 W.G. Davey
An analysis of the fission cross-sections of Th^{232}, U^{233}, U^{234}, U^{235}, U^{236}, Np^{237}, U^{238}, Pu^{239}, Pu^{240}, Pu^{241}, Pu^{242} from 1 keV to 10 MeV
Nucl. Sci. Eng., Vol 26 (1966)

32 R. Hakansson
private communication

33 H. Bachmann et al.
private communication

34 W. Frisch
Stabilitätsprobleme bei dampfgekühlten schnellen Reaktoren
KFK-Report 759 (1968), Kernforschungszentrum Karlsruhe

35 W. Frisch et al.
Safety aspects of steam-cooled fast breeder reactors
KFK-Report 613 (1967), Kernforschungszentrum Karlsruhe

36 W. Frisch and E. Schönfeld
Rechenprogramme für Dynamik und Stabilität eine schnellen Leistungsreaktors
KFK-Report 465 (1966), Kernforschungszentrum Karlsruhe

37 W. Frisch et al.
Systems analysis of a fast steam-cooled reactor of 1000 MWe
Proceedings of the IAEA Symposium on Fast Reactor Physics and Related Safety Problems, Karlsruhe, 1967
SM 101/10; KFK 636; Eur 3680e

38 F. Erbacher et al.
Parametric study of the dynamic behaviour and stability of a steam-cooled fast reactor with an integrated coolant cycle.
Proceedings of the IAEA Symposium on Fast Reactor Physics and Related Safety Problems, Karlsruhe, 1967
SM 101/18; KFK 637; Eur 3681e

39 W. Frisch and G. Woite
Analoges Rechenmodell für dampfgekühlte schnelle Reaktoren mit Direktkreislauf
KFK-Report 657, Eur 3693d (1967), Kernforschungszentrum Karlsruhe

40 L. Krebs
Die Stabilität von starr zurückgeführten Regelstrecken ohne Ausgleich am Beispiel des dampfgekühlten Reaktors
KFK-Report 656, Eur 3691d (1967), Kernforschungszentrum Karlsruhe

41 K. Hornyik
REX - A digital computer program for calculating the dynamic behaviour of steam- and gas-cooled breeder reactors
KFK-Report 699 (1968) Kernforschungszentrum Karlsruhe

42 K. Thurnay
private communication

Appendix A

The maximum percentage atom burn-up of the D-1 design

For the calculations the percentage atom burn-up is required. The maximum allowed burn-up is defined in Megawattdays per ton (MWd/T).

The maximum allowed burn-up B_{max} is defined as the maximal axial averaged burn-up in the fuel rods situated in the core where the radial flux distribution has its maximum. Successive change of 1/3 of the core loading results in a maximal averaged core burn-up.

$$\bar{B} = B_{max} \frac{\bar{\phi}_{rad}}{\phi_{rad,max}} \frac{1}{3}\left(1 + \frac{2}{3} + \frac{1}{3}\right)$$

$$\bar{B} = B_{max} \frac{\bar{\phi}_{rad}}{\phi_{rad,max}} \frac{2}{3} \qquad \text{(A.1)}$$

Between MWd/T and atom percent the following equivalency may be derived:

$$1 \text{ MWd} = 10^6 \cdot 24\ 3600 \text{ Wsec}$$
$$1 \text{ eV} = 1.602 \cdot 10^{-19} \text{ Wsec}$$

Energy released per fission 190 MeV (not included are about 10 MeV neutrino energy).

Also

$$1 \text{ MWd/T} = \frac{24\ 3600\ 10^6}{1.602 \cdot 10^{-19}\ 190\ 10^6} \text{ fissions/T}$$

1 Ton contains $10^6 \frac{N}{A}$ atoms

N Avogadro number
A mass number

So

$$1 \text{ MWd/T} = \frac{24\ 3600\ 10^6}{1.602\ 10^{-19}\ 190\ 10^6\ \frac{N}{A}\ 10^6} \text{ fissions/total number of atoms}$$

or

$$1 \text{ MWd/T} = \frac{24\ 3600\ 10^6\ A\ 10^2}{1.602\ 10^{-19}\ 190\ 10^6\ N\ 10^6} \text{ atom percent}$$

For Pu^{239}

$$1 \text{ MWd/T} \triangleq 1.128\ 10^{-4} \text{ atom percent} \qquad \text{(A.2)}$$

with

$$B_{max} = 55000 \text{ MWd/T}$$

$$\frac{\phi_{rad}}{\phi_{rad,max}} = 0.836$$

The percentage atom burn-up for the D-1 design at maximum allowed burn-up becomes with equations (A.1) and (A.2)

$$B.U. = \frac{2}{3}\ 0.836\ 55000\ 1.128\ 10^{-4} = \underline{3.45} \text{ atom percent}$$

Appendix B

The perturbation code applied

For the analyses of the group dependent distribution of the reduced steam-density coefficient and of the Doppler effect a perturbation code has been used.

The basic equations for this code will be derived here. We start with the multi-group diffusion equations for the flux and adjoint flux (equations 3.4 and 3.5). (The space dependence is omitted and $\phi_i^+ = \psi_i$)

$$VD_i\nabla\phi_i + \Sigma^i_{rem}\phi_i = \sum_{j\neq i} \Sigma_{j\to i}\phi_j + \frac{\chi_i}{k_{eff}} \sum_j \nu\Sigma^j_f \phi_j \qquad (B.1)$$

$$VD_i\nabla\psi_i + \Sigma^i_{rem}\psi_i = \sum_{j\neq i} \Sigma_{i\to j}\psi_j + \frac{\nu\Sigma^i_f}{k_{eff}} \sum_j \chi_j \psi_j \qquad (B.2)$$

These equations may be written in the following matrix form

$$M\phi = \frac{\chi}{k_{eff}} \langle \nu\Sigma^T_f, \phi \rangle \qquad (B.3)$$

$$M^T\psi = \frac{\nu\Sigma_f}{k_{eff}} \langle \chi^T, \psi \rangle \qquad (B.4)$$

with

$$M = \begin{pmatrix} VD_1\nabla + \Sigma^1_{rem} & 0 & \cdots & 0 & 0 & \cdots & 0 \\ -\Sigma_{1\to 2} & VD_2\nabla + \Sigma^2_{rem} & \cdots & 0 & 0 & \cdots & 0 \\ \vdots & \vdots & & \vdots & \vdots & & \vdots \\ -\Sigma_{1\to i} & -\Sigma_{2\to i} & \cdots & \Sigma_{i-1\to i} & VD_i\nabla + \Sigma^i_{rem} & \cdots & 0 \\ \vdots & \vdots & & \vdots & \vdots & & \vdots \\ -\Sigma_{1\to n} & -\Sigma_{2\to n} & \cdots & \Sigma_{i-1\to n} & \Sigma_{i\to n} & \cdots & VD_n\nabla + \Sigma^n_{rem} \end{pmatrix}$$

M^T transponed of matrix M

$$\phi = \begin{pmatrix} \phi_1 \\ \phi_2 \\ \vdots \\ \phi_n \end{pmatrix} \quad \psi = \begin{pmatrix} \psi_1 \\ \psi_2 \\ \vdots \\ \psi_n \end{pmatrix} \quad \chi = \begin{pmatrix} \chi_1 \\ \chi_2 \\ \vdots \\ \chi_n \end{pmatrix} \quad \nu\Sigma_f = \begin{pmatrix} \nu\Sigma^1_f \\ \nu\Sigma^2_f \\ \vdots \\ \nu\Sigma^n_f \end{pmatrix}$$

$(\nu\Sigma_f)^T = (\nu\Sigma_f^1, \nu\Sigma_f^2, \ldots, \nu\Sigma_f^n)$ transponed of $\nu\Sigma_f$

$\chi^T = (\chi_1, \chi_2, \ldots, \chi_n)$ " " χ

$\langle \nu\Sigma_f^T, \phi \rangle = \sum_j \nu\Sigma_f^j \phi_j$

$\langle \chi^T, \psi \rangle = \sum_j \chi_j \psi_j$

For equation (B.3) we take the transponed of both sides

$$(M^T\psi)^T = \psi^T M$$

$$\left(\frac{\nu\Sigma_f}{k_{eff}} \langle \chi^T, \psi \rangle\right)^T = \frac{\nu\Sigma_f^T}{k_{eff}} \langle \chi^T, \psi \rangle = \frac{\nu\Sigma_f^T}{k_{eff}} \langle \psi^T, \chi \rangle$$

with $\psi^T = \phi^+ \qquad \phi^+ = (\phi_1^+, \phi_2^+, \ldots, \phi_n^+)$

$$\phi^+ M = \frac{\nu\Sigma_f^T}{k_{eff}} \langle \phi^+, \chi \rangle \tag{B.5}$$

Now, we consider 2 states of the system.

For state 1 equation (B.3) reads

$$M_1 \phi_1 = \frac{\chi}{k_{eff_1}} \langle \nu\Sigma_{f_1}^T, \phi_1 \rangle \tag{B.6}$$

For state 2 equation (B.5) reads

$$\phi_2^+ M_2 = \frac{\nu\Sigma_{f_2}^T}{k_{eff_2}} \langle \phi_2^+, \chi \rangle \tag{B.7}$$

For both states the fission spectrum is taken the same.

Multiplication of equation (B.6) with ϕ_2^+ from the left side gives

$$\phi_2^+ M_1 \phi_1 = \frac{\phi_2^+, \chi}{k_{eff_1}} \langle \nu\Sigma_{f_1}^T, \phi_1 \rangle \tag{B.8}$$

Multiplication of equation (B.7) with ϕ_1 from the right side

$$\phi_2^+ M_2 \phi_1 = \frac{\nu\Sigma_{f_2}^T, \phi_1}{k_{eff_2}} \langle \phi_2^+, \chi \rangle \tag{B.9}$$

Subtracting (B.9) from (B.8) and integration over energy region and reactor volume give

$$\int_V dV\left[\langle\phi_2^+(M_1-M_2)\phi_1\rangle\right] = \int_V dV\left[\frac{\langle\phi_2^+,\chi\rangle}{keff_1}\langle\nu\Sigma_{f_1}^T,\phi_1\rangle - \frac{\langle\nu\Sigma_{f_2}^T,\phi_1\rangle}{k_{eff_2}}\langle\phi_2^+,\chi\rangle\right] \qquad (B.10)$$

If

$$M_2 = M_1 + \delta M$$
$$\nu\Sigma_{f_2} = \nu\Sigma_{f_1} + \delta\nu\Sigma_f$$

equation (B.10) becomes

$$\int_V dV\left[-\langle\phi_2^+\delta M\phi_1\rangle\right] = \int_V dV\left[\langle\phi_2^+,\chi\rangle\left\{\frac{\langle\nu\Sigma_{f_1}^T,\phi_1\rangle}{k_{eff_1}} - \frac{\langle\nu\Sigma_{f_1}^T,\phi_1\rangle}{k_{eff_2}} - \frac{\langle\delta\nu\Sigma_f^T,\phi_1\rangle}{k_{eff_2}}\right\}\right]$$

or

$$\int_V dV\left[-\langle\phi_2^+\delta M\phi_1\rangle + \frac{\langle\delta\nu\Sigma_f^T,\phi_1\rangle\langle\phi_2^+,\chi\rangle}{k_{eff_2}}\right] =$$

$$\int_V dV\left[\langle\phi_2^+,\chi\rangle\langle\nu\Sigma_{f_1}^T,\phi_1\rangle\left\{\frac{1}{k_{eff_1}} - \frac{1}{k_{eff_2}}\right\}\right] \qquad (B.11)$$

Now, we only consider small variations between state 1 and state 2, with state 1 just critical

In this case we assume to be allowed to take

$$\phi_1 = \phi_2 = \phi$$
$$\phi_1^+ = \phi_2^+ = \phi^+$$
$$k_{eff_2} = k_{eff_1} + \delta k = 1 + \delta k.$$

Also we obtain

$$\left(\frac{1}{k_{eff_1}} - \frac{1}{k_{eff_2}}\right) = 1 - \frac{1}{1+\delta k} = \frac{1+\delta k-1}{1+\delta k} \approx \delta k$$

$$\frac{\langle \delta \nu \Sigma_f^T, \phi_1 \rangle \langle \phi_2^+, \chi \rangle}{k_{eff_2}} \approx \langle \delta \nu \Sigma_f^T, \phi \rangle \langle \phi^+, \chi \rangle$$

Then equation (B.11) reads

$$\int_V dV \left[-\langle \phi^+ \delta M \phi \rangle + \langle \delta \nu \Sigma_f^T, \phi \rangle \langle \phi^+, \chi \rangle \right] = \int_V dV \left[\langle \phi^+, \chi \rangle \langle \nu \Sigma_f^T, \phi \rangle \delta k \right]$$

or

$$\delta k = \frac{\int_V dV \left[-\langle \phi^+ \delta M \phi \rangle + \langle \delta \nu \Sigma_f^T, \phi \rangle \langle \phi^+, \chi \rangle \right]}{\int_V dV \left[\langle \phi^+, \chi \rangle \langle \nu \Sigma_f^T, \phi \rangle \right]} \qquad (B.12)$$

The denominator is independent of the perturbations and is put equal to F. (Equation (B.12) then reads

$$\delta k = \frac{1}{F} \int_V dV \left[-\langle \phi^+ \delta M \phi \rangle + \langle \delta \nu \Sigma_f^T, \phi \rangle \langle \phi^+, \chi \rangle \right] \qquad (B.13)$$

The integrant may be written as a sum over the energy groups in the following way

$$\langle \phi^+ \delta M \phi \rangle = \sum_i \left\{ \phi_i^+ \phi_i \left(\nabla \delta D_i \nabla + \delta \Sigma_{rem}^i \right) \right\} - \sum_{i,j} \delta \Sigma_{j \to i} \phi_j \phi_i^+$$

$$= \sum_i \delta D_i \nabla \phi_i^+ \nabla \phi_i + \sum_i (\delta \Sigma_\gamma^i + \delta \Sigma_f^i) \phi_i \phi_i^+ - \sum_{i,j} \delta \Sigma_{j \to i} \phi_j (\phi_i^+ - \phi_j^+) \qquad (B.14)$$

and

$$\langle \delta \nu \Sigma_f^T, \phi \rangle \langle \phi^+ \chi \rangle = \sum_{i,j} \delta \nu \Sigma_f^j \phi_j \phi_i^+ \chi_i \qquad (B.15)$$

From (B.13), (B.14) and (B.15) follows

$$\delta k = \frac{1}{F}\int_V dV\left[-\sum_i \delta D_i \nabla\phi_i^+\nabla\phi_i - \sum_i(\delta\Sigma_\gamma^i+\delta\Sigma_f^i)\phi_i\phi_i^+\right.$$

$$\left.+\sum_{i,j}\delta\Sigma_{j\to i}\phi_j(\phi_i^+-\phi_j^+)+\sum_{i,j}\delta\nu\Sigma_f^j\phi_j\phi_i^+\chi_i\right] \qquad (B.16)$$

The splitting up of δk in group dependent contributions is not well defined because of the components in δk with sum over i and j simultaneously.

The splitting of the component

$$\sum_{ij}\delta\Sigma_{j\to i}\phi_j(\phi_i^+-\phi_j^+)+\sum_{ij}\delta\nu\Sigma_f^j\phi_j\phi_i^+\chi_i \qquad (B.17)$$

may be based on 2 principes:

a) In group i the reactivity effects due to the cross-section variations in this group are taken together.

b) In group i the reactivity effects due to the variations of the neutron population of this group are taken together.

Method a) gives for (B.17)

$$\sum_i\left\{\sum_j\delta\Sigma_{i\to j}\phi_i\phi_j^+-\sum_j\delta\Sigma_{i\to j}\phi_i\phi_i^+\right\}+\sum_i\left\{\delta\nu\Sigma_f^i\phi_i\sum_j\chi_j\phi_j^+\right\}$$

or

$$\sum_i\left\{\sum_j\delta\Sigma_{i\to j}\phi_i\phi_j^+-\sum_j\delta\Sigma_{i\to j}\phi_i\phi_i^+ +\delta\nu\Sigma_f^i\phi_i\sum_j\chi_j\phi_j^+\right\} \qquad (B.18)$$

Method b) gives

$$\sum_i\left\{\sum_j\delta\Sigma_{j\to i}\phi_j\phi_i^+-\sum_j\delta\Sigma_{i\to j}\phi_i\phi_i^+\right\}+\sum_i\left\{\chi_i\phi_i^+\sum_j\delta\nu\Sigma_f^j\phi_j\right\}$$

or

$$\sum_i \left\{ \sum_j \delta\Sigma_{j\to i}\phi_j\phi_i^+ - \sum_j \delta\Sigma_{i\to j}\phi_i\phi_i^+ + \chi_i\phi_i^+ \sum_j \delta\nu\Sigma_f^j\phi_j \right\} \qquad \text{(B.19)}$$

Also equation B.16 may be written as

$$\delta k = \sum_i \delta k_i \qquad \text{(B.20)}$$

with

method a)

$$\delta k_i = \frac{1}{F}\int_V dV\Big[-\delta D_i \nabla\phi_i^+\nabla\phi_i - (\delta\Sigma_\gamma^i + \delta\Sigma_f^i)\phi_i\phi_i^+ + \sum_j \delta\Sigma_{i\to j}\phi_i\phi_j^+ + -\delta\Sigma_b^i\,\phi_i\phi_i^+ + \delta\nu\Sigma_f^i\phi_i \sum_j \chi_j\phi_j^+\Big] \qquad \text{(B.21)}$$

method b)

$$\delta k_i = \frac{1}{F}\int_V dV\Big[-\delta D_i \nabla\phi_i^+\nabla\phi_i - (\delta\Sigma_\gamma^i + \delta\Sigma_f^i)\phi_i\phi_i^+ + \sum_j \delta\Sigma_{j\to i}\phi_j\phi_i^+ + -\delta\Sigma_b^i\,\phi_i\phi_i^+ + \chi_i\phi_i^+ \sum_j \delta\nu\Sigma_f^j\phi_j\Big] \qquad \text{(B.22)}$$

The NUSYS program 2240 by Bachmann enables the calculation of the equations (B.16), (B.21) and (B.22). The flux and adjoint flux have to be calculated with a one-dimensional diffusion approximation.

In figure 13 the energy dependence of the R.S.D.C. is calculated both with the help of formulae (B.21) and (B.22).

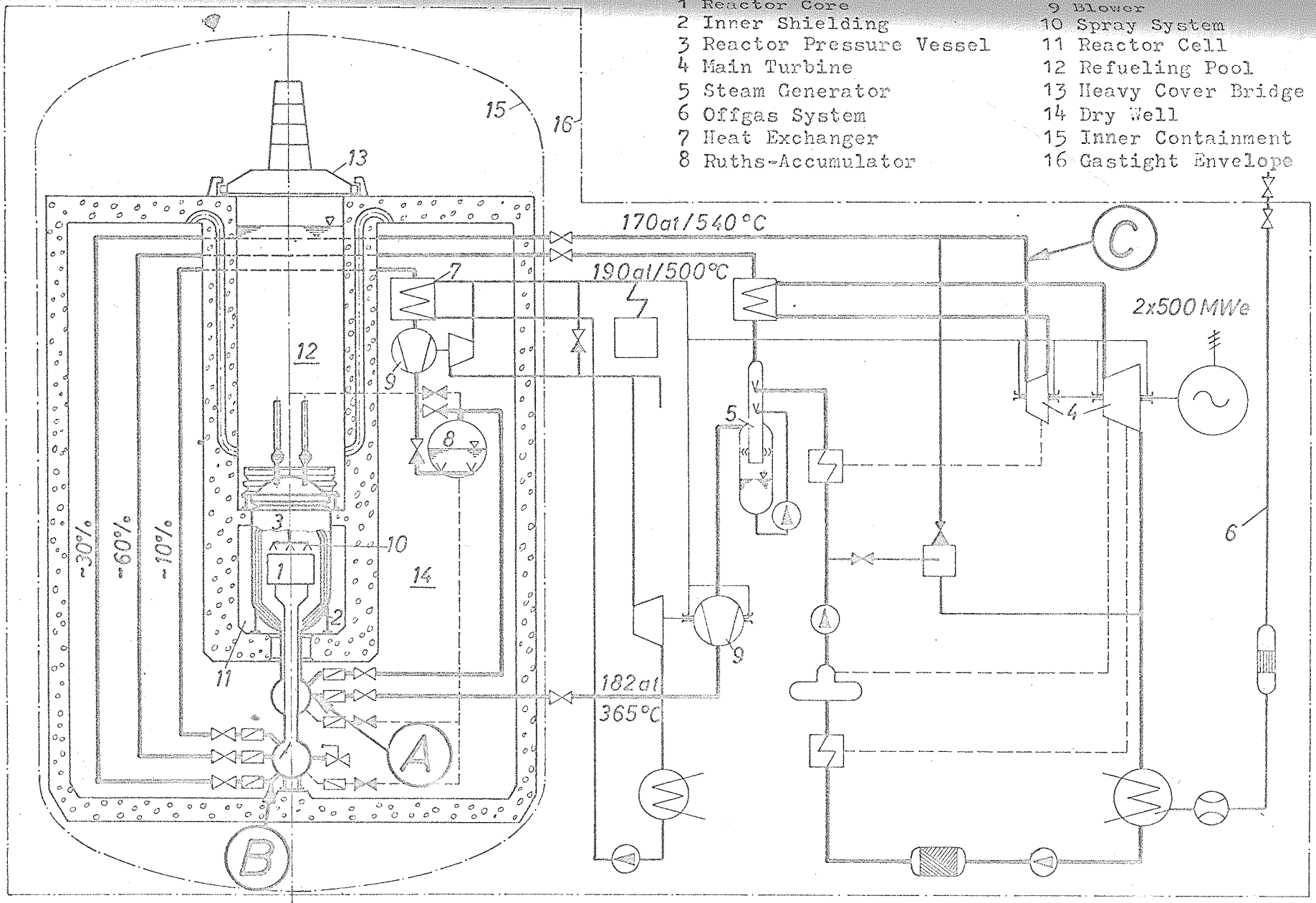

Fig. 1 Simplified Flow Diagram and Containment System

Fig. 2

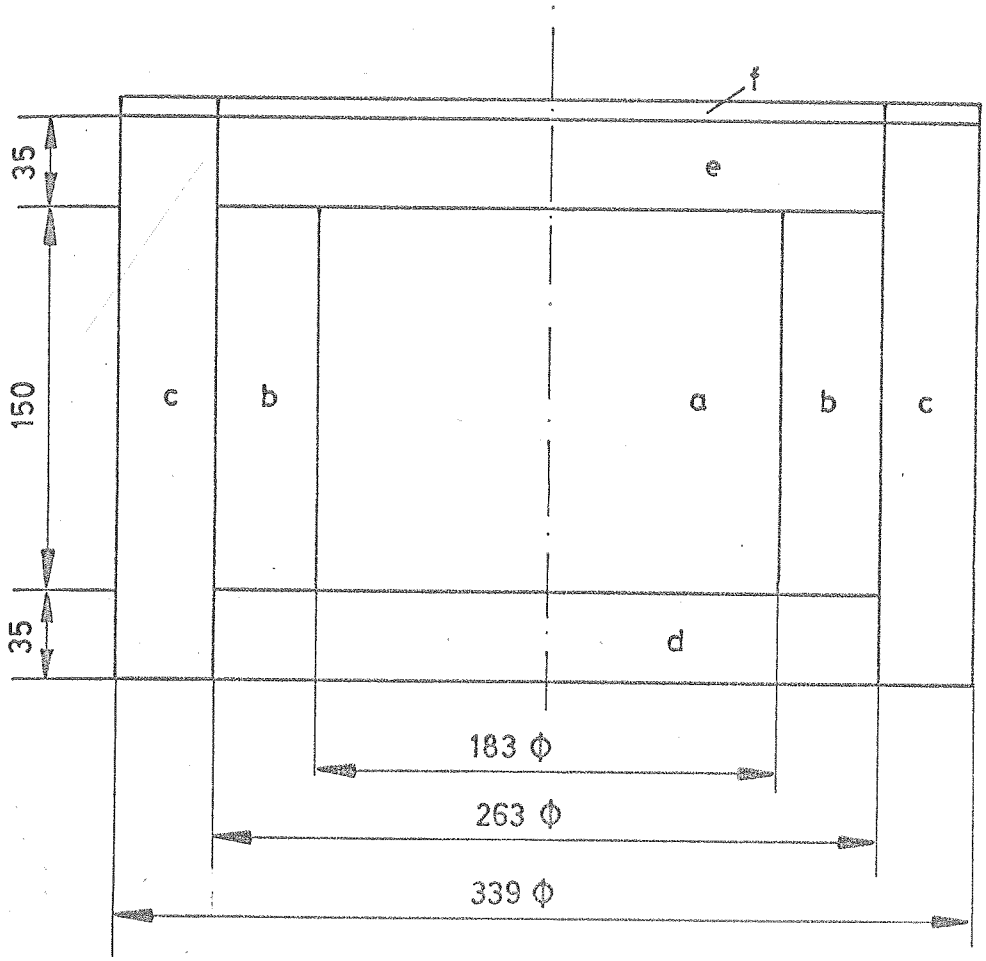

measures in cm

a) inner fission region
b) outer fission region
c) radial blanket
d) lower axial blanket
e) upper axial blanket
f) gasplenum

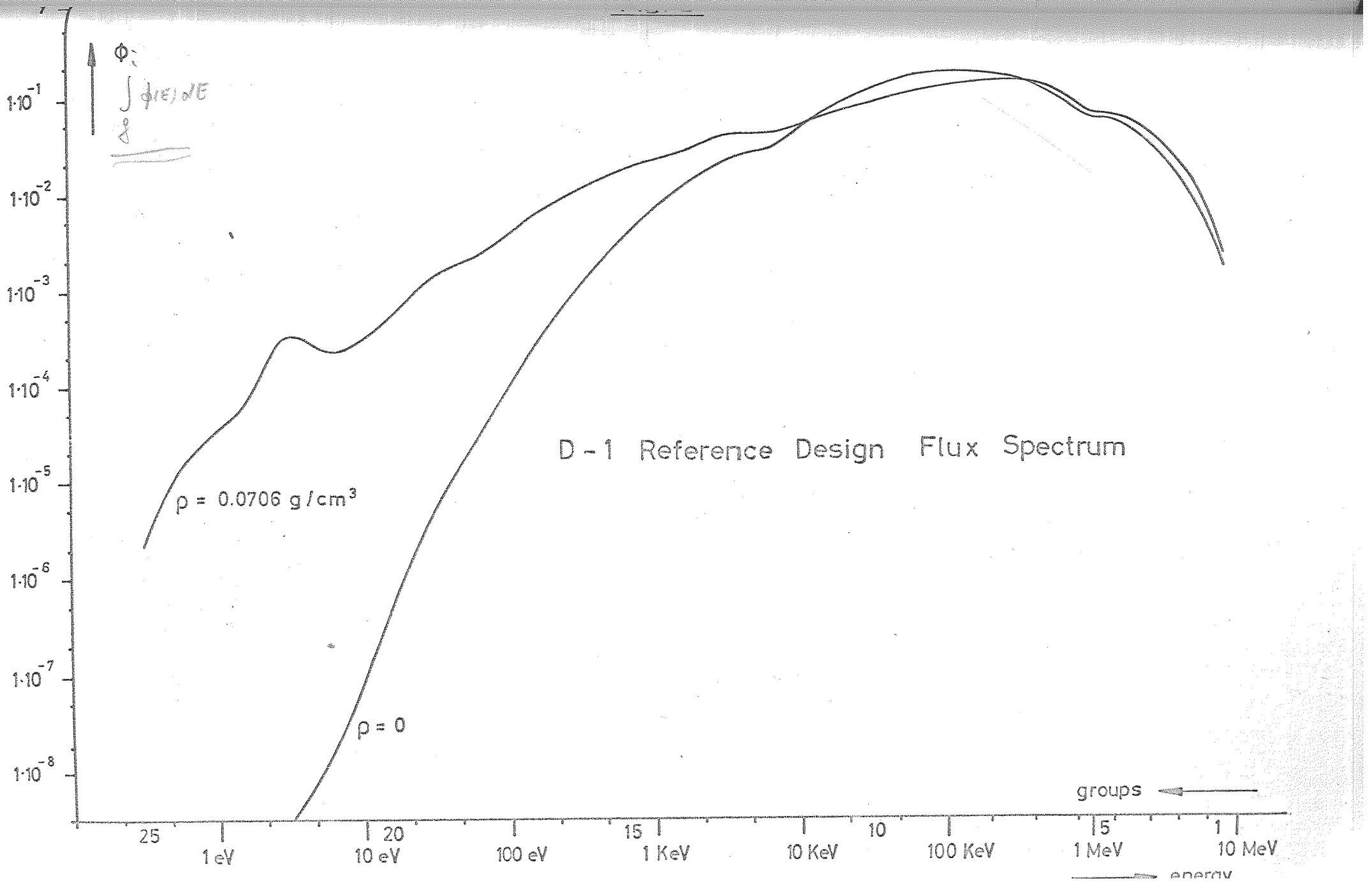

Fig. 4

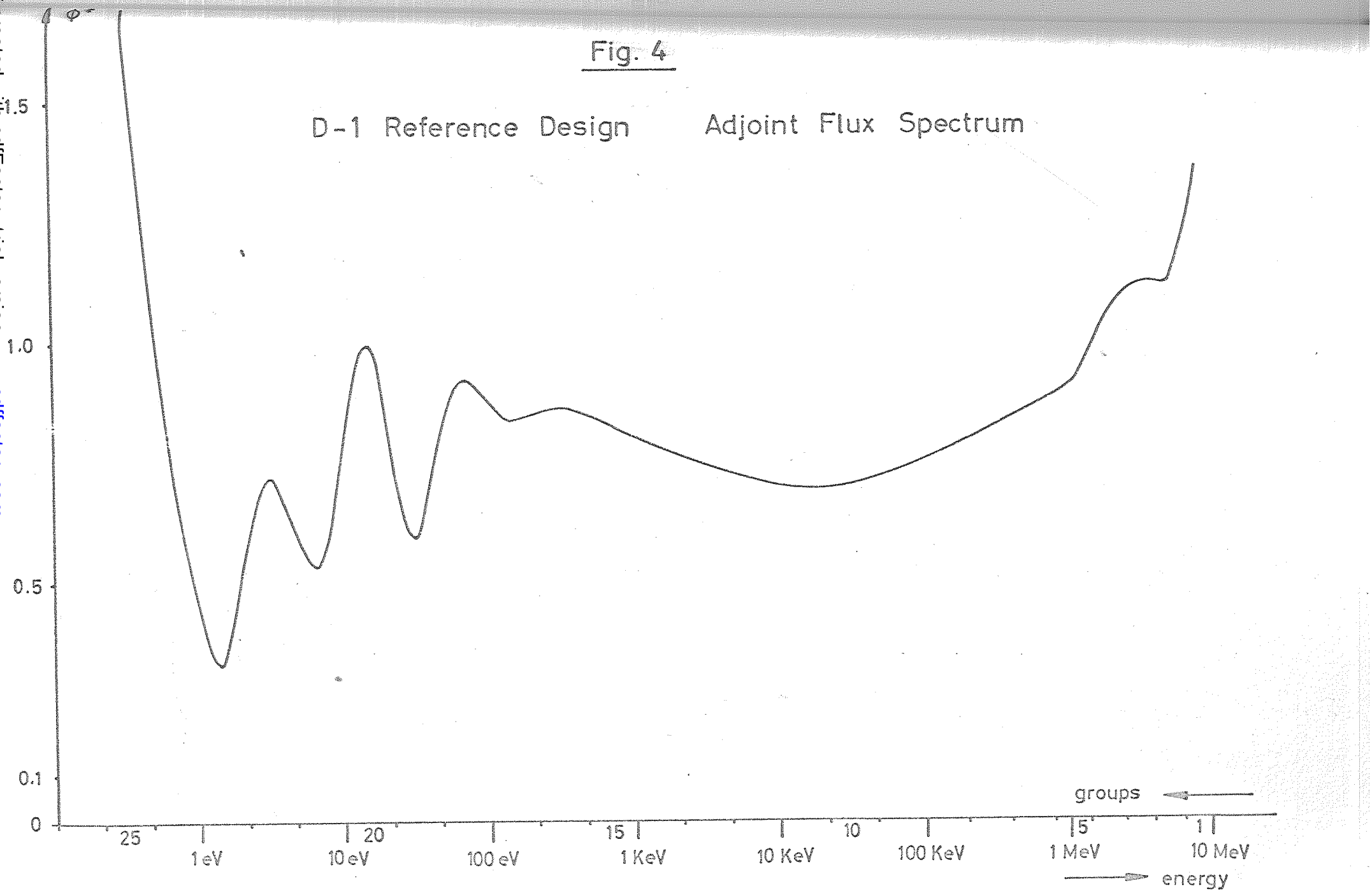

Fig. 5

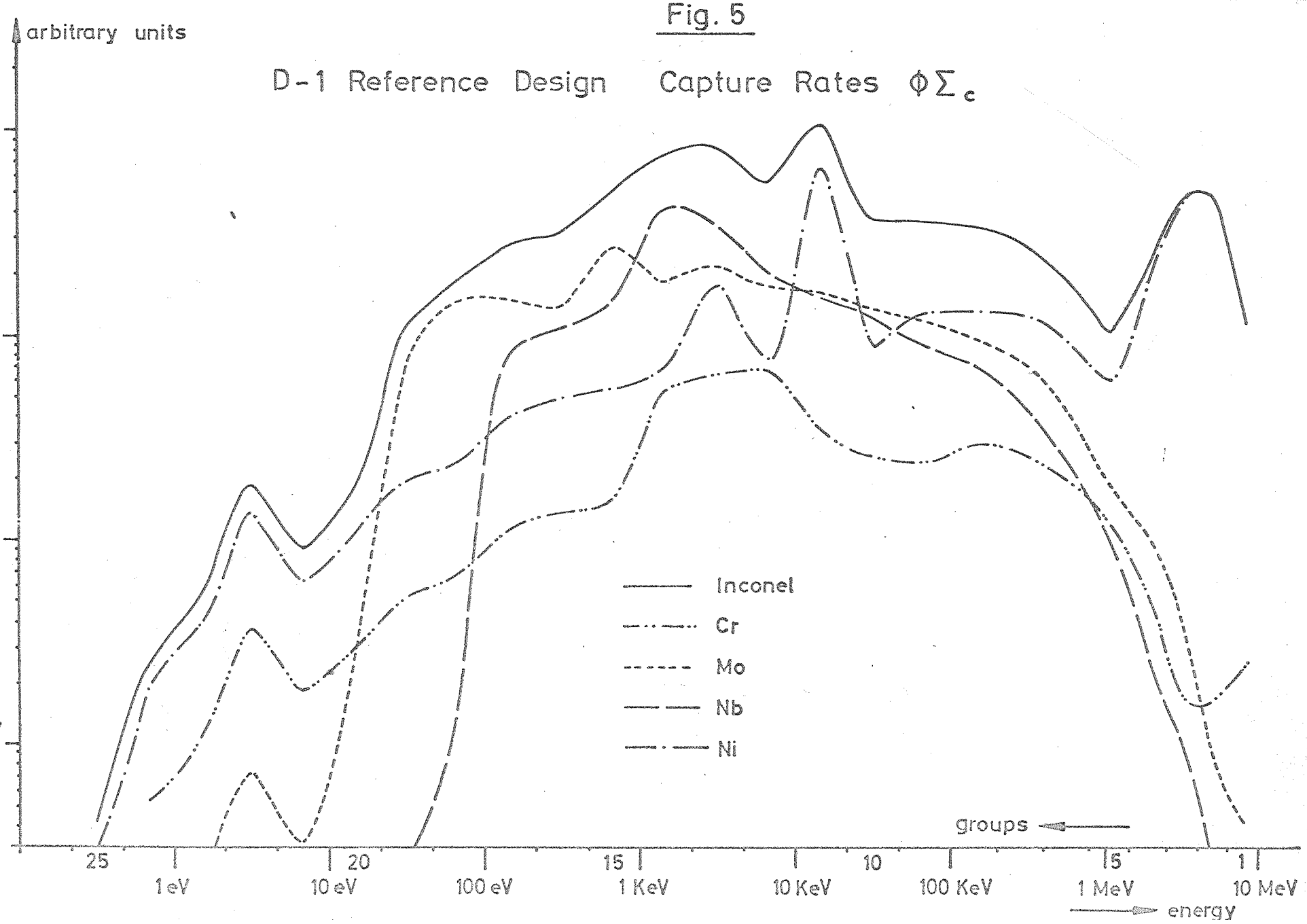

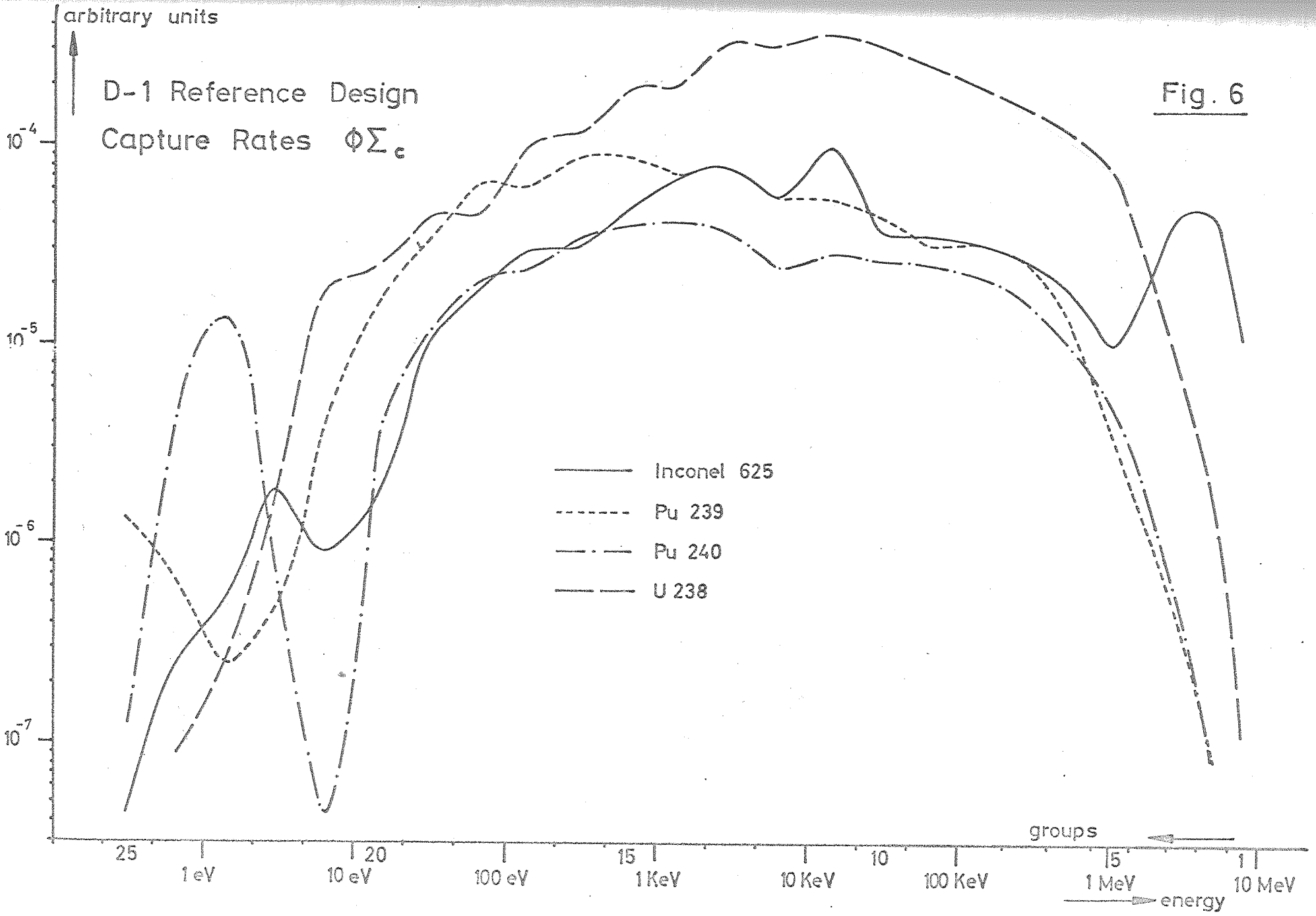

Fig. 7

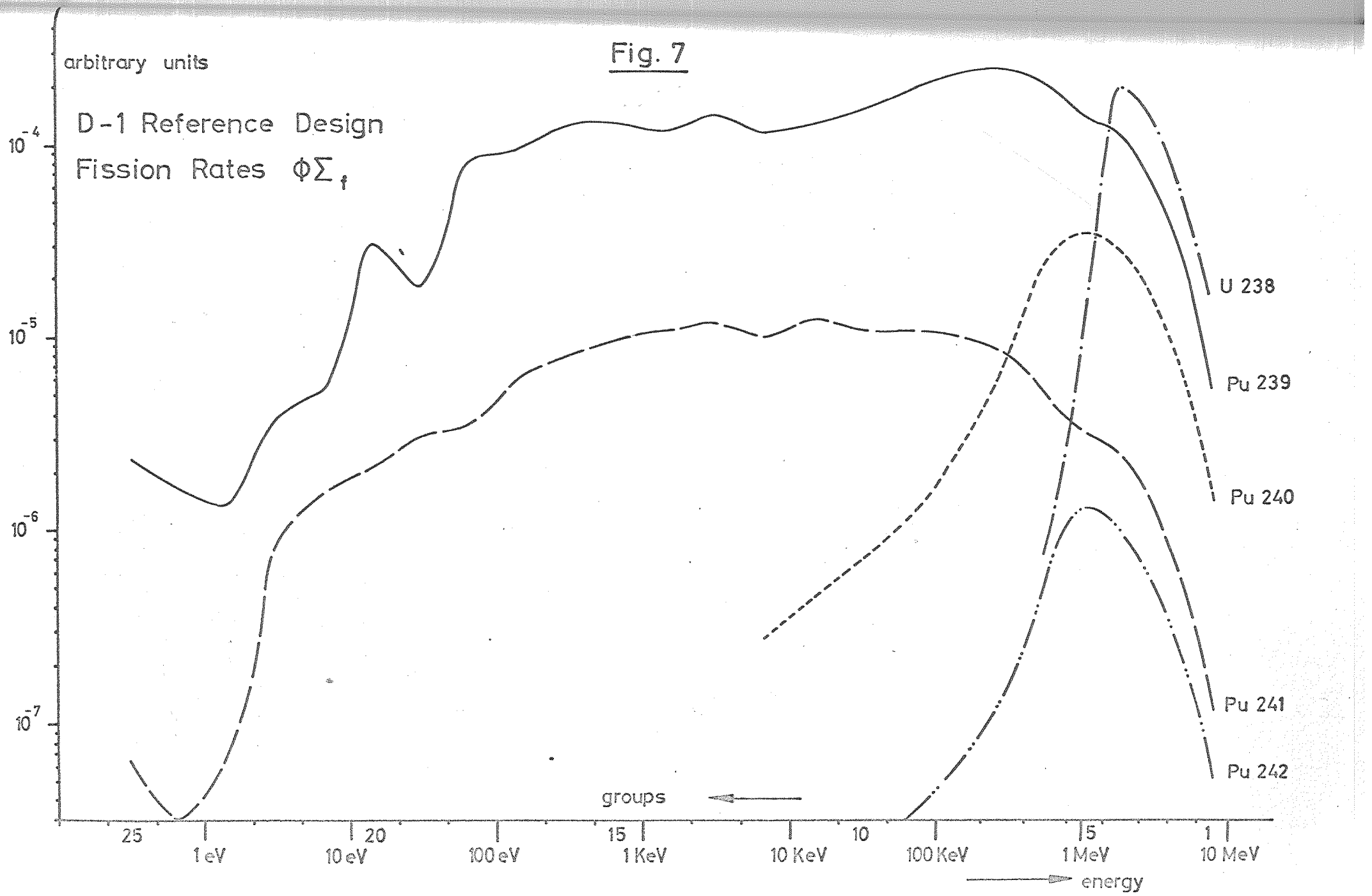

Fig. 8

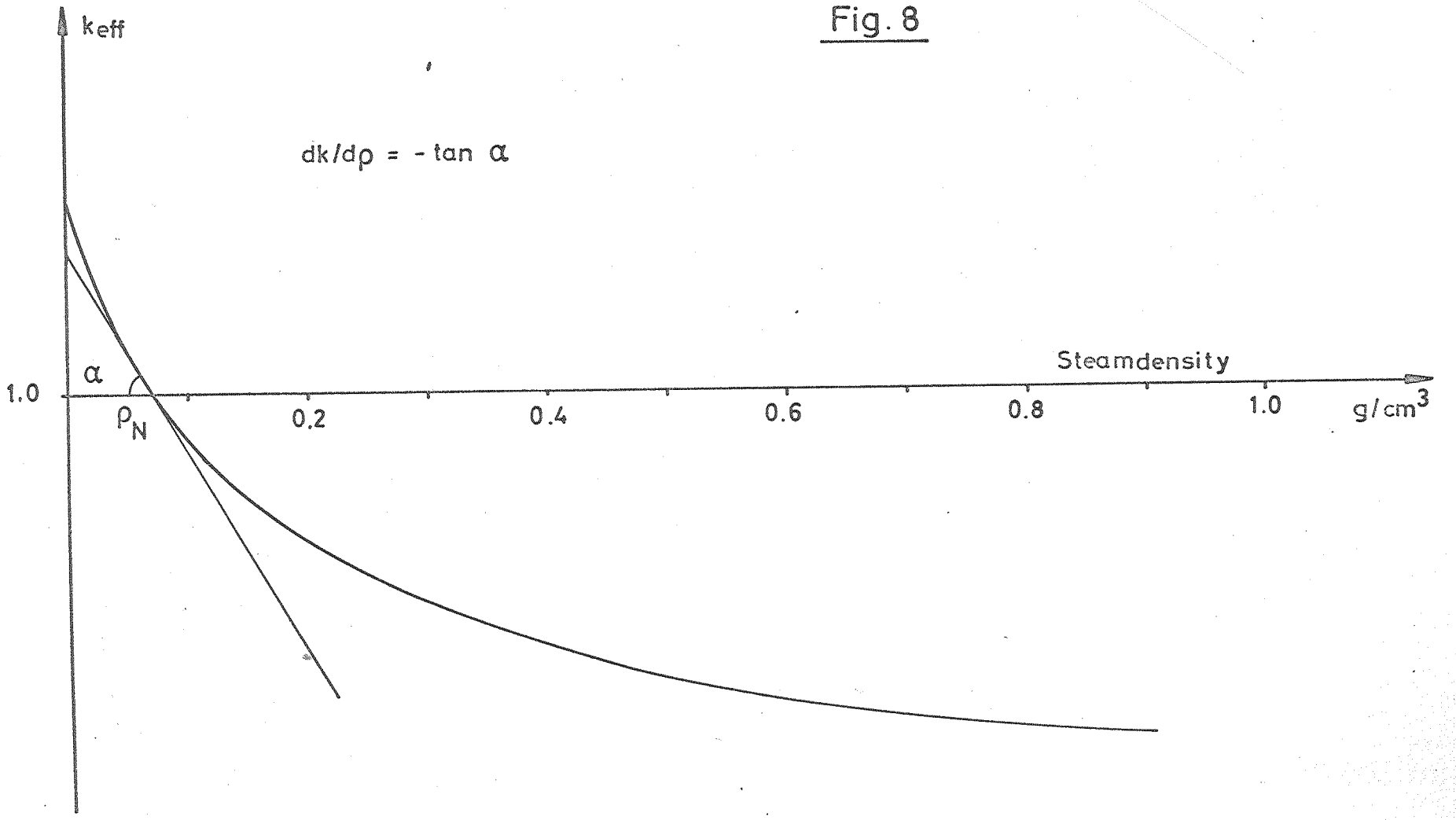

Fig. 9

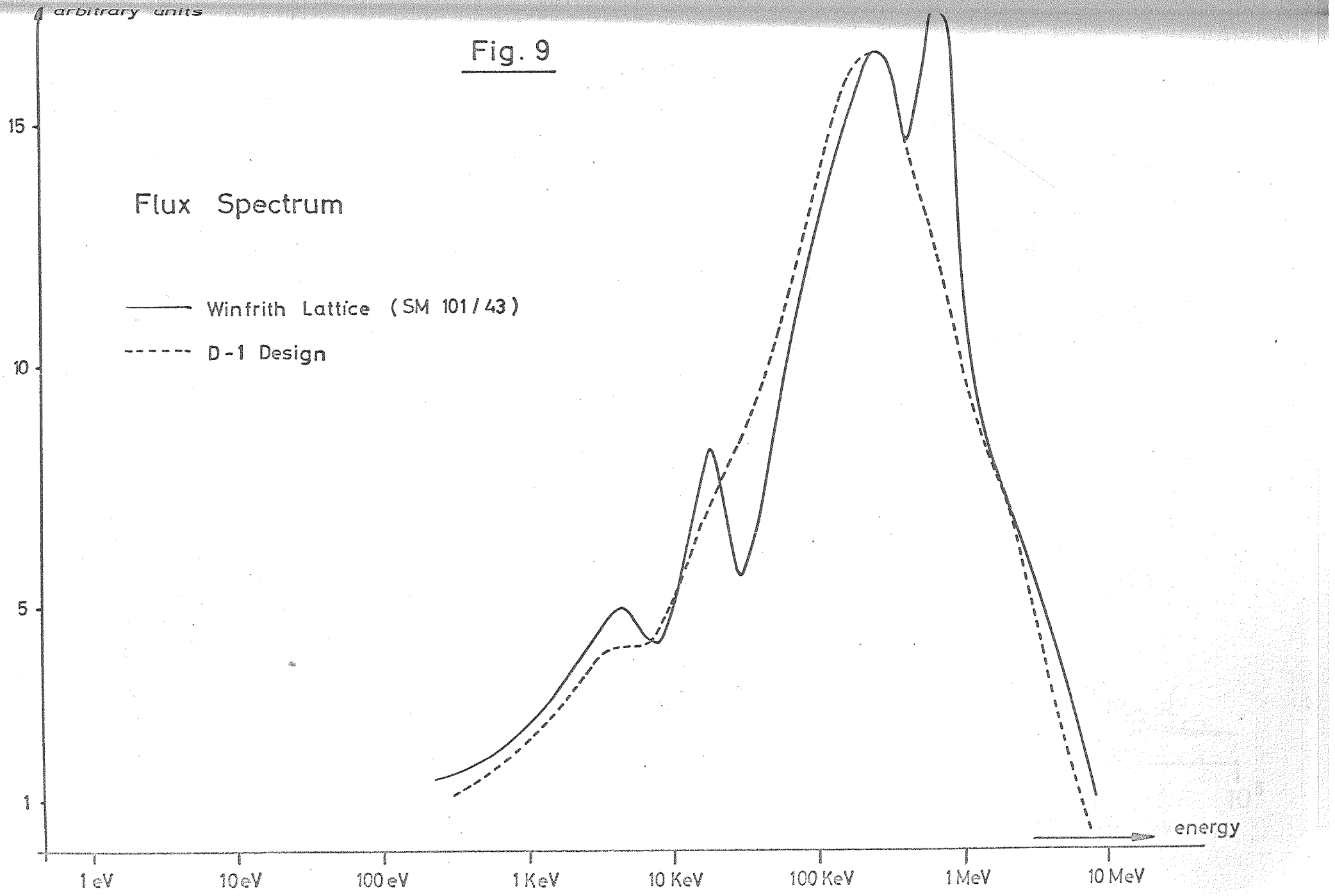

Fig. 10

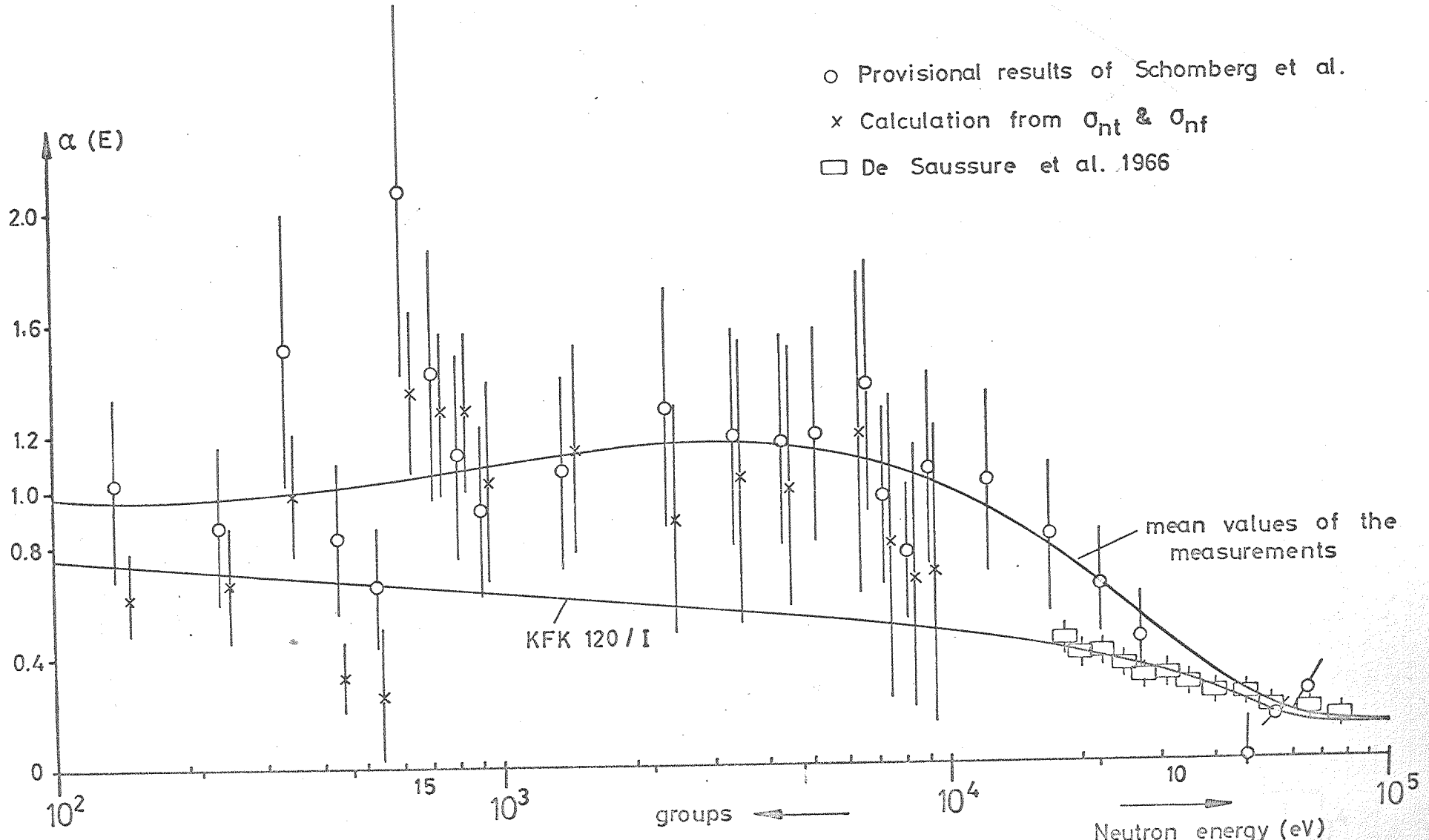

$\alpha = \frac{\sigma_\gamma}{\sigma_f}$ for Pu 239

Fig. 11

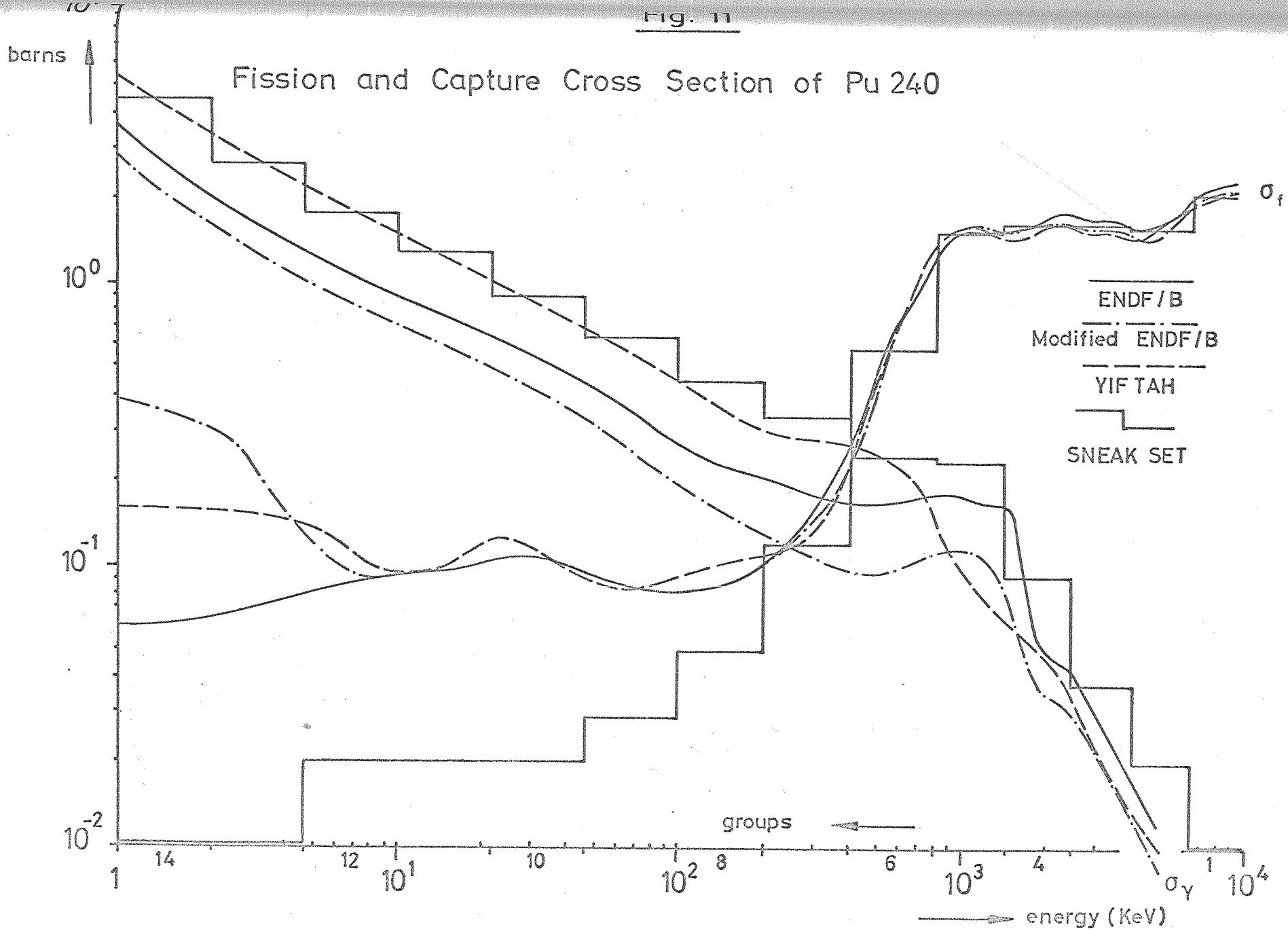

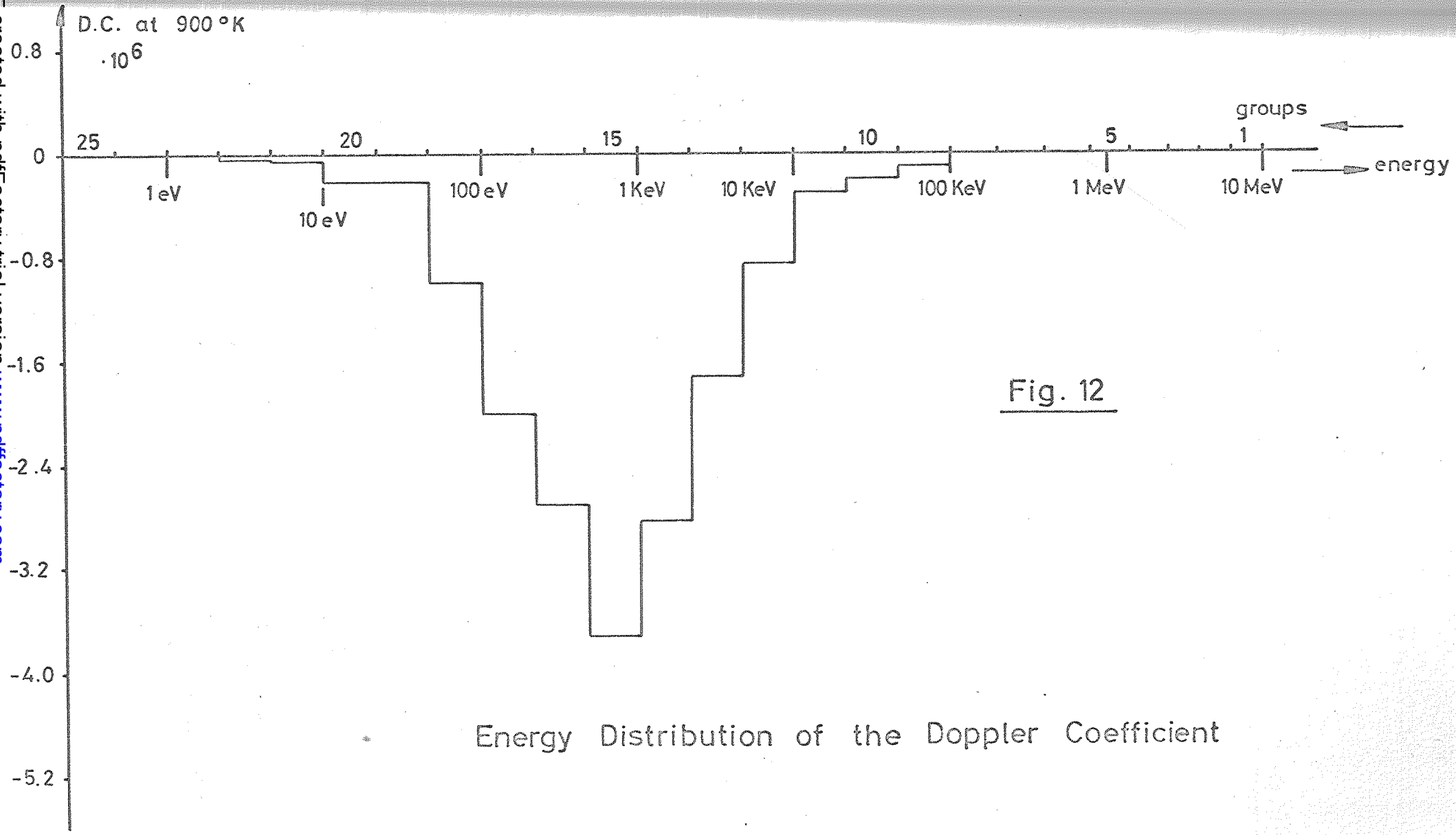

Fig. 12

Energy Distribution of the Doppler Coefficient

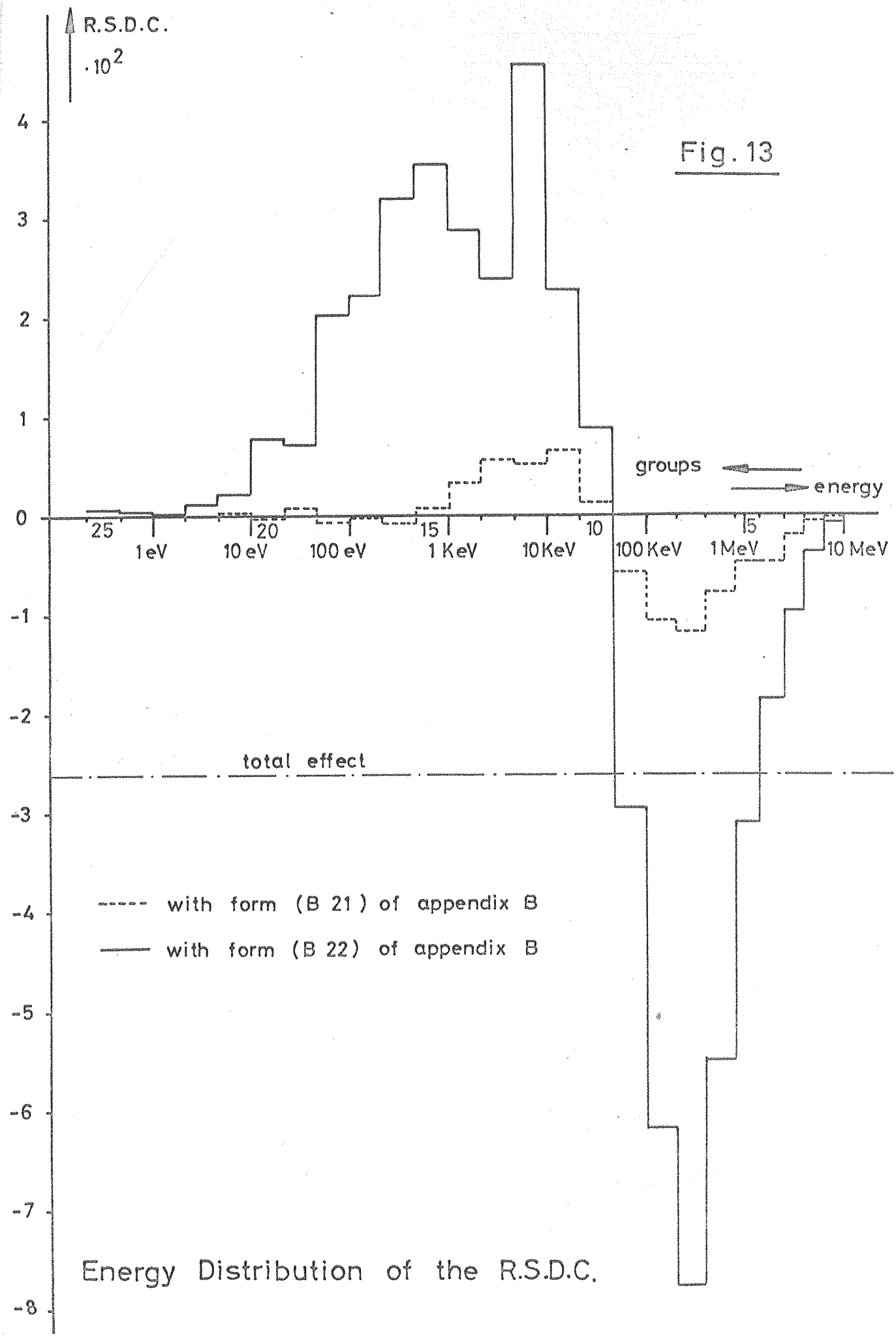

Fig. 13

Energy Distribution of the R.S.D.C.

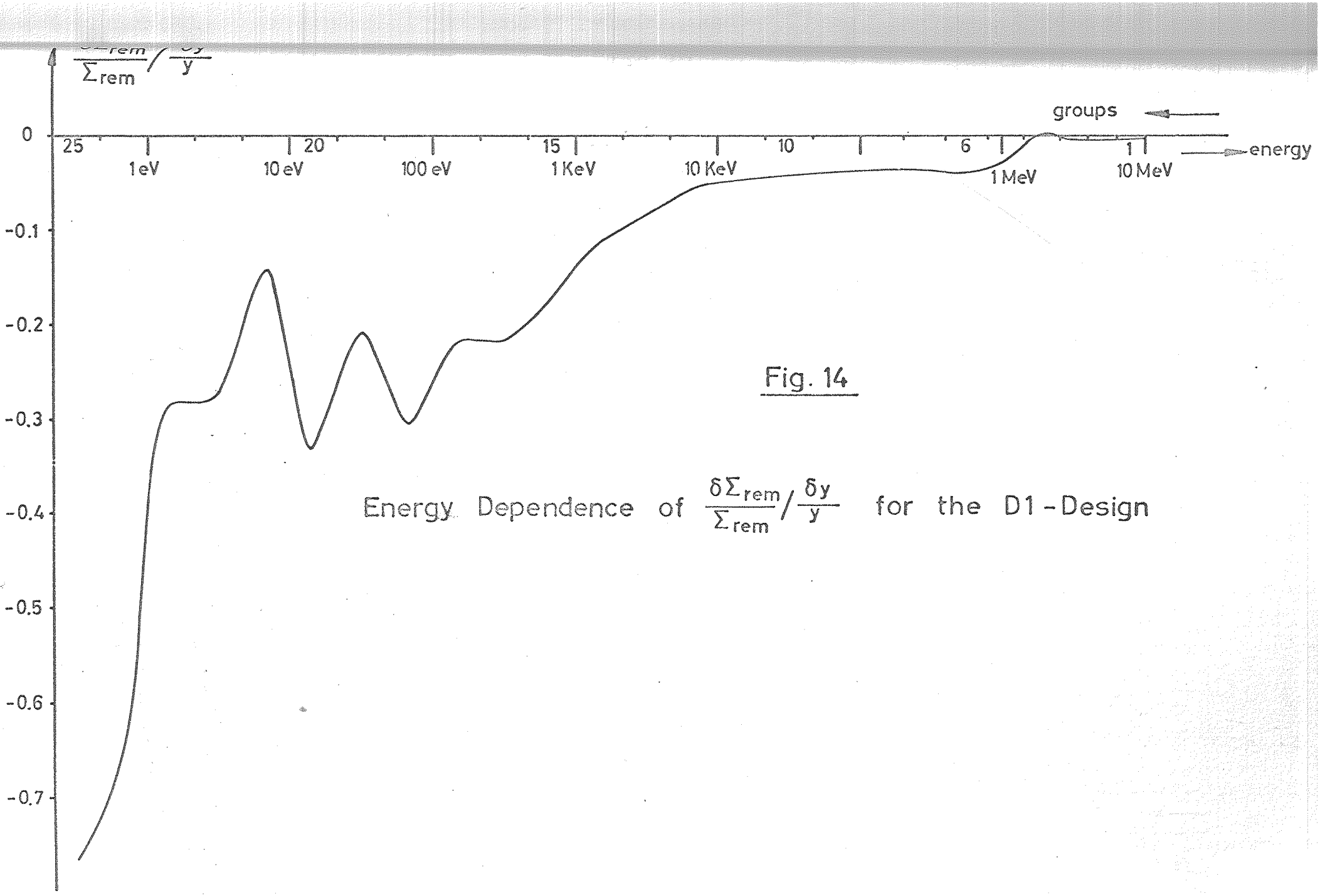

Fig. 14

Energy Dependence of $\frac{\delta\Sigma_{rem}}{\Sigma_{rem}} / \frac{\delta y}{y}$ for the D1-Design

Fig. 15

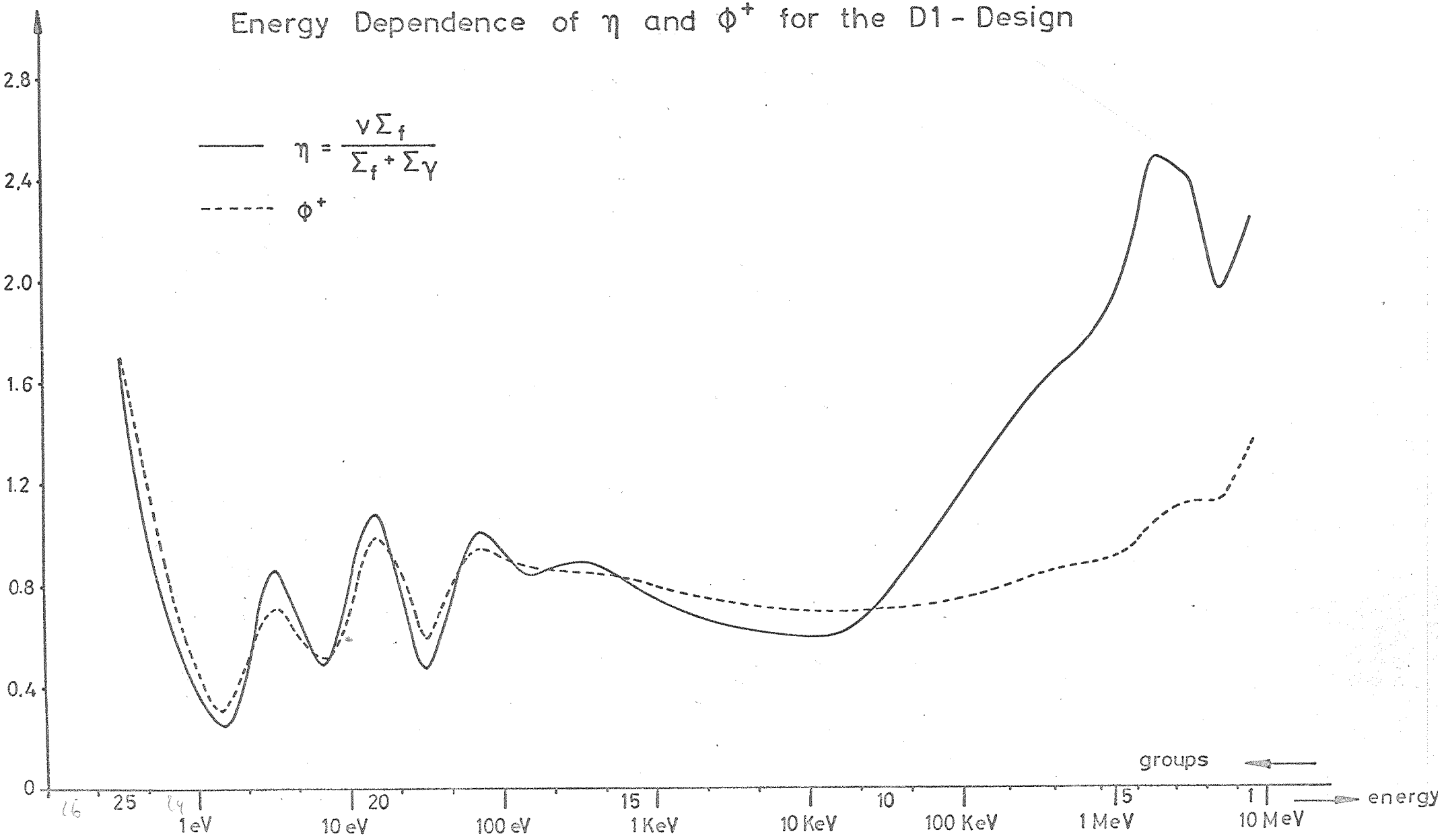

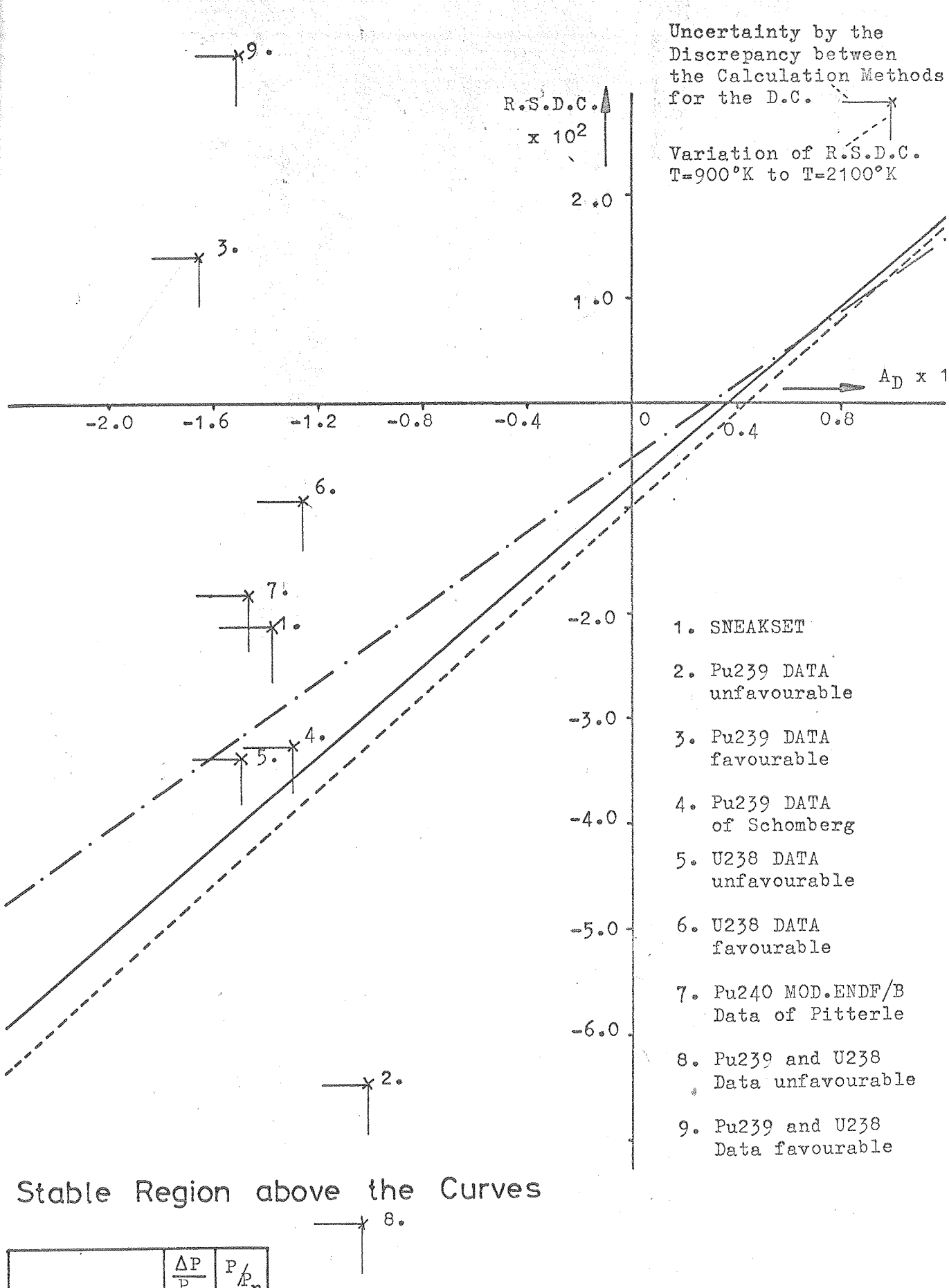

	$\frac{\Delta P}{P}$	P/P_n
———	0.01	1
- - - - - - -	0.75	1
——— · ——— ·	0.01	0.6

Fig. 16

Fig. 17

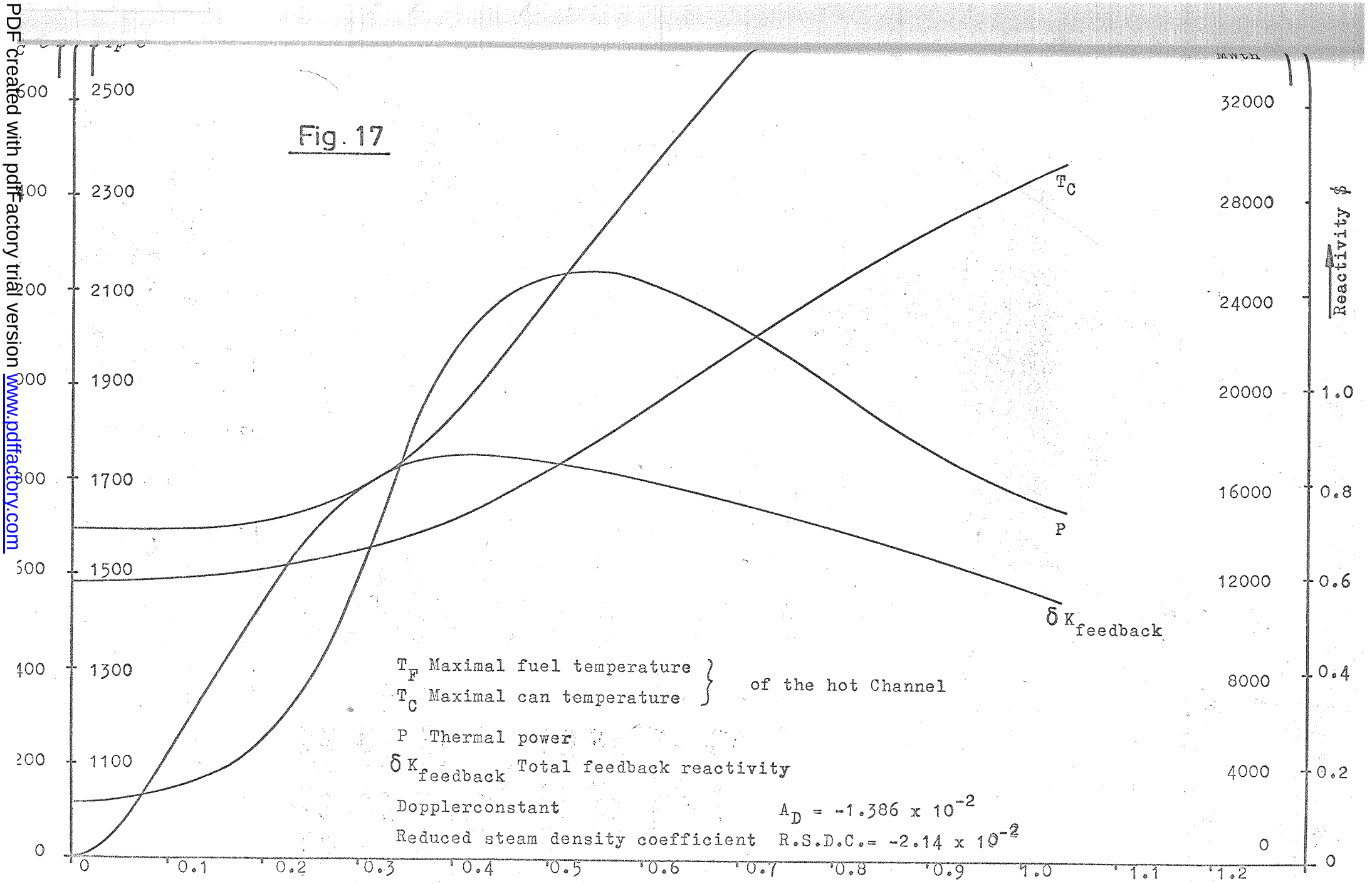

Behaviour of some Significant Quantities of the D-1 Core after a main pipe Rupture near the Reactor Inlet (without Scram)

Fig. 18

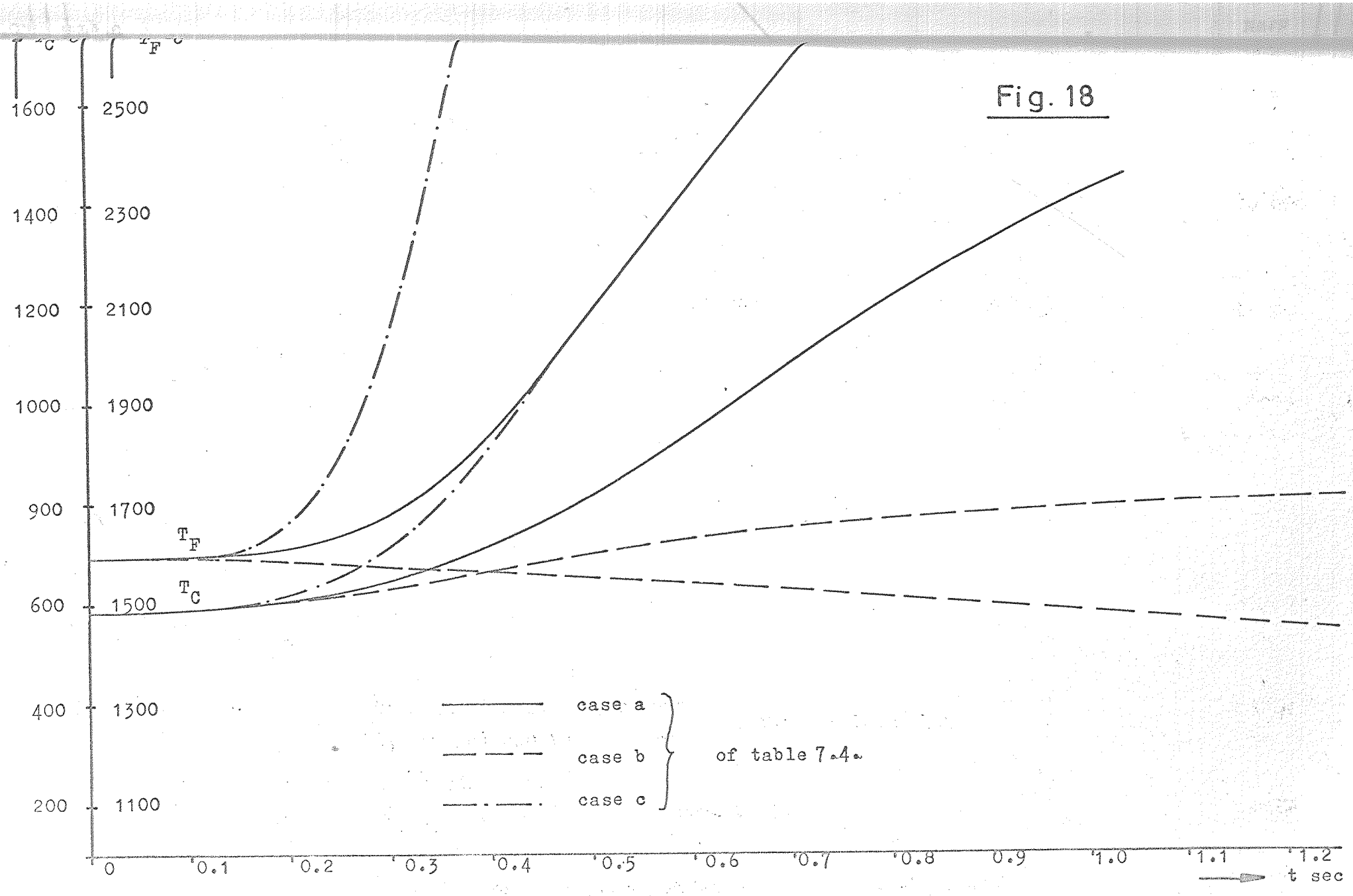

The Maximal Fuel and Can Temperature in the Hot Channel after a Main Pipe Rupture near the Reactor Inlet (Without Scram)

Fig. 19

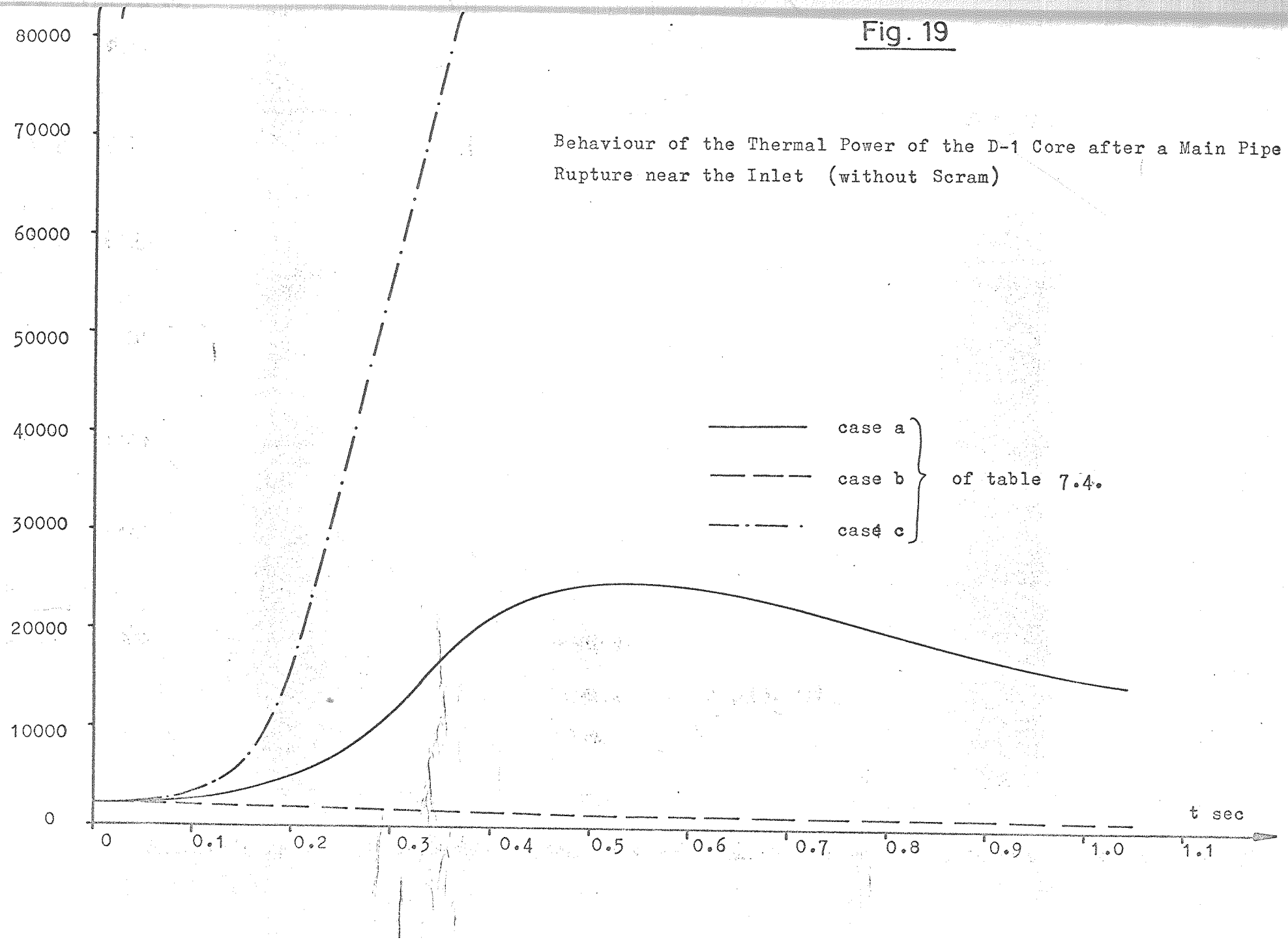

Behaviour of the Thermal Power of the D-1 Core after a Main Pipe Rupture near the Inlet (without Scram)

Fig. 20

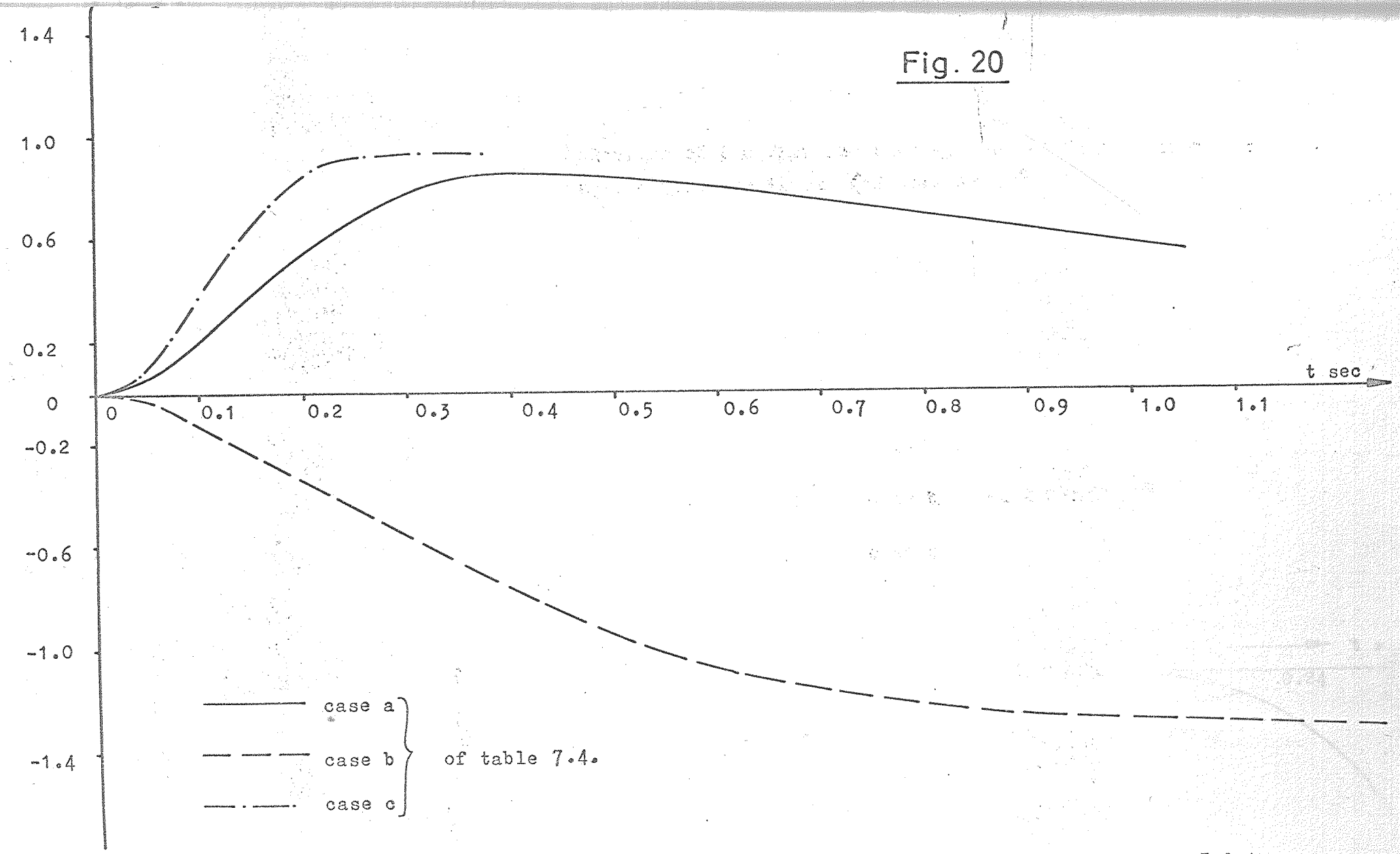

The Total Feedback Reactivity of the D-1 Core after a Main Pipe Rupture near the Reactor Inlet (Without Scram)

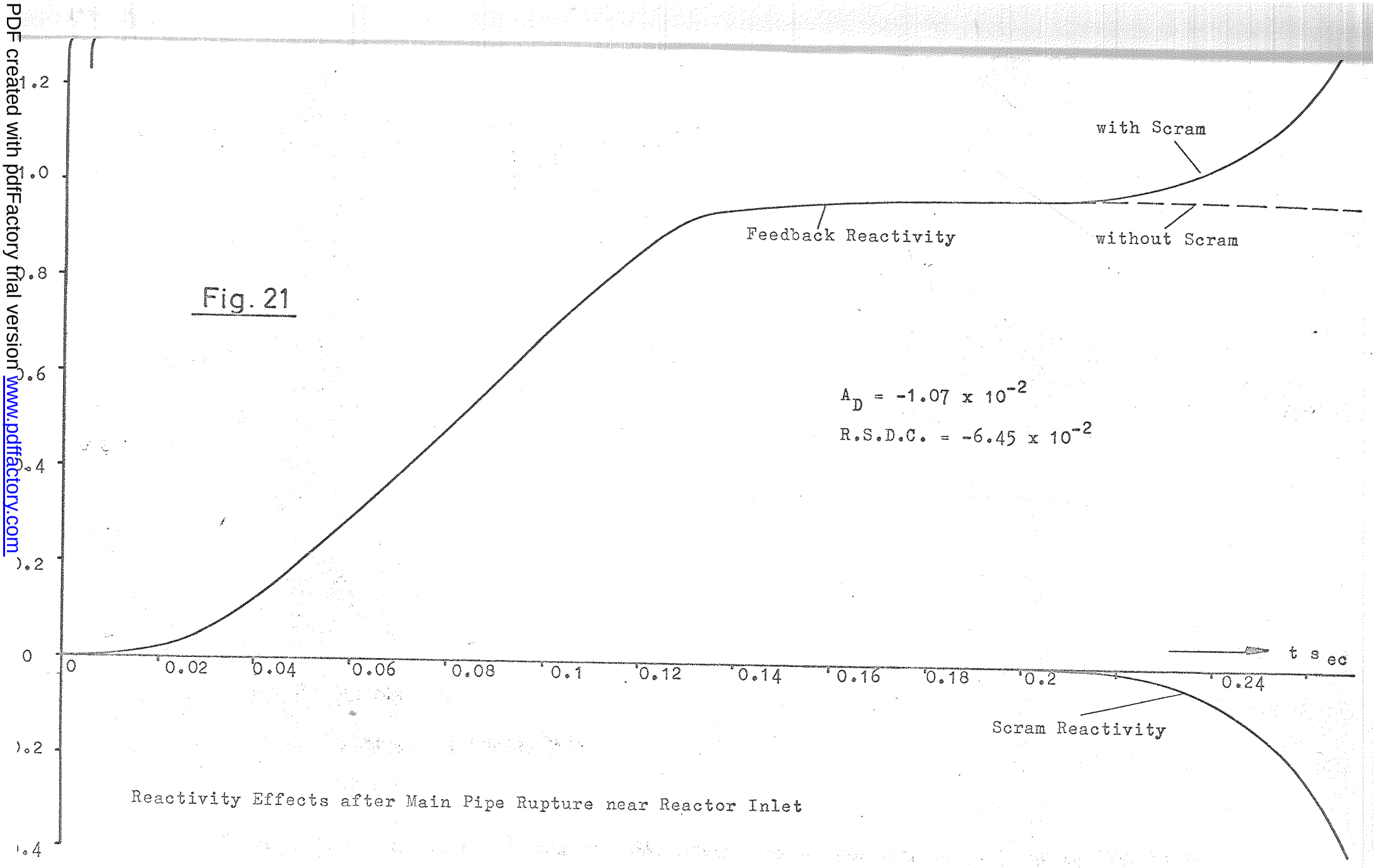

Fig. 21

Reactivity Effects after Main Pipe Rupture near Reactor Inlet

Fig. 22

Fuel and Can Temperature after Main Pipe Rupture Reactor Inlet

$A_D = -1.07 \times 10^{-2}$

R.S.D.C. $= -6.45 \times 10^{-2}$

obtained with most unfavourable Pu 239 Data

a without Scram
b with Scram

T_C Can Temperature

T_F Fuel Temperature

in hot Channel